CERN

Cours/Lecture Series

1994 – 1995 ACADEMIC TRAINING PROGRAMME

LECTURE SERIES

SPEAKER	:	E. IAROCCI / INFN, Frascati, Italy
TITLE	:	New detector techniques
TIME	:	13, 14, 15, 16 & 17 March, 11.00 to 12.00 hrs
PLACE	:	Auditorium

ABSTRACT

The lectures will concentrate on the particle detectors which are under development for LHC. Many of them feature enough conceptual simplicity so to be useful examples to introduce the basic principles of the various detector types.

The main detector areas will be covered as follows :

1. Detectors of ionization charge, in liquids gases, and solids. These mostly cover the tracking devices. The emphasis will be on the operation of the detector elements.
2. Calorimeters based on liquids and scintillators. Here the emphasis will be on the subsystem aspects.

SIS/H/346

1995/DSU-CP-MP
Distr. int. & ext.

Detectors for LHC

mainly : an introduction to the detector technologies of ATLAS and CMS starting from basic principles

Outline:

- Detectors of ionization charge
  - in gases and liquids
  - in solids
- Calorimeters
  - with noble liquids
  - with scintillating media

Detectors of ionization charge in gases and liquids

- Currents induced by the motion of charges
- Noble liquid ionization chamber
- Avalanche and proportional amplification in gas
  - Transition Radiation Tracker
  - Drift Tubes
  - Cathode Strip Chambers
  - RPCs and Thin Gap Chambers

* GMSCs : after the Solid State detectors

References:

ATLAS and CMS Tech. Proposal and related DRDC papers + Internal Notes + ...

Detectors of ionization charge

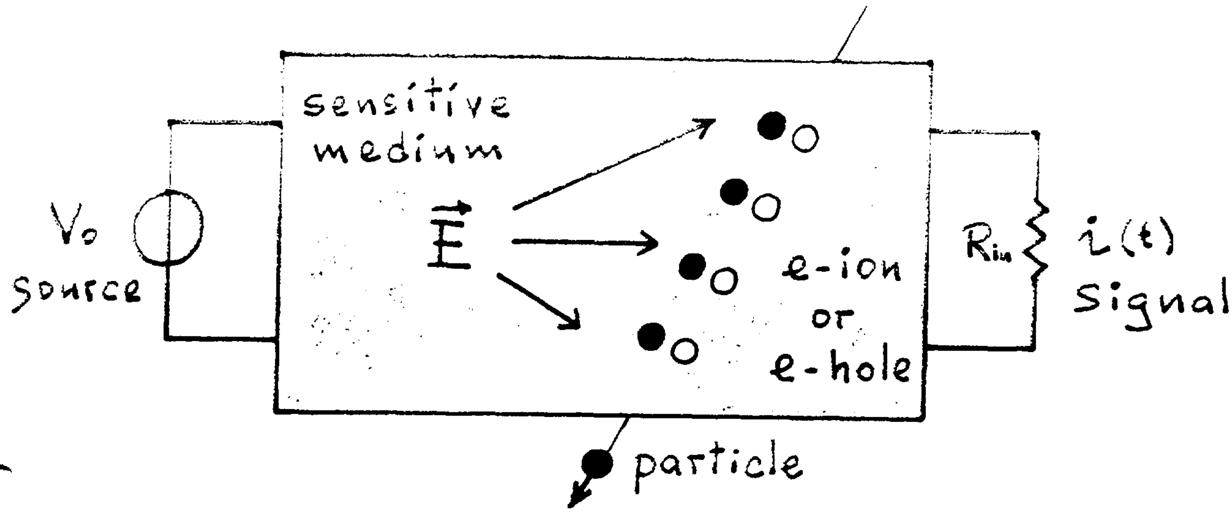

Sensitive medium :

any insulator where electrons(*) can move freely :

- non electronegative gas or liquid (e - ion pairs) ; electron multiplication needed in gas
- insulating crystal (e-h pairs) :
  - reverse biased semiconductor junction
  - diamond

(*) The same electric force acts on ions and electrons, but due to their much higher mobility, most of the power is transferred to electrons

The generation of signals is usually localized within $\lesssim (1cm)^3$ cells.

Since $1cm/c \sim 30ps$ the quasi stationary electric approximation can be used (Poisson equation).

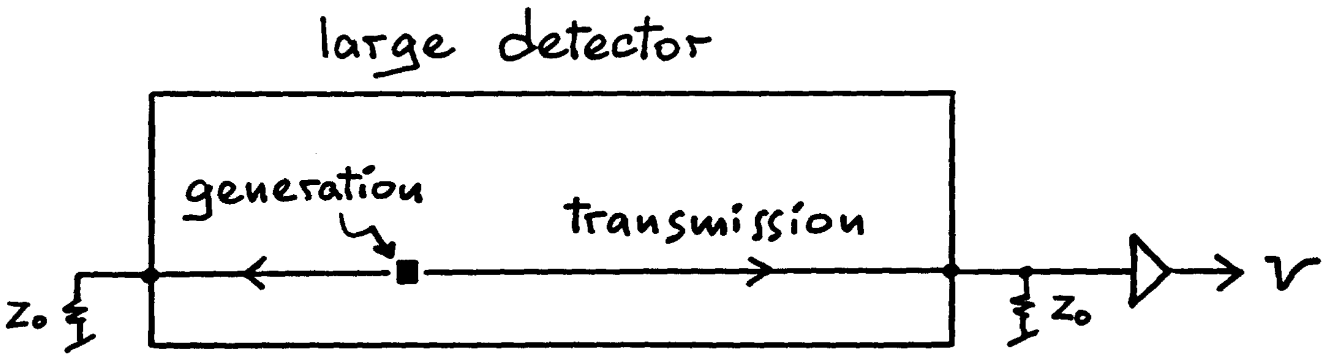

On large detectors the transmission of signals usually is on pair of electrodes at velocity $c/\sqrt{\varepsilon_r}$.

At high rates it can be necessary to arrange the pair of electrodes as a transmission line with matching resistors at both ends.

Current associated to a charge drifting in a static electric field between two electrodes

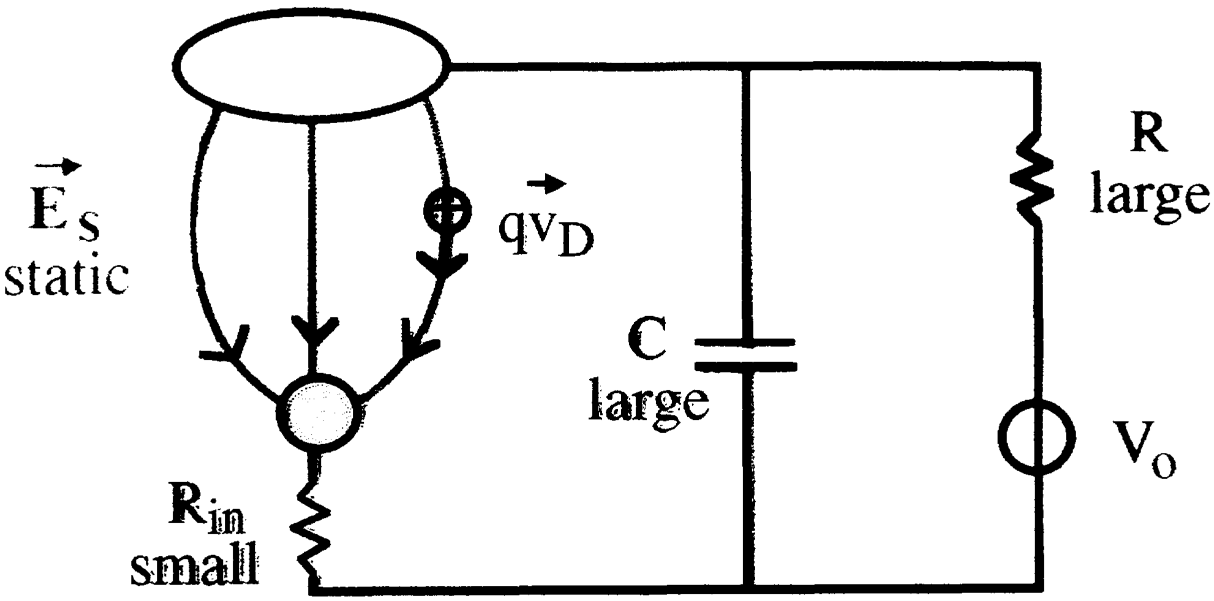

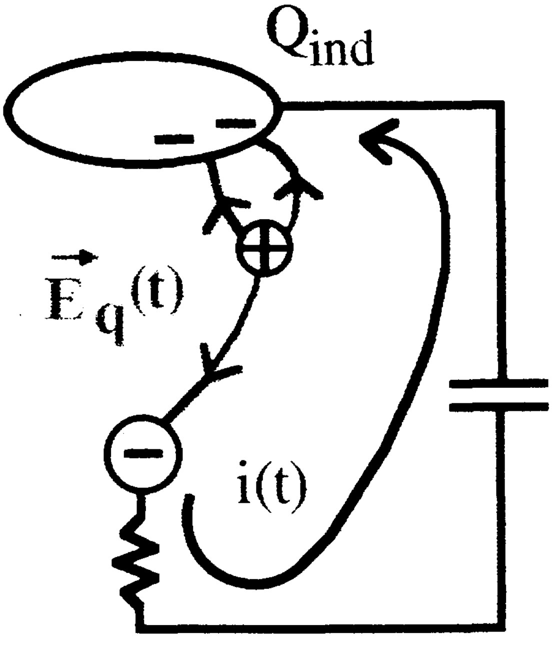

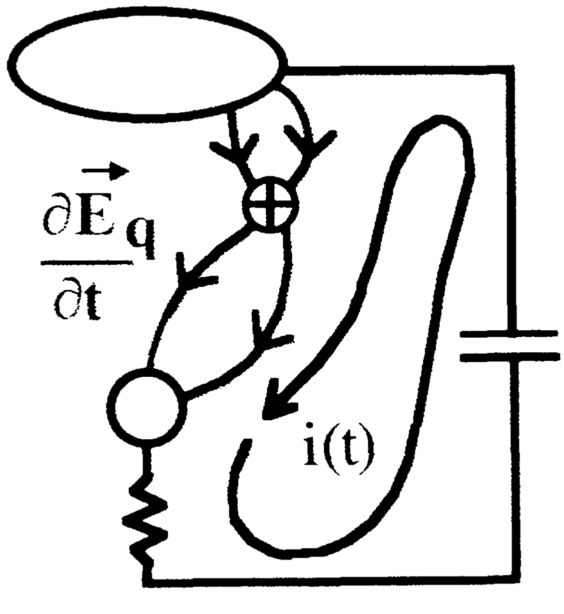

$$i(t) = \frac{d\,Q_{ind}}{d\,t} =$$

current induced by the charge in motion (Faraday picture)

i(t) loop closed by displacement current (Maxwell picture)

Calculation of the induced current in the case of only two electrodes

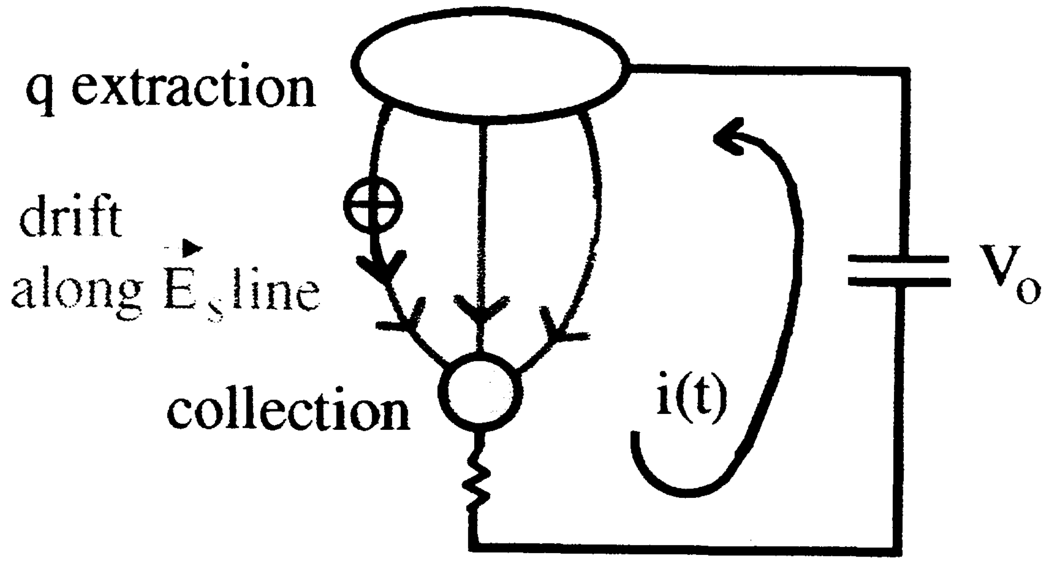

- Power by V_0 on i(t) = power by $\vec{E}_S$ on $q\vec{v}_D$

$$V_0 \; i(t) = (q \, E_S) \, v_D$$

$$\longrightarrow \; i(t) = q \, \frac{E_S(t)}{V_0} \, v_D(t)$$

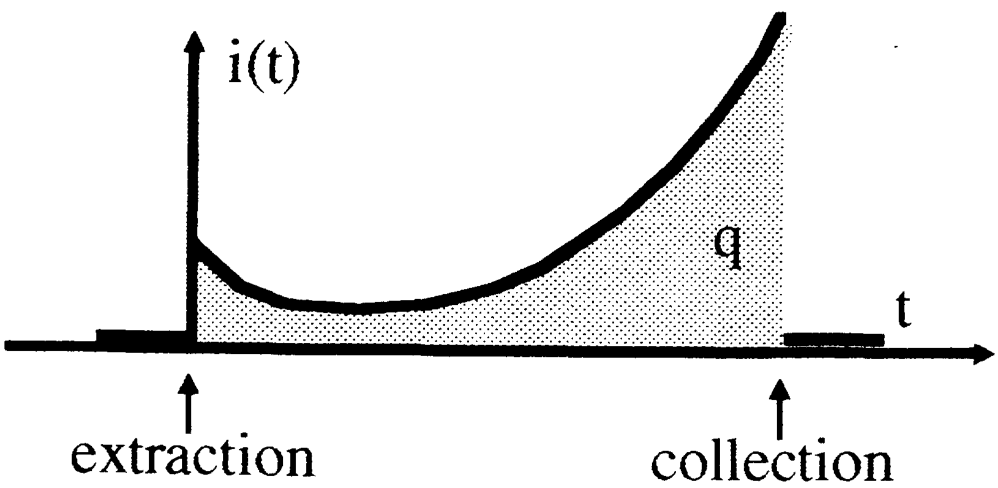

Induced current in the case of more than two electrodes

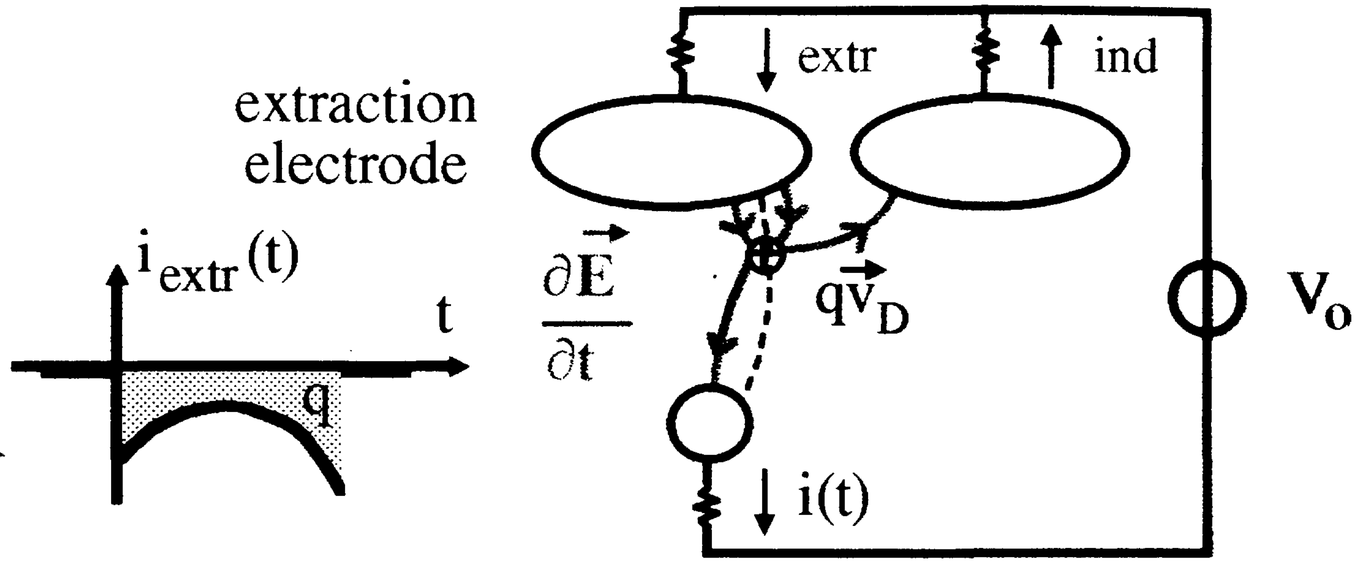

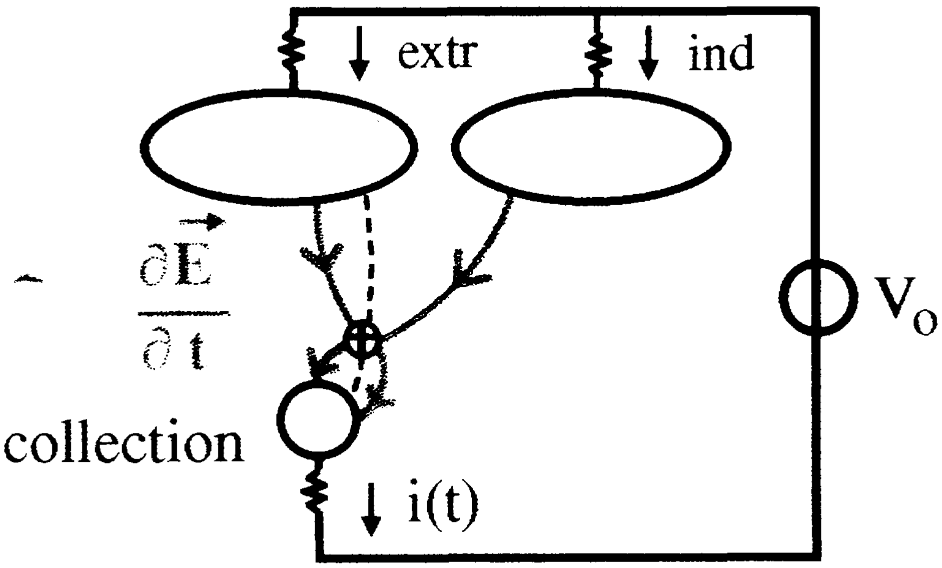

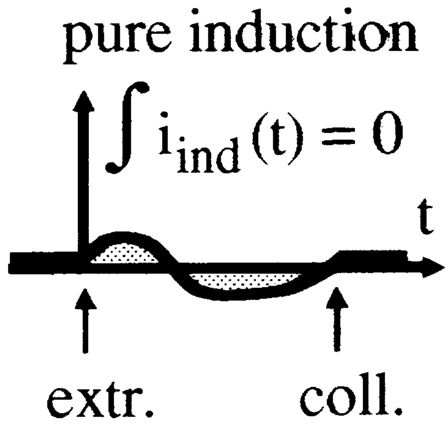

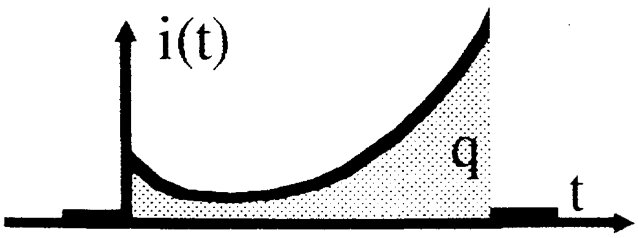

$$i(t) = q\frac{E_S}{V_O}v_D$$

Calculation of induced current on any electrode by the weighting field

(V. Radeka, Ann. Rev. Nucl. Part. Sci. 1988,38,217)

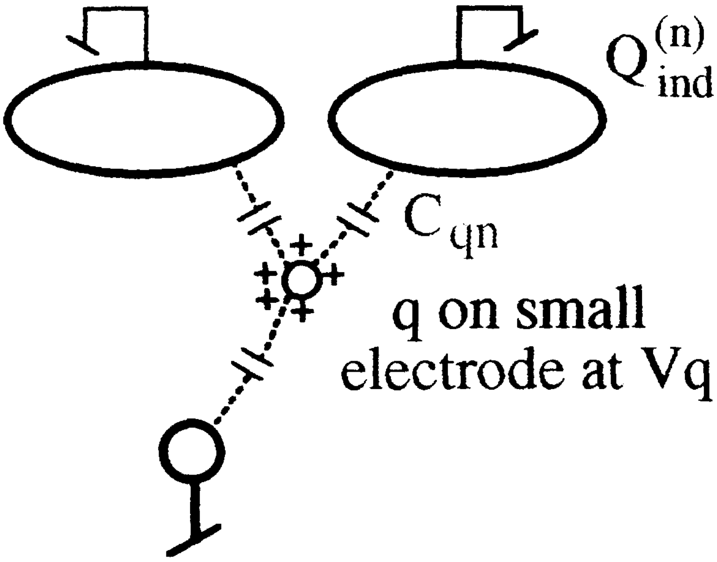

$$\frac{Q_{ind}^{(n)}}{q} = \frac{C_{qn}}{C_{tot}}$$

$$\longrightarrow Q_{ind}^{(n)} = C_{qn}\,\frac{q}{C_{tot}} = C_{qn} V_q = \left(\frac{q}{V_n}\right) V_q$$

Reciprocity Theorem

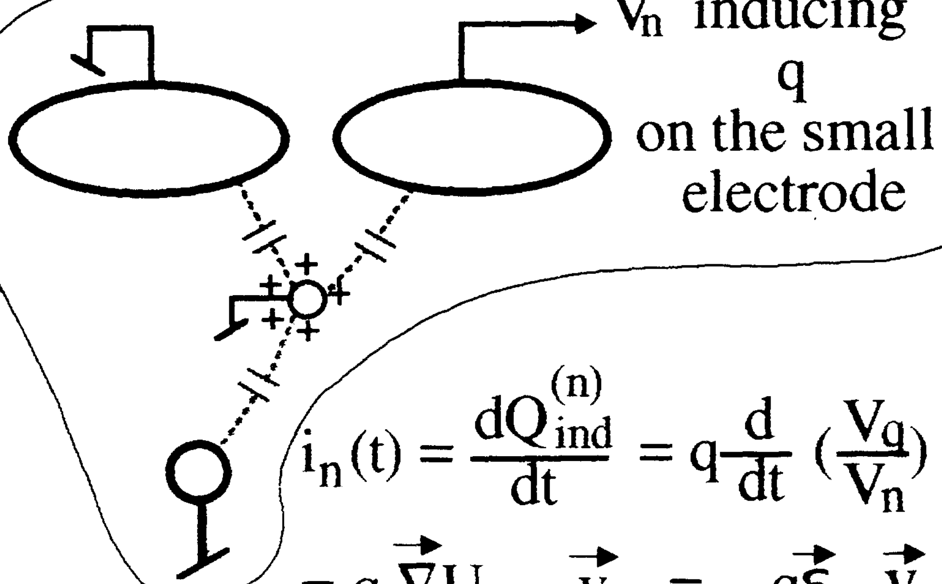

$$i_n(t) = \frac{dQ_{ind}^{(n)}}{dt} = q\frac{d}{dt}\left(\frac{V_q}{V_n}\right) = q\frac{d}{dl}\left(\frac{V_q}{V_n}\right)\frac{dl}{dt} =$$

$$= q\,\underbrace{\vec{\nabla} U}_{\text{adimensional scalar field}} \cdot \vec{v}_D = -q\underbrace{\vec{\varepsilon}}_{\text{weighting field}} \cdot \vec{v}_D$$

Note: 2 electrodes $\vec{\varepsilon} = \vec{E}_S / V_O$

In general in detectors e-ion (e - h) pairs are produced at some position in the sensitive volume

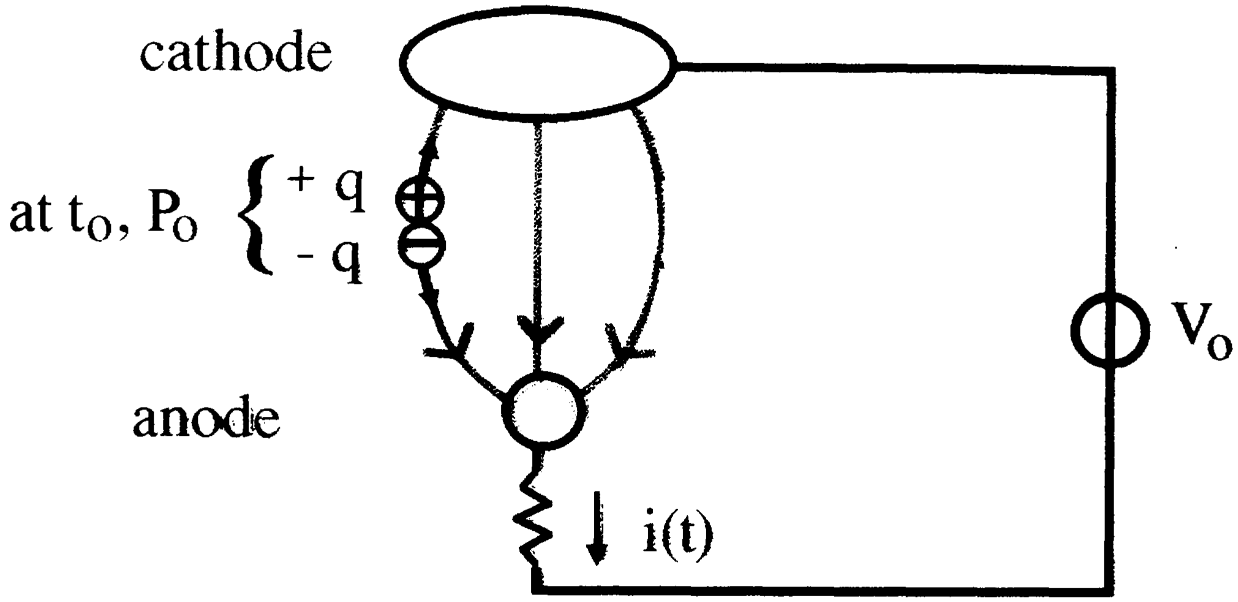

$$i(t) = i_e + i_{ion} = q\frac{E_s^{(e)}}{V_o} v_e + q\frac{E_s^{(ion)}}{V_o} v_{ion}$$

- electron charge signal:

$$Q_e = \int_{t_o}^{\text{collection}} i_e(t)\, dt = \frac{q}{V_o} \int_{P_o}^{\text{anode}} E_s \frac{dl}{dt} dt =$$

$$= q\frac{\Delta V}{V_o} \underset{\substack{\uparrow \\ \text{if } E_s \text{ uniform}}}{=} q\,\frac{\text{electron path}}{\text{electrode distance}}$$

- ions: similar but much slower

$$\longrightarrow \quad Q_e + Q_{ion} = q$$

Current signal in a parallel plate ionization chamber

→ Noble liquid calorimetry

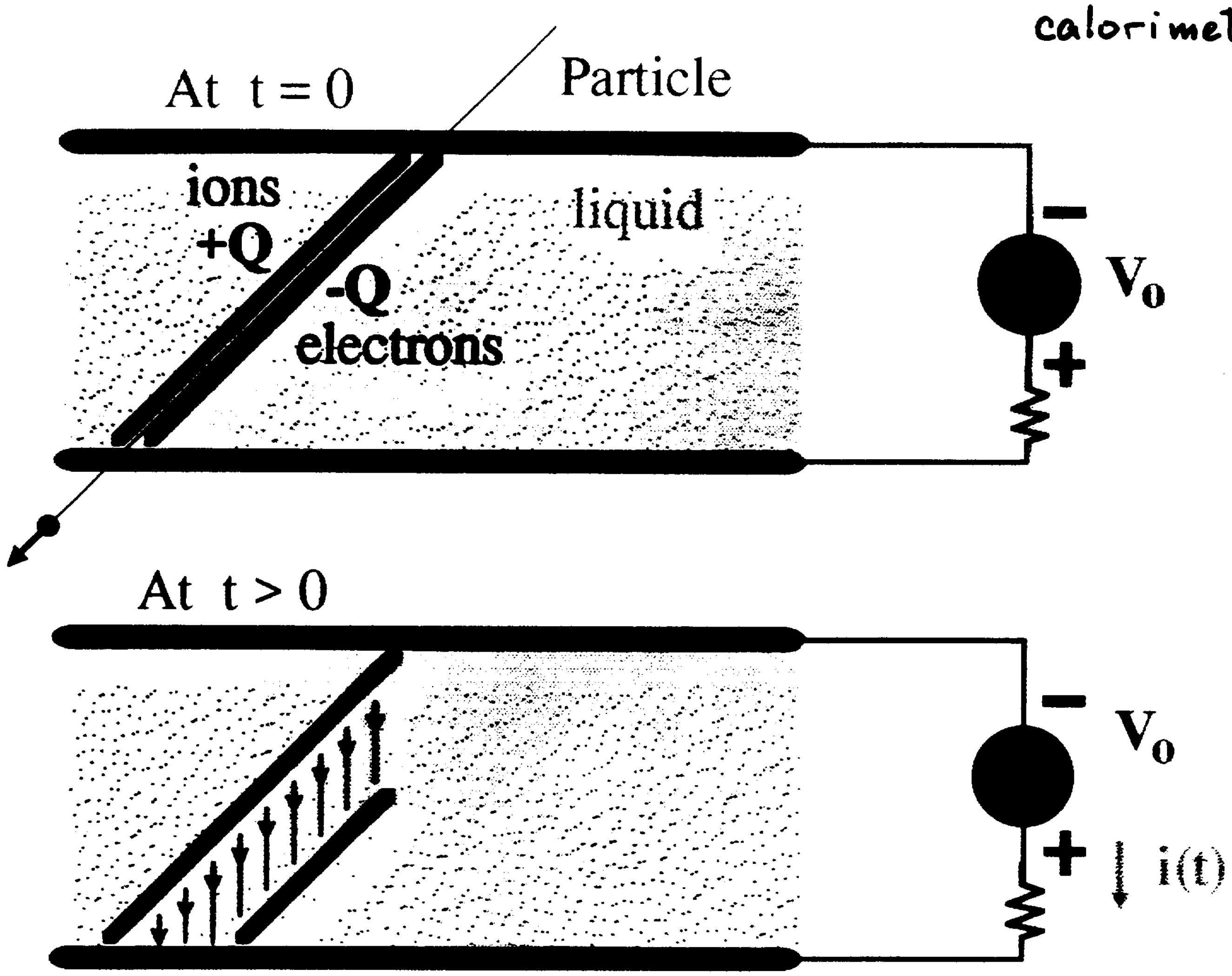

$$i(t) = \frac{E}{V_0}\, q(t)\, v_D = \frac{E}{V_0}\, Q\left(1 - \frac{v_D}{d}\, t\right) v_D$$

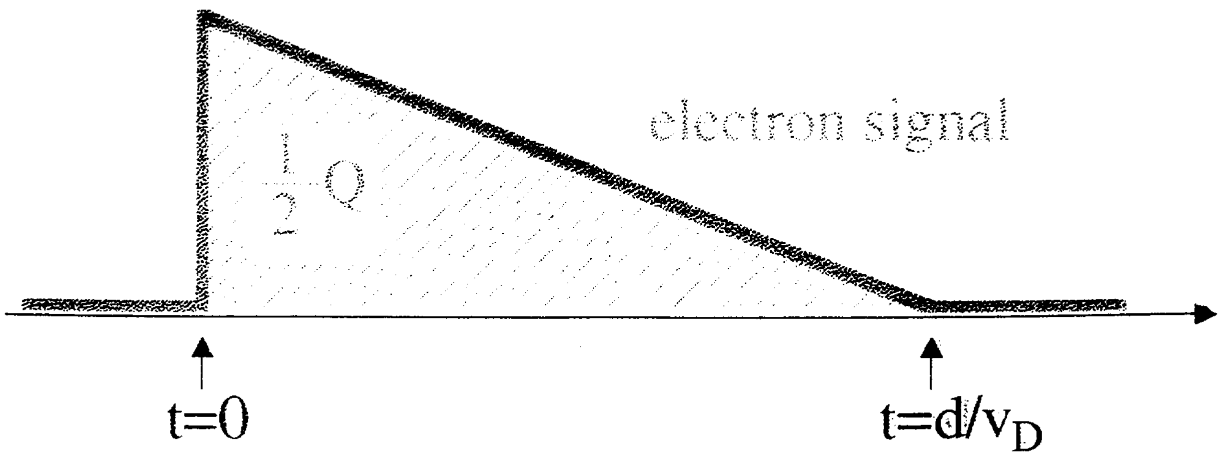

ICARUS 3-D non distructive imaging read-out

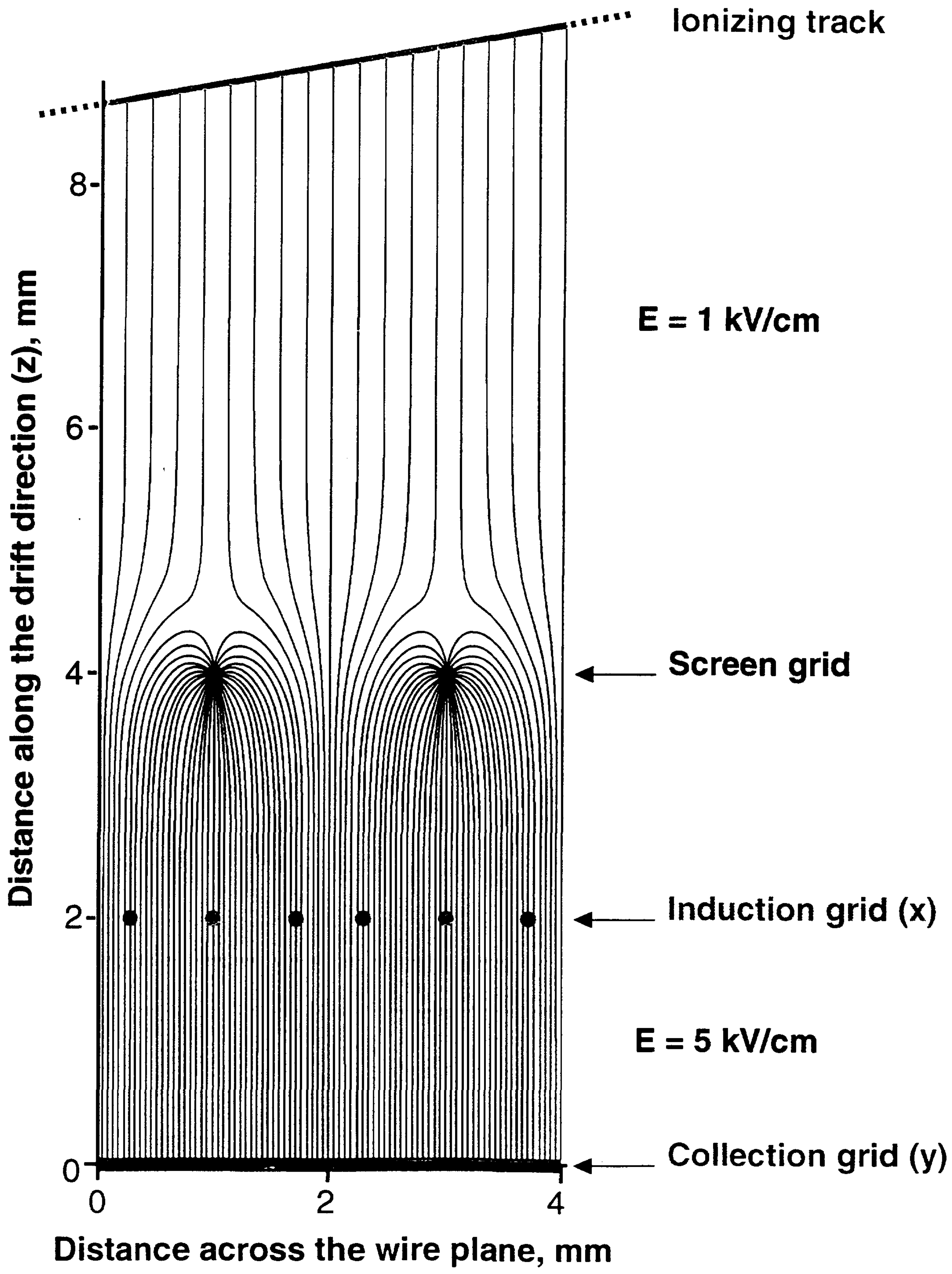

Data Filtering

(Signal Power on a 9 samples window)

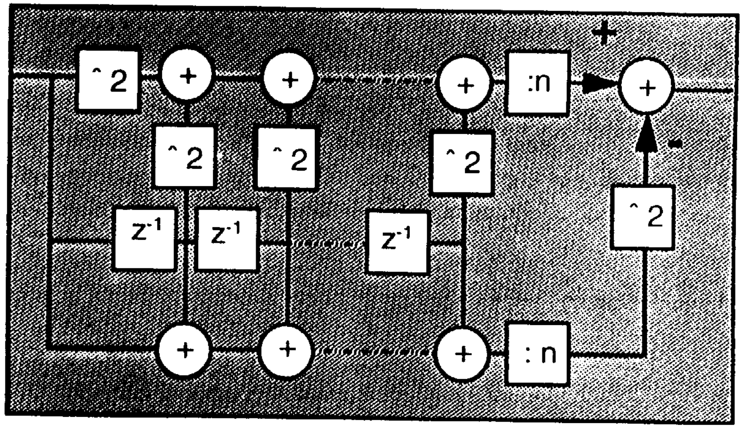

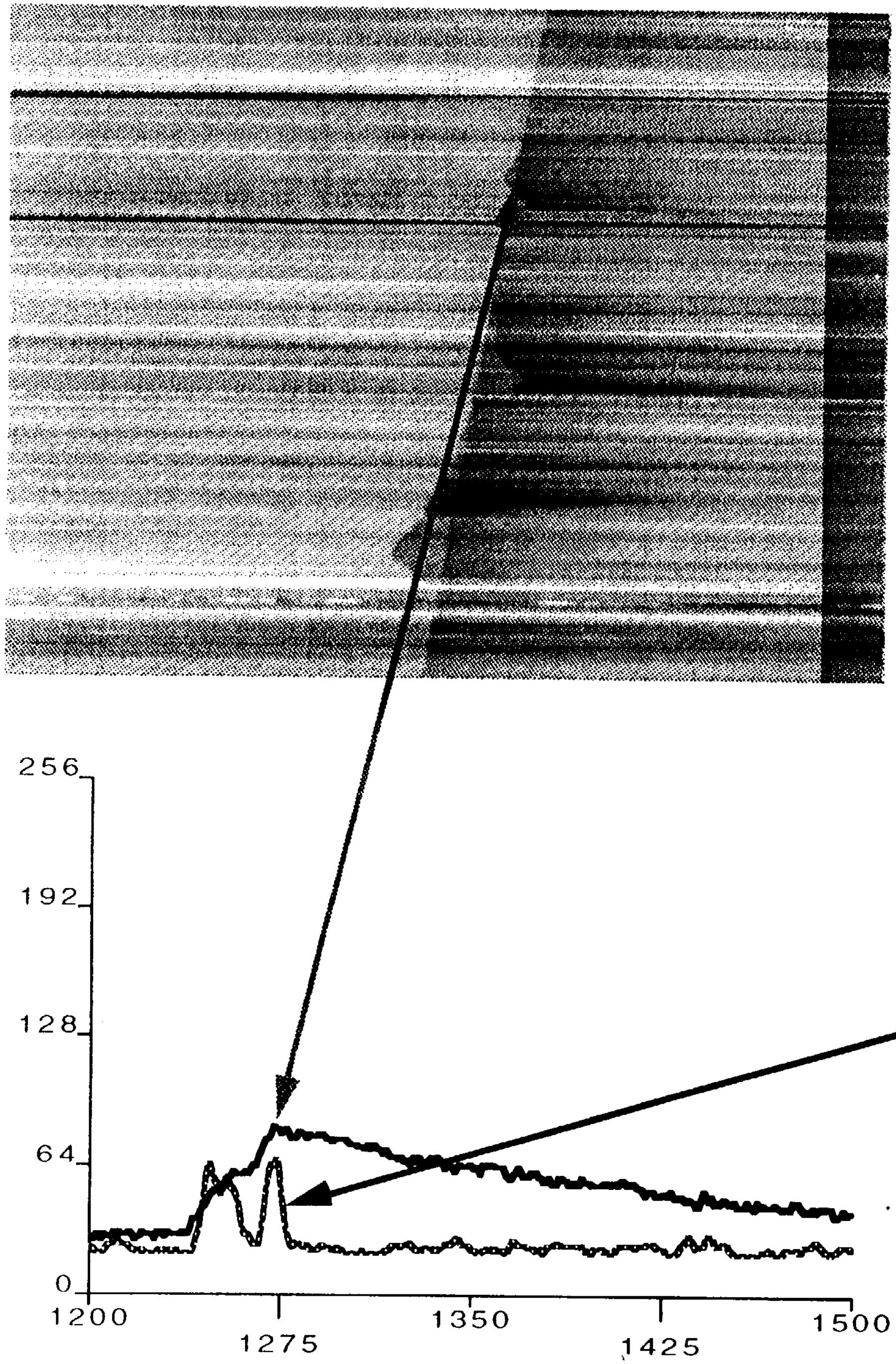

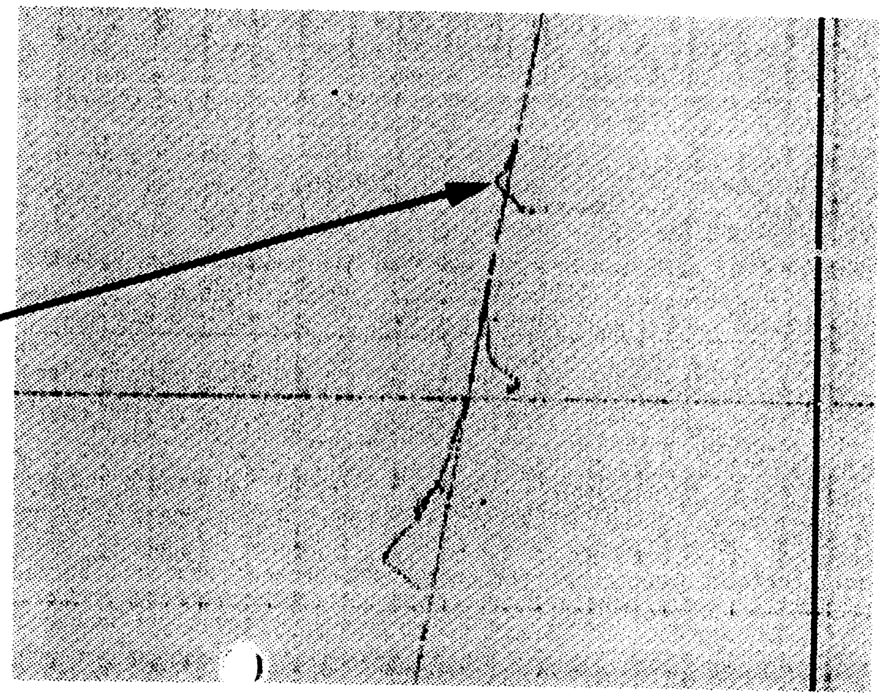

THE IONIZATION PROCESS IN GASES AND LIQUIDS

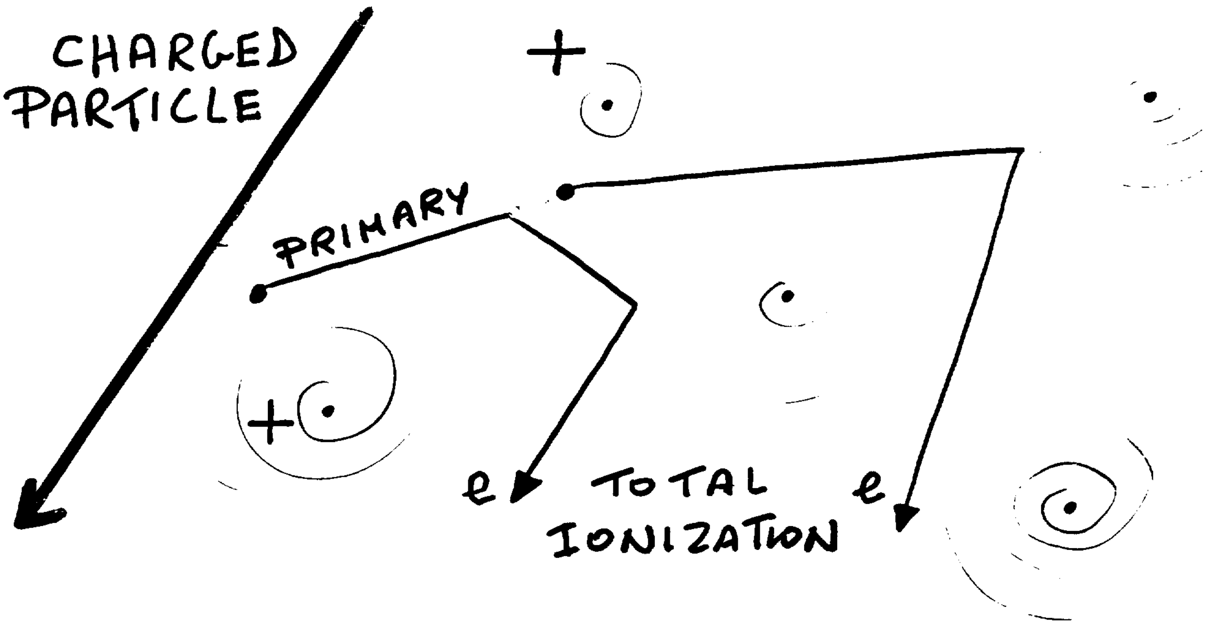

$$\frac{\Delta N_{PRIMARY}}{\Delta x} \rightarrow \text{GAUSSIAN} \qquad \frac{\Delta N_{TOTAL}}{\Delta x} \rightarrow \text{LANDAU}$$

SOME NON ELECTRONEGATIVE GASES (1 bar)

		$N_{PRIMARY}/cm$	N_{TOTAL}/cm
NOBLE	He	5	8
	Ar	24	94
	Xe	44	307
QUENCHING	CH_4	26	53
	C_4H_{10}	90	195
	CO_2	36	91

GAS DEVICES NEED e AVALANCHE MULTIPLICATION

Proportional Tube

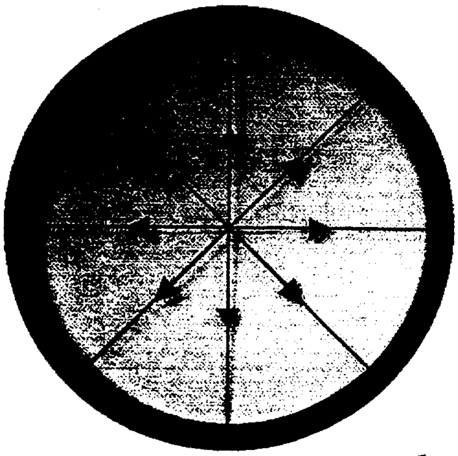

- cathode tube: 3÷100 mm
- anode wire: 20÷ 100 μm
- non electronegative gas
- $E \propto 1/r$

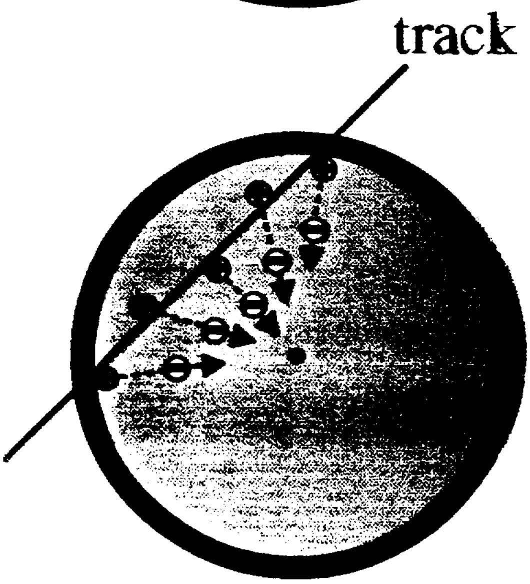

- electronic drift ~ 1mm/20ns
- negligible ionic drift

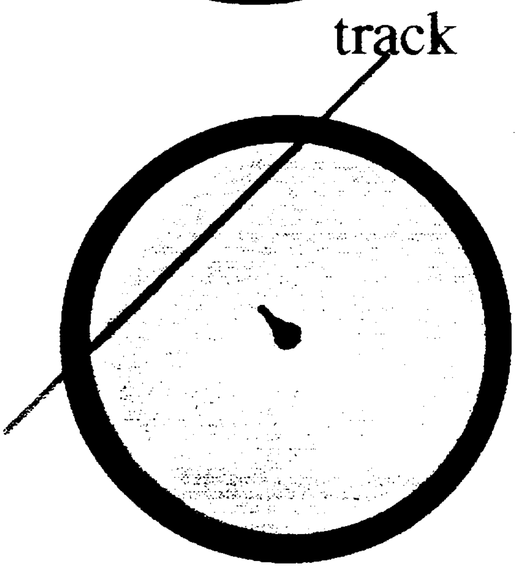

- electronic avalanche
  $N=N_o e^{\alpha(E)x}$ near the wire
- E_{max} ~ 200 kV/cm

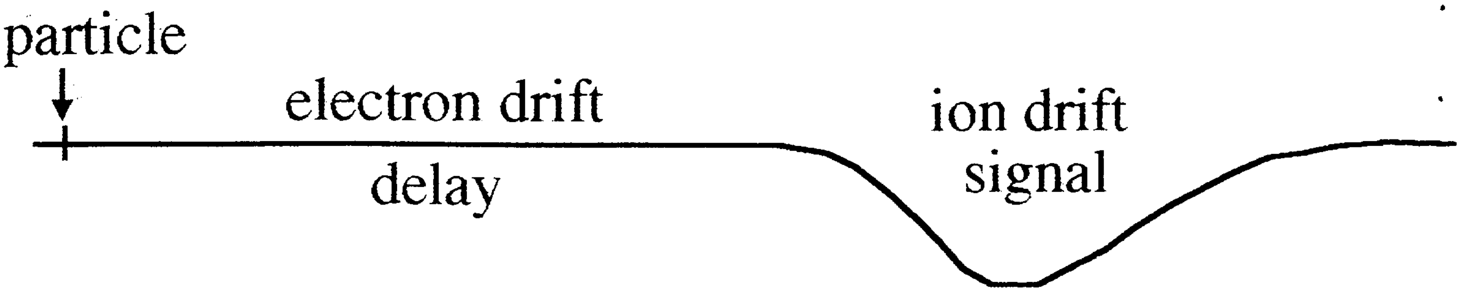

ATLAS: the combined Straw Tracker and Transition Radiation Detector (RD6)

ø 4 mm x 50 cm Drift Tubes

interleaved with polypropilene foils or foam radiator

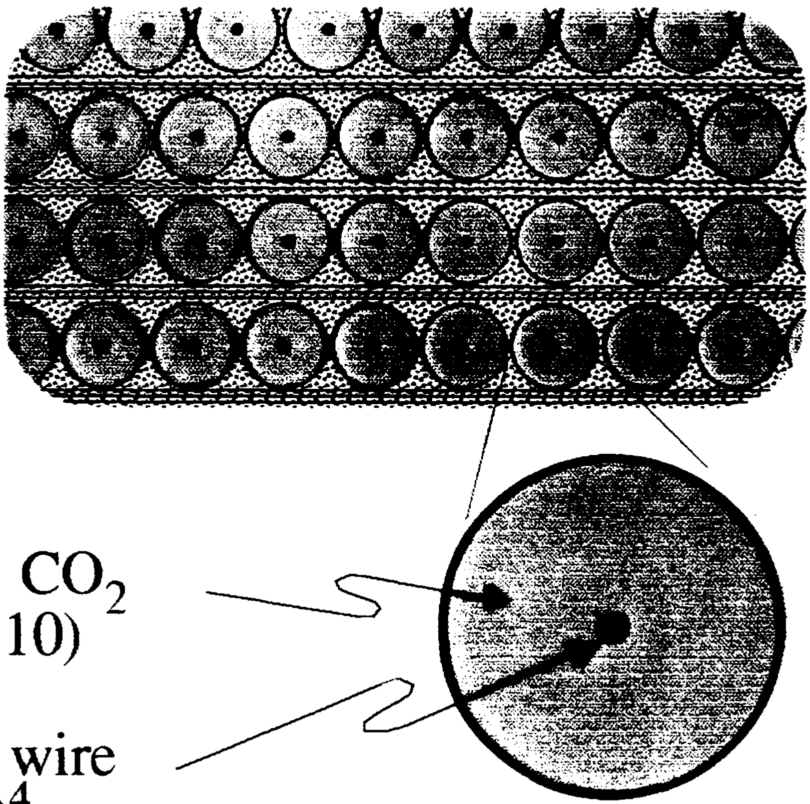

$Xe + CF_4 + CO_2$
(70 + 20 + 10)

50 μm anode wire
gain: $2{,}5 \times 10^4$
drift - time: 38 ns max

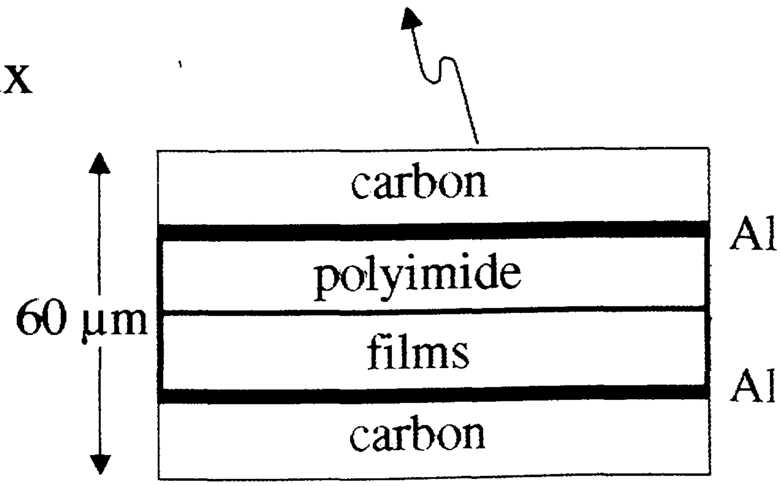

- Identification and tracking of high γ particles
electrons > 10 GeV, muons and pions >100 GeV

The structure of the TRT

Radial straws in end-cap, longitudinal in barrel

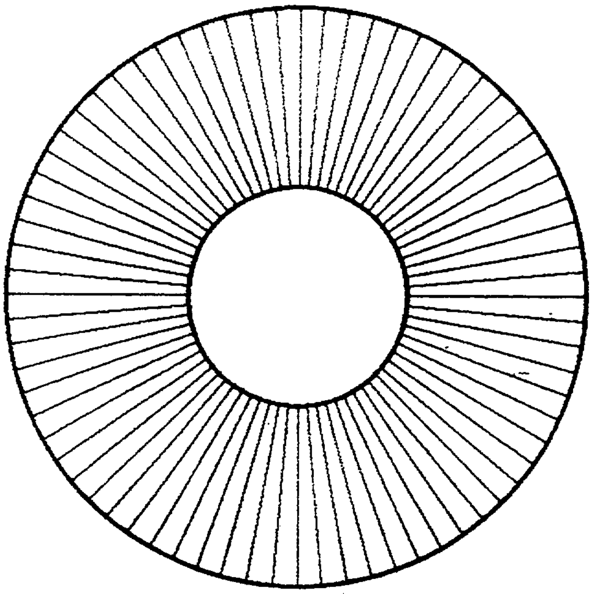

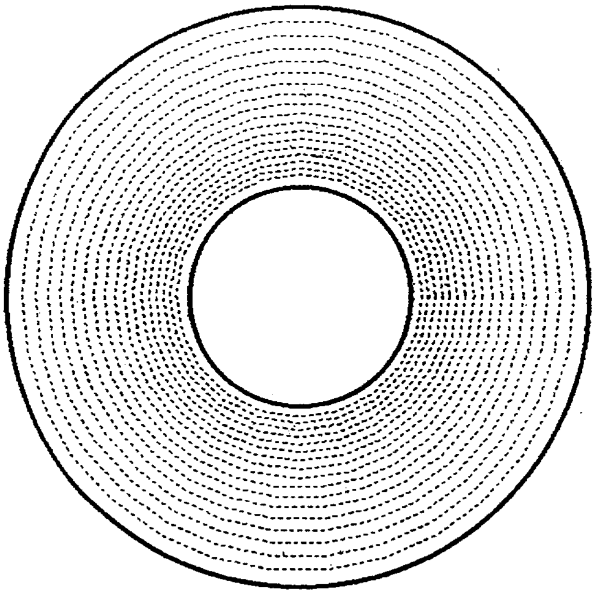

end-cap wheel

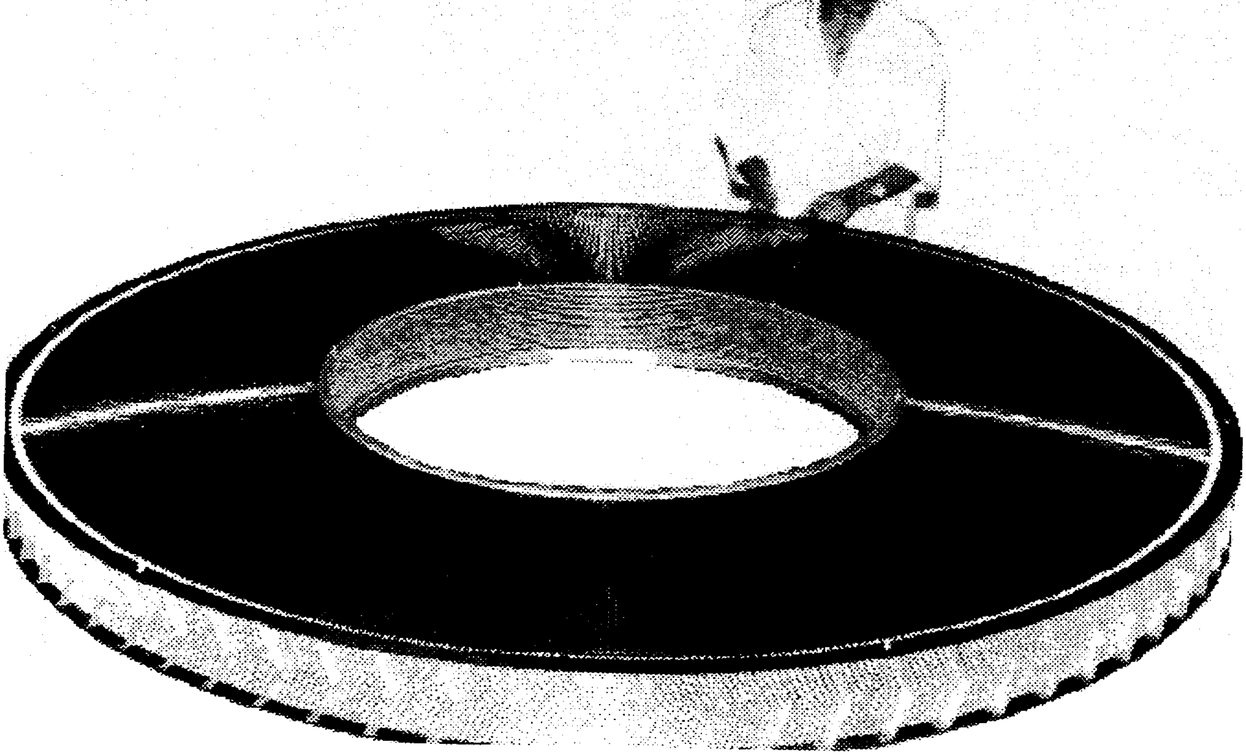

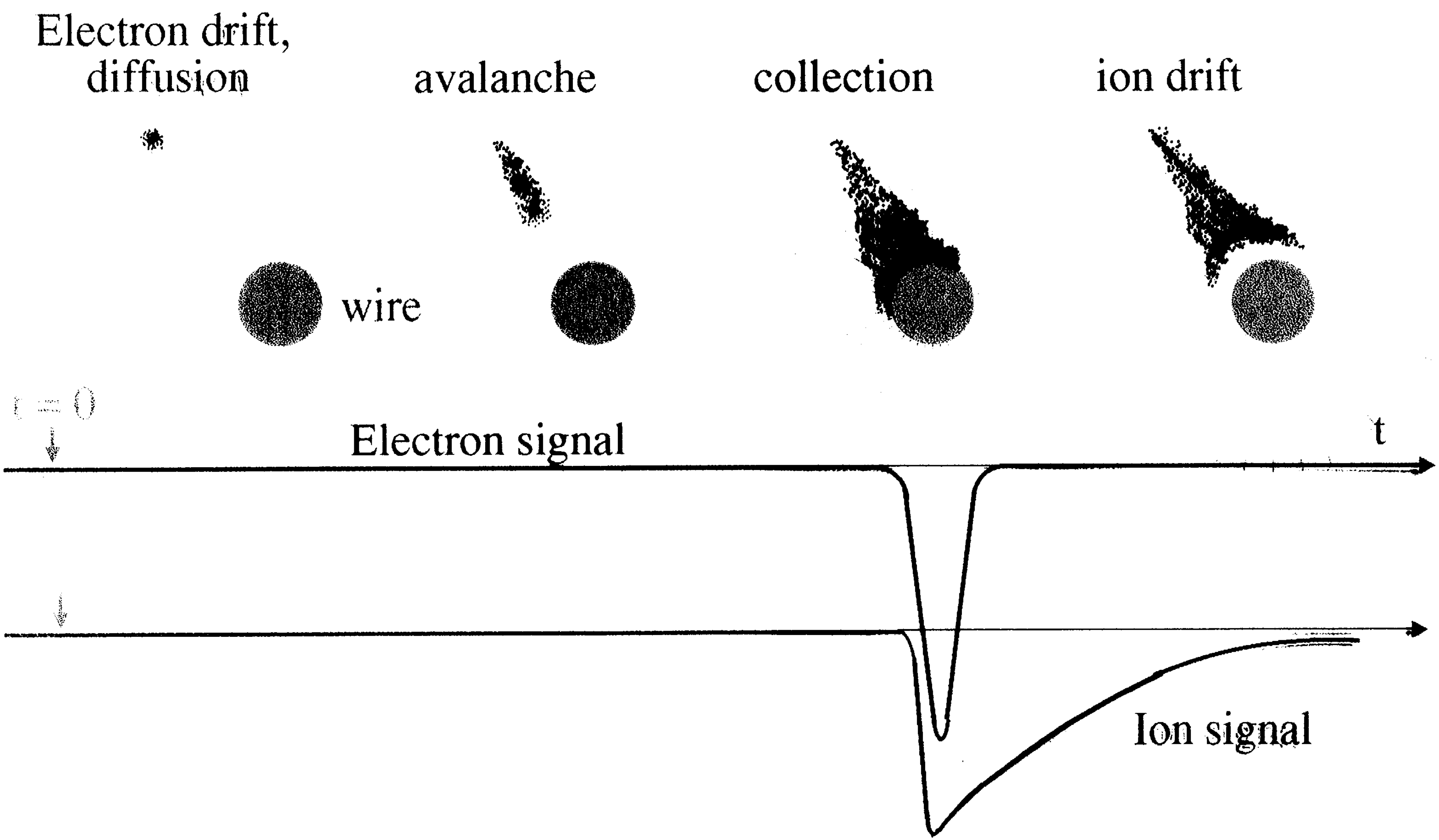
Electron drift,
diffusion
avalanche
collection
ion drift
wire
t = 0
Electron signal
t
Ion signal

Current signals with ^{55}Fe: 5,9 keV X rays
$\longrightarrow$ 200 e clusters

Ar + CH_4
0.8 + 0.2

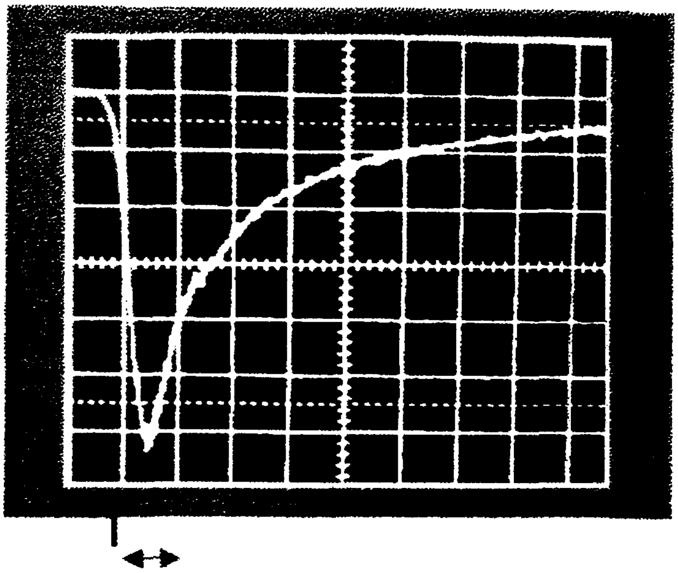

10 ns

X_e + CF_4 + CO_2

0.7 + 0.2 + 0.1

high T.R. detection efficiency

gain stabilizer

high drift velocity

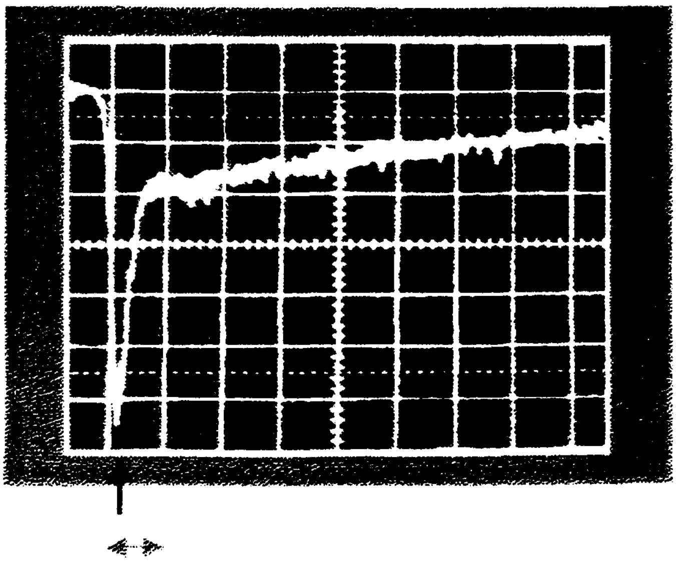

10 ns

the electron signal contributes 3% of total charge and 50% of signal for 10 ns shaping

Straw tube charge signal:

$$Q(t) = \int_0^t i(t')\,dt'$$

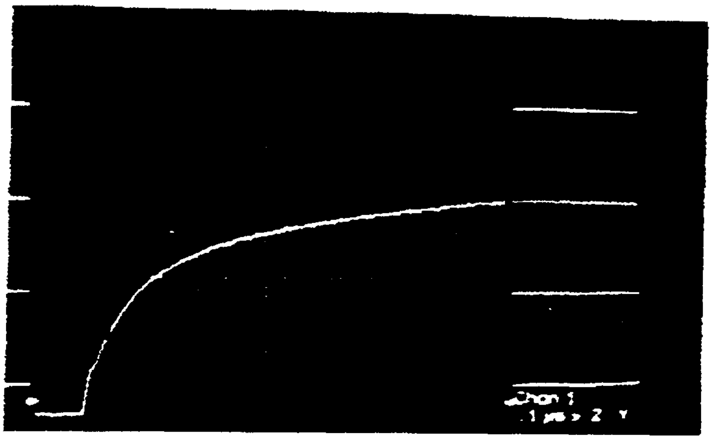

$\longleftarrow$ 1 µs $\longrightarrow$

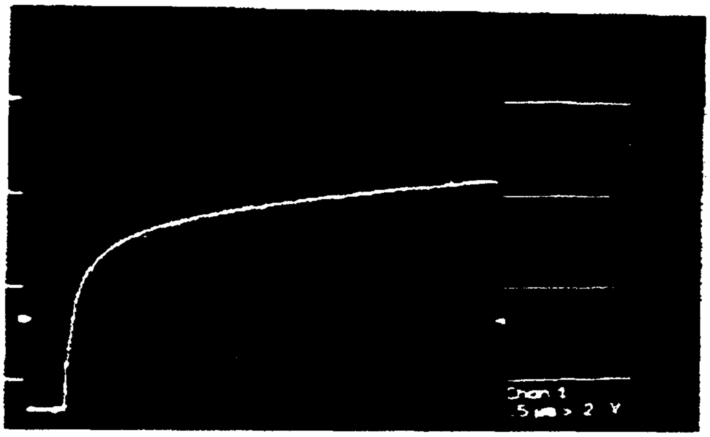

$\longleftarrow$ 5 µs $\longrightarrow$

Total charge collection time with Xe: 60 µs (with Ar: 28 µs)

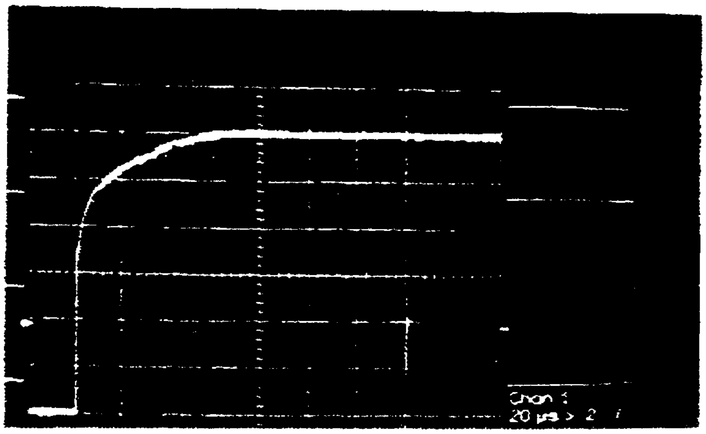

$\longleftarrow$ 200 µs $\longrightarrow$

TRT

A detailed study of the ion current signal shape

From $i_{ion}(t) = q \dfrac{E_s}{V_0} V_D$ in cylindrical geometry

$$\xrightarrow{\text{Radeka}} \quad i_{ion}(t) = \frac{i_0}{1 + t/\tau}, \quad \text{with} \quad \tau = \frac{a^2 \ln(b/a)}{2 \mu_{ion} V_0}.$$

With available value of μ_{Xe^+} :

$$\tau = 11.4 \text{ ns}$$

From fit on experimental pulse shapes:

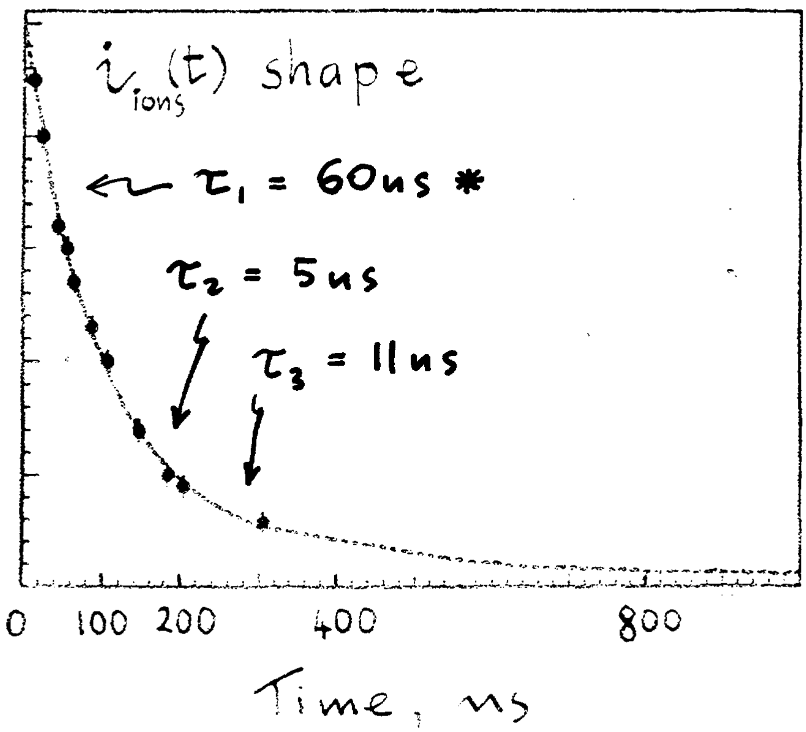

The digital readout of TRT straws

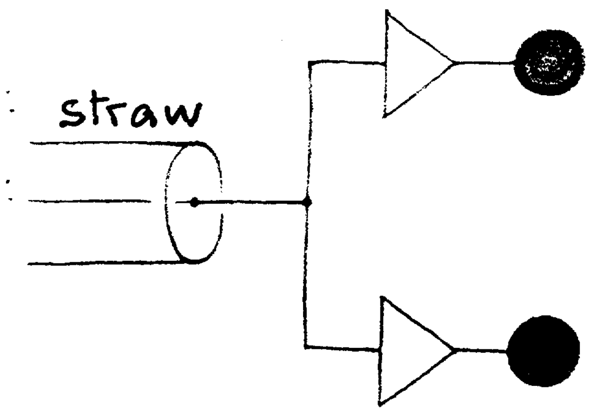

low threshold = 0.2 keV
$\longrightarrow$ all tracks

high threshold = 5.5 keV
$\longrightarrow$ T.R. hits + double tracks +
+ δ rays

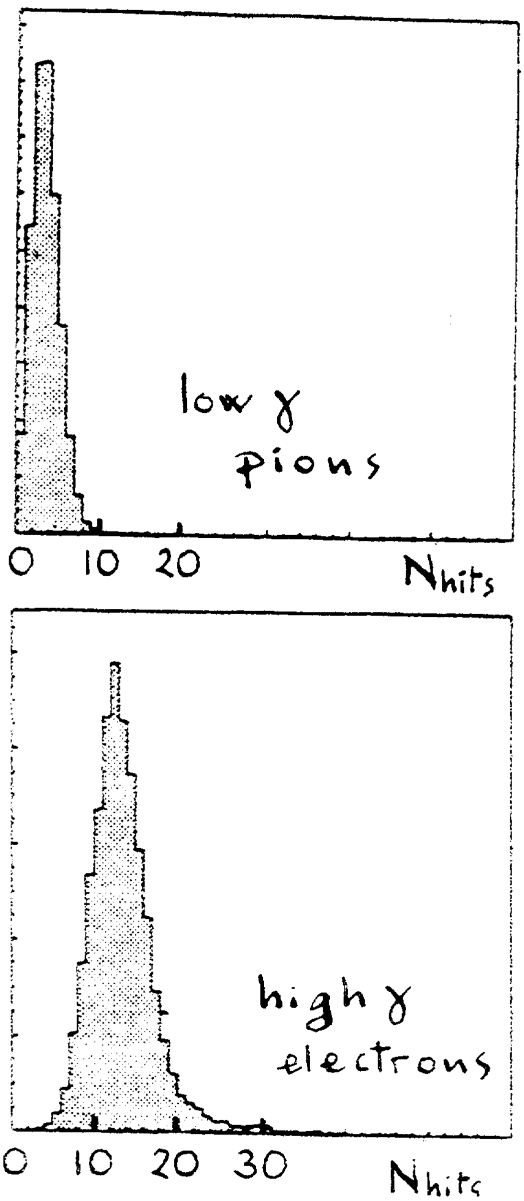

Distributions of number of hits above the high threshold.

TRD Event Display

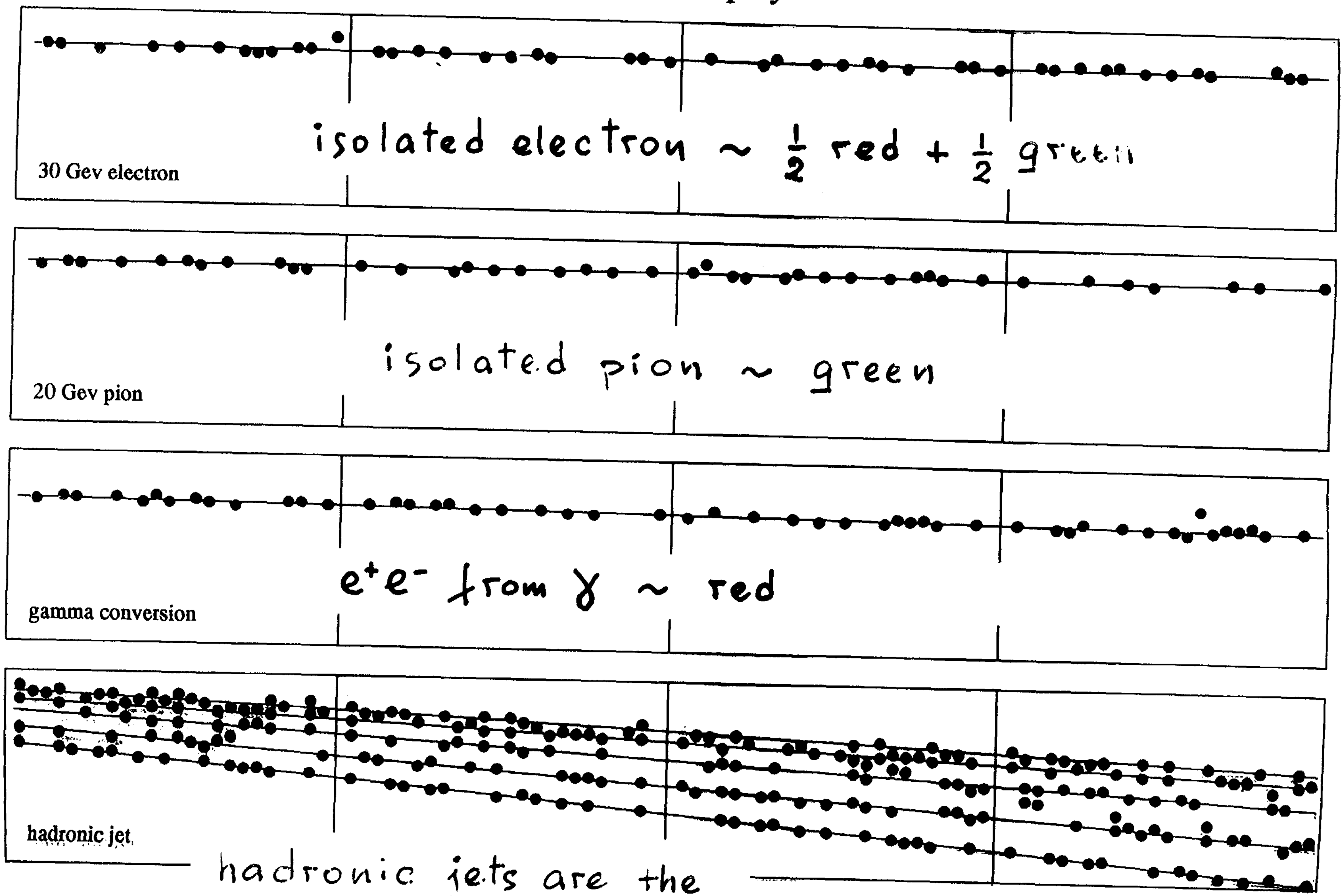

hadronic jets are the main source of fake electrons

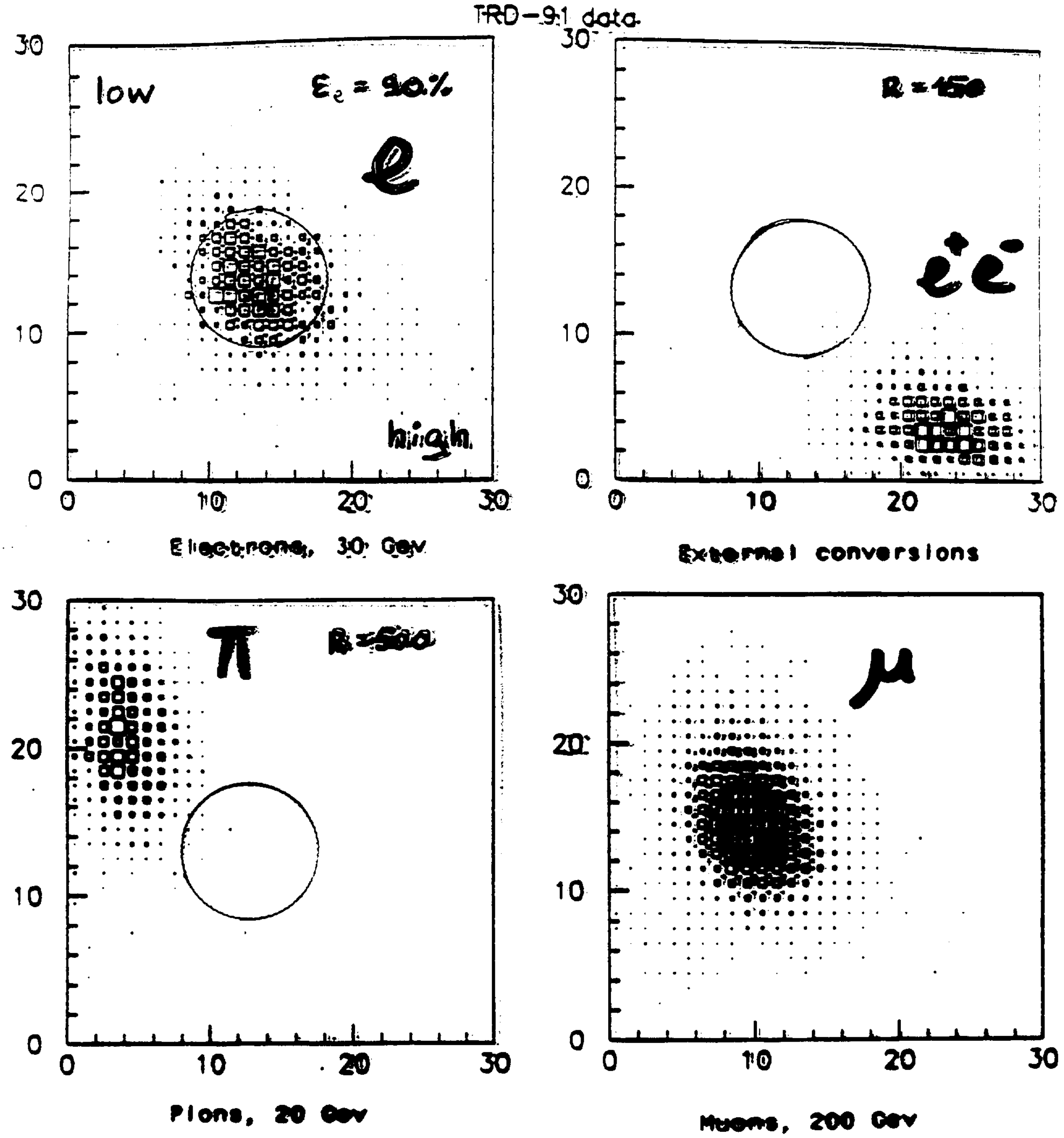

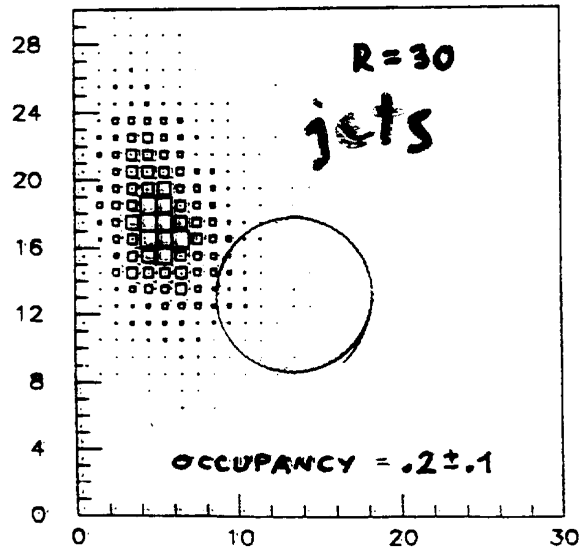

Low threshold hits
vs
high threshold hits

TARGET RUN

Pion rejection as a function of occupancy

20 GeV pions detection efficiency

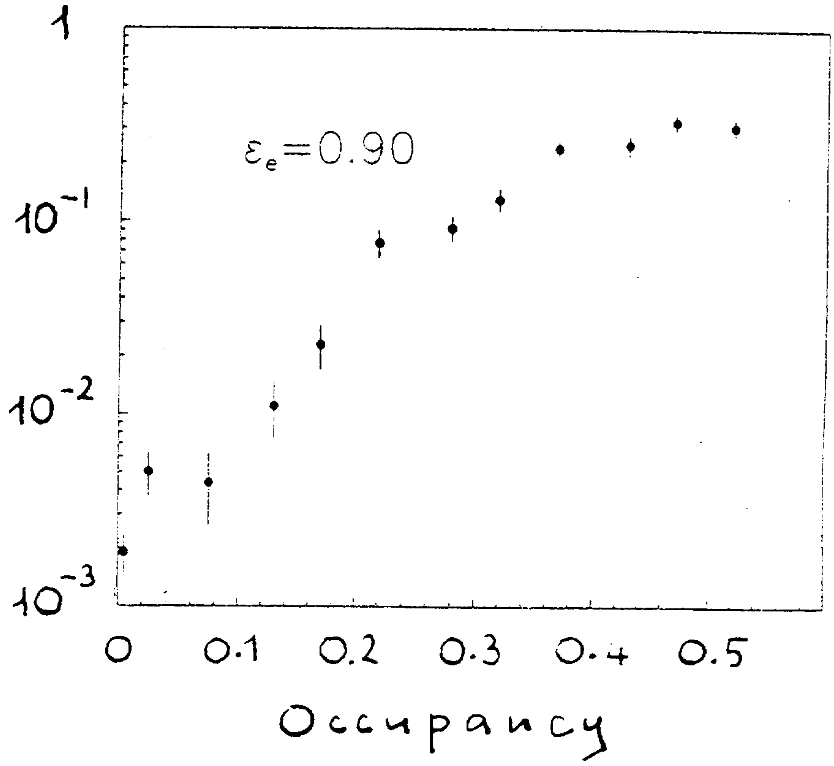

R = 20 for ε_e = 90% at the maximum LHC occupancy

TRD—event display

π^-(20 GeV/c)+ B=0.232 T

Without drift time

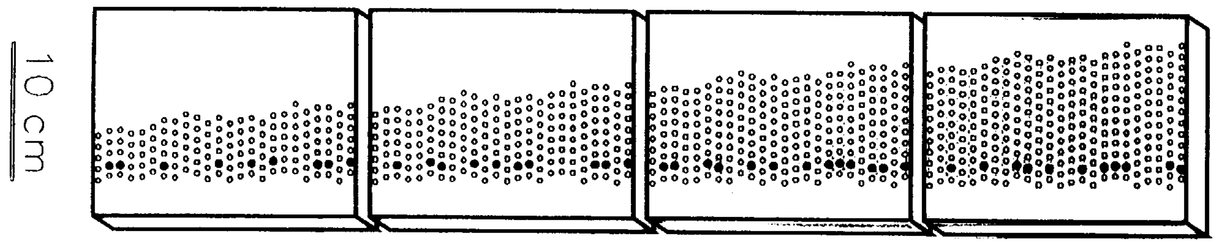

With drift time • – $2\sigma = 300\ \mu$

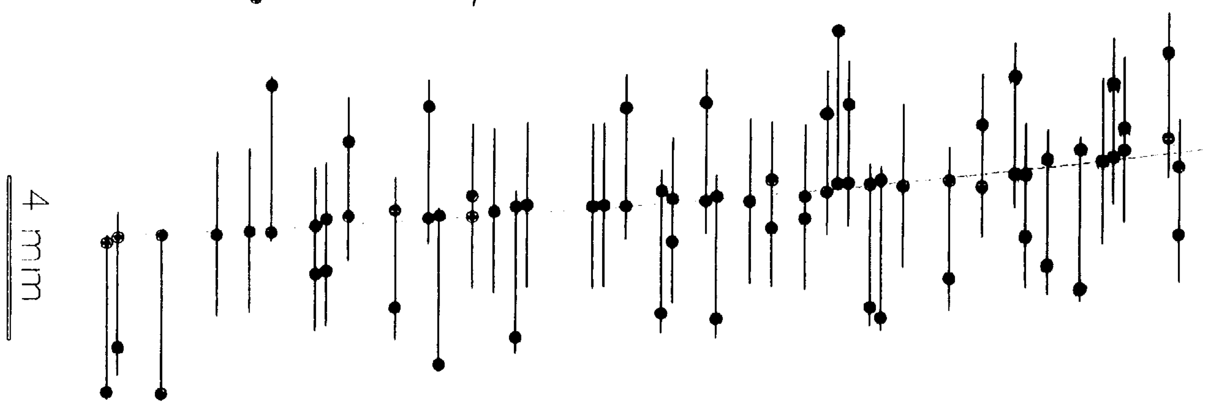

With drift time readout: $\sigma_x = 150 \mu m$

Test beam $\rightarrow \Delta p/p = 4.2 \times 10^{-3} P_T$ for BL = 0.3 T.m

TRD at LHC $\rightarrow \Delta p/p = 8 \times 10^{-4} P_T$ for BL = 2 T.m

Electron drift velocity in the straw tube vs electric field and distance from axis without and with 2T magnetic field

The force on drifting electrons:

$$\vec{F} = q_e \vec{E} + q_e \vec{v} \times \vec{B}$$

The Lorentz force improves the v_D vs E relation

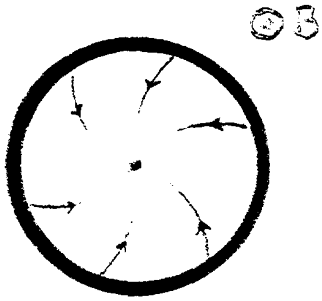

electron path

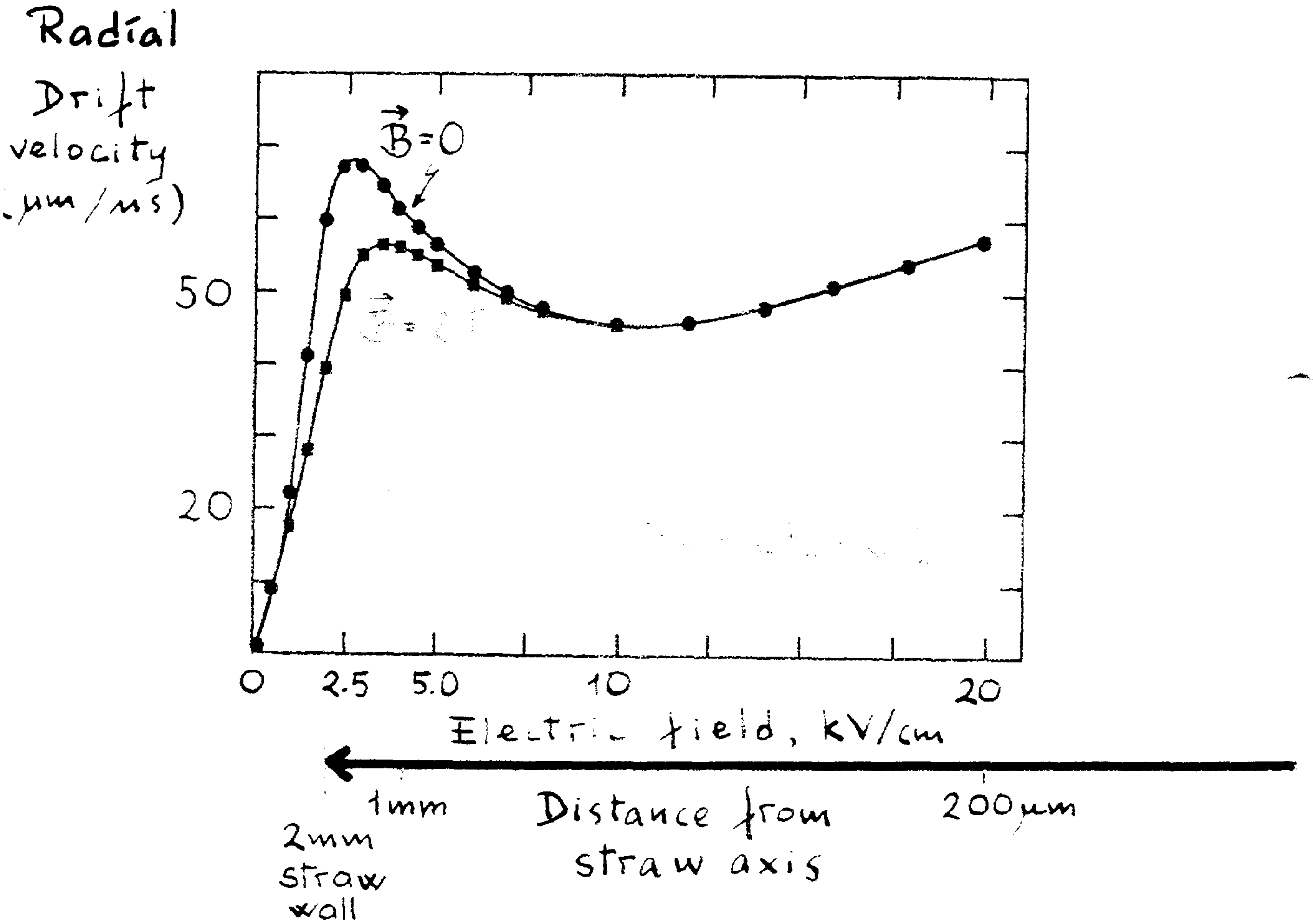

Drift time to distance relation

(the gas mixture is mainly optimized for Transition Radiation detection)

Driftime (ns)

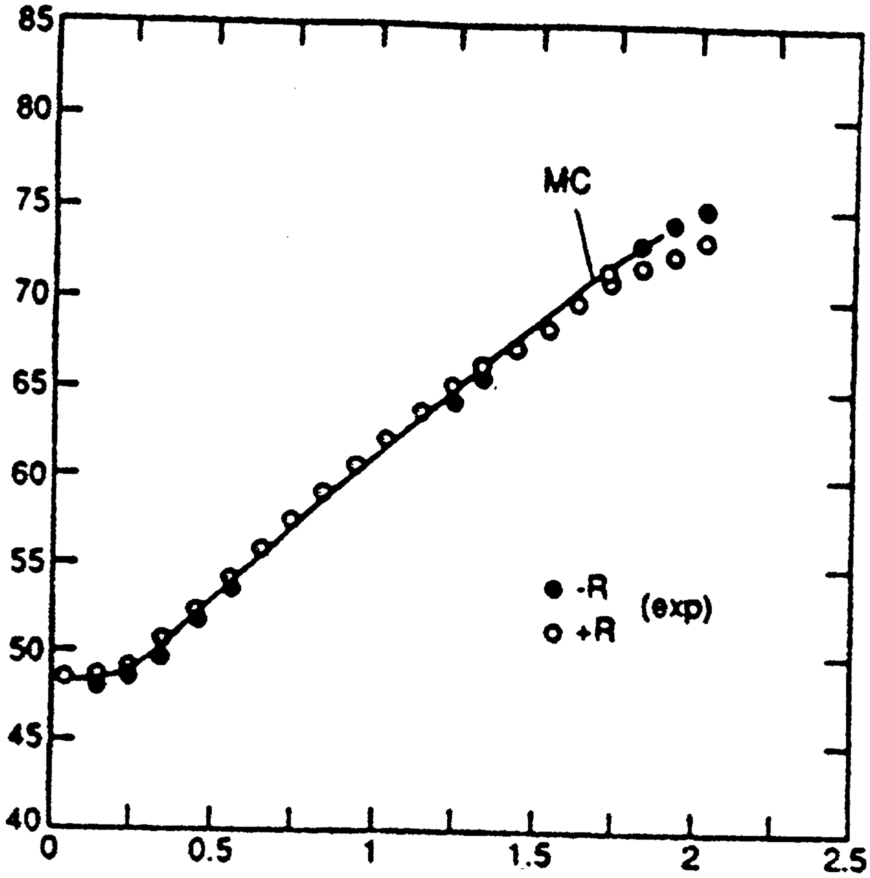

Distance from axis (mm)

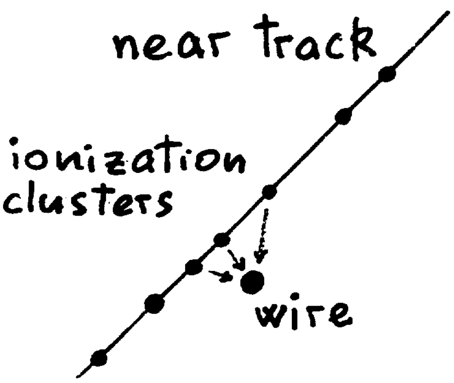

The measured time is that of arrival of the first cluster above threshold (0.2 keV)
→ non linearity at small distance of track from wire

At high rate the space charge of drifting ions affects the electric field distribution : E weaker near the wire

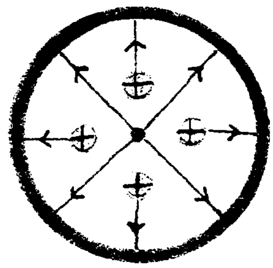

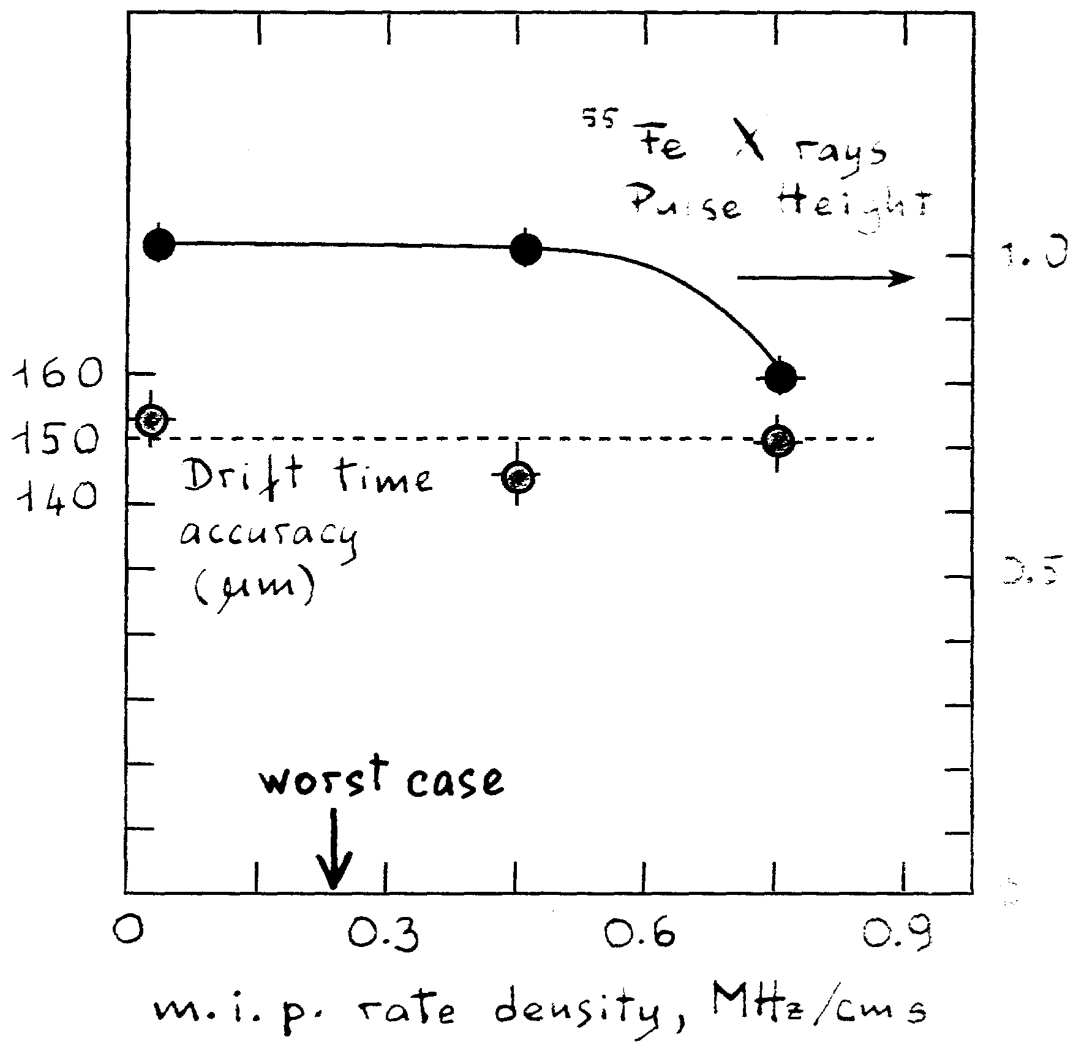

Predicted straw signal shapes after preamplifier and shaper for tail suppression
(10 ns shaping time)

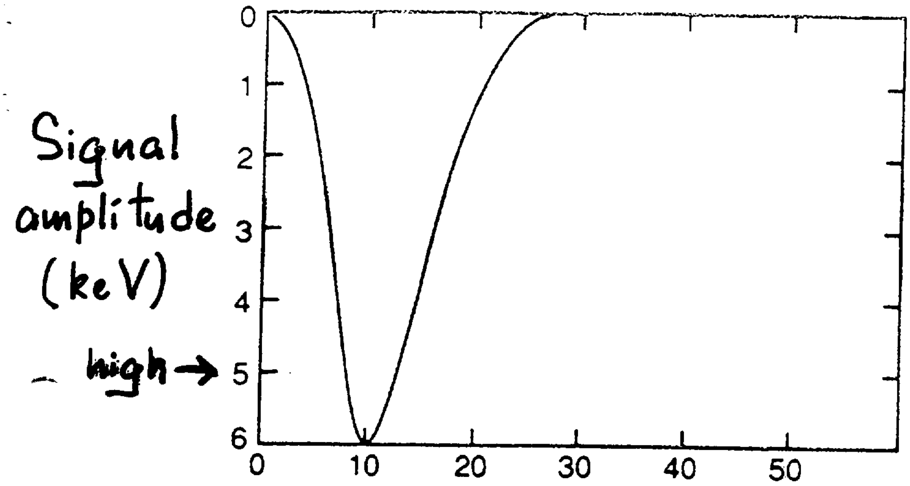

^{55}Fe X ray :
single cluster
$\sim 2 \cdot 10^2$ electrons

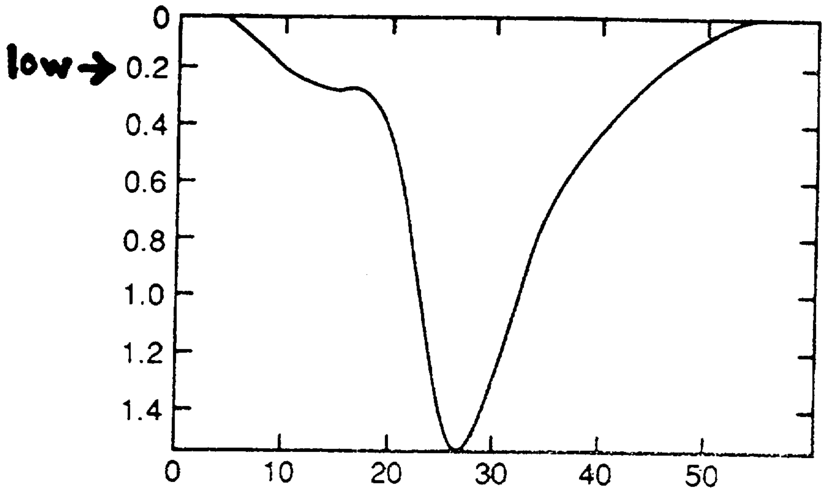

2 GeV pion
near the wire

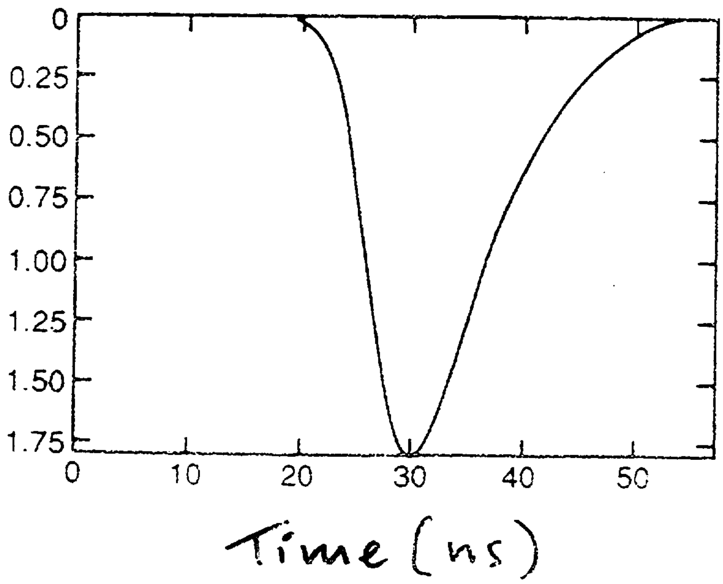

2 GeV pion
1 mm from wire

Charge collection
time $\gtrsim$ 25 ns
LHC bunch
crossing period

Single-straw drift-time accuracy and efficiency vs rate

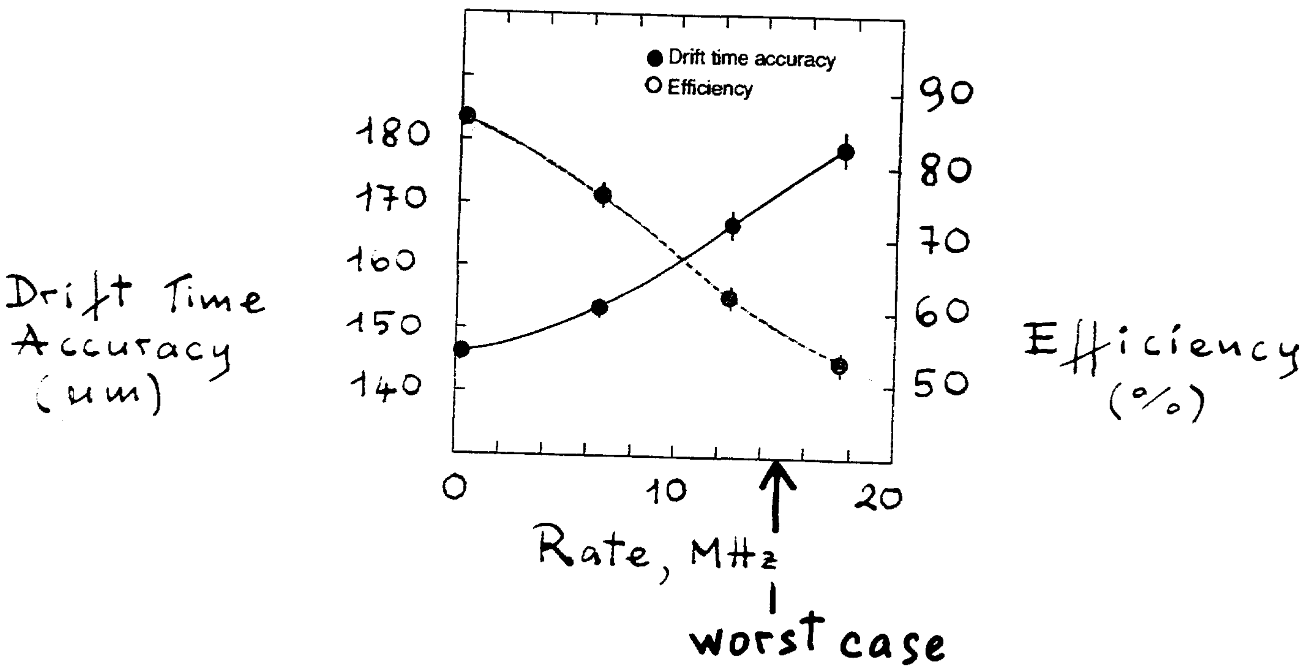

- Single straw power $= V_0 \langle i \rangle =$ Several mW's: cooling systems under study
- Gas aging: no effect observed for a total integrated charge of 5C/cm ~ 10 LHC years ($Xe + CF_4 + CO_2$, 70 + 20 + 10, at gain 10^4)

TRT end cap

Simulation at maximum luminosity
with test beam performance

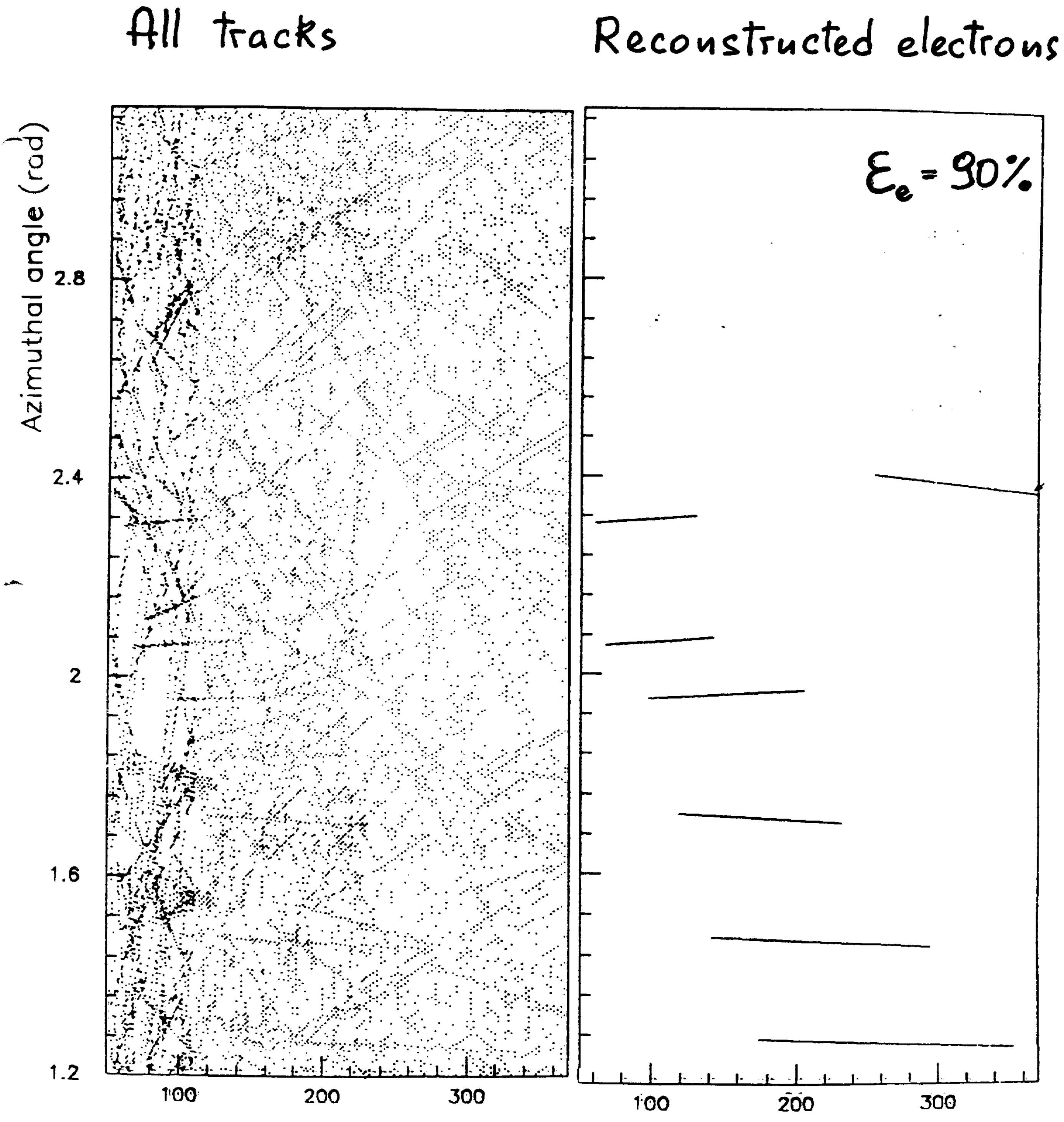

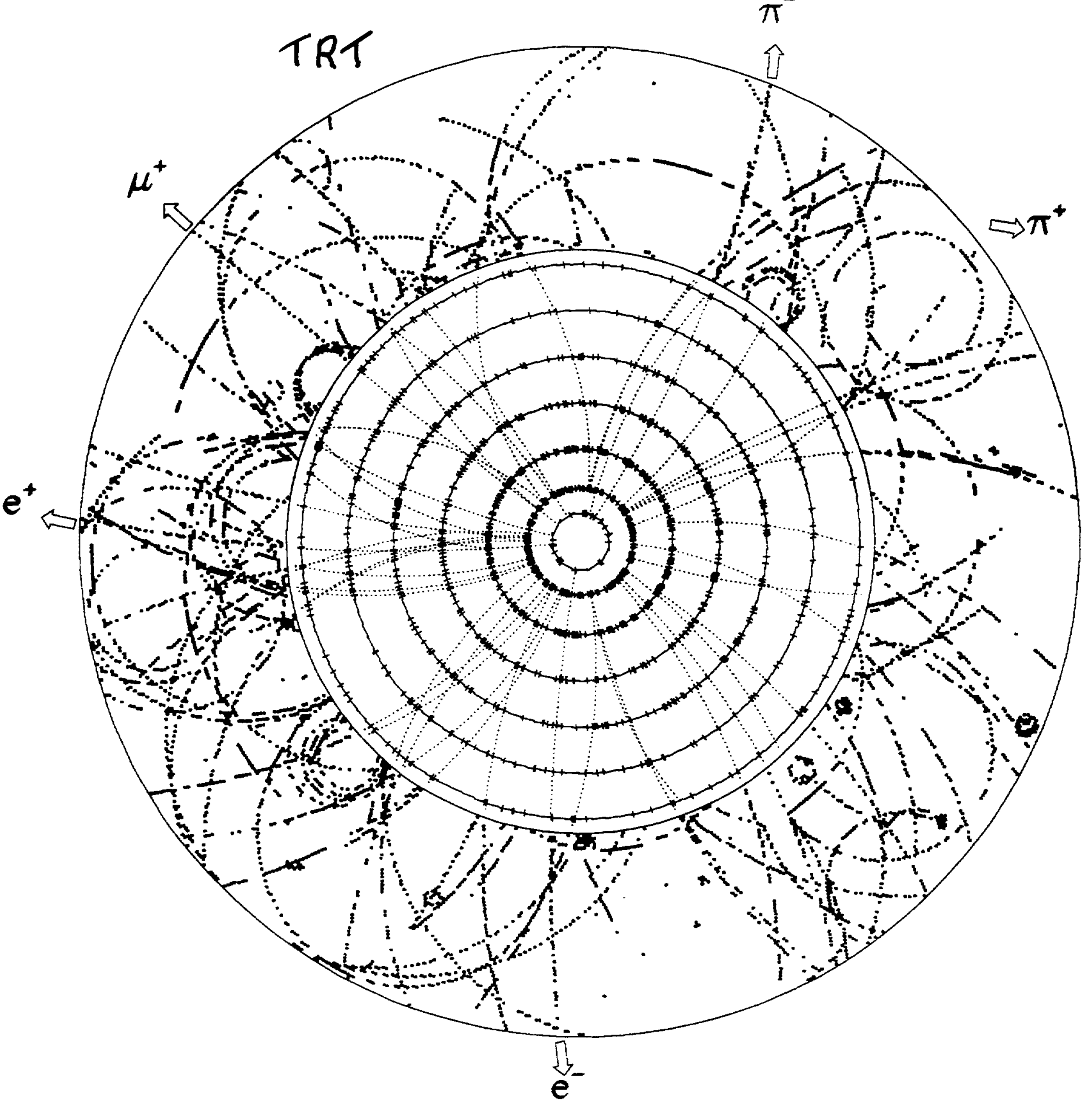

TRT
π^-
μ^+
π^+
e^+
e^-

The general features of μ detectors

- Precision chambers for momentum measurement
  - Barrel : lower rates and $\vec{B}$ fields
    $\rightarrow$ drift time method
  - End Cap: higher rates and $\vec{B}$ fields
    $\rightarrow$ induced charge centroid method

- Timing chambers for bunch crossing identification
  - Barrel : RPC
  - End Cap: RPC or Thin gap wire chambers

The challenging aspects

- few 10^5 wire/strips per system
- at high rates : $10 \div 10^3$ Hz/cm^2
- with accuracies $100 \div 200\ \mu m$
- in inhomogeneous $\vec{B}$ field (Lorentz angle)
- with non flammable gas mixtures
- with $\lesssim 100\ \mu m$ position monitoring over ~ 20 m lengths

ATLAS barrel Monitored Drift Tubes in the Air Toroid

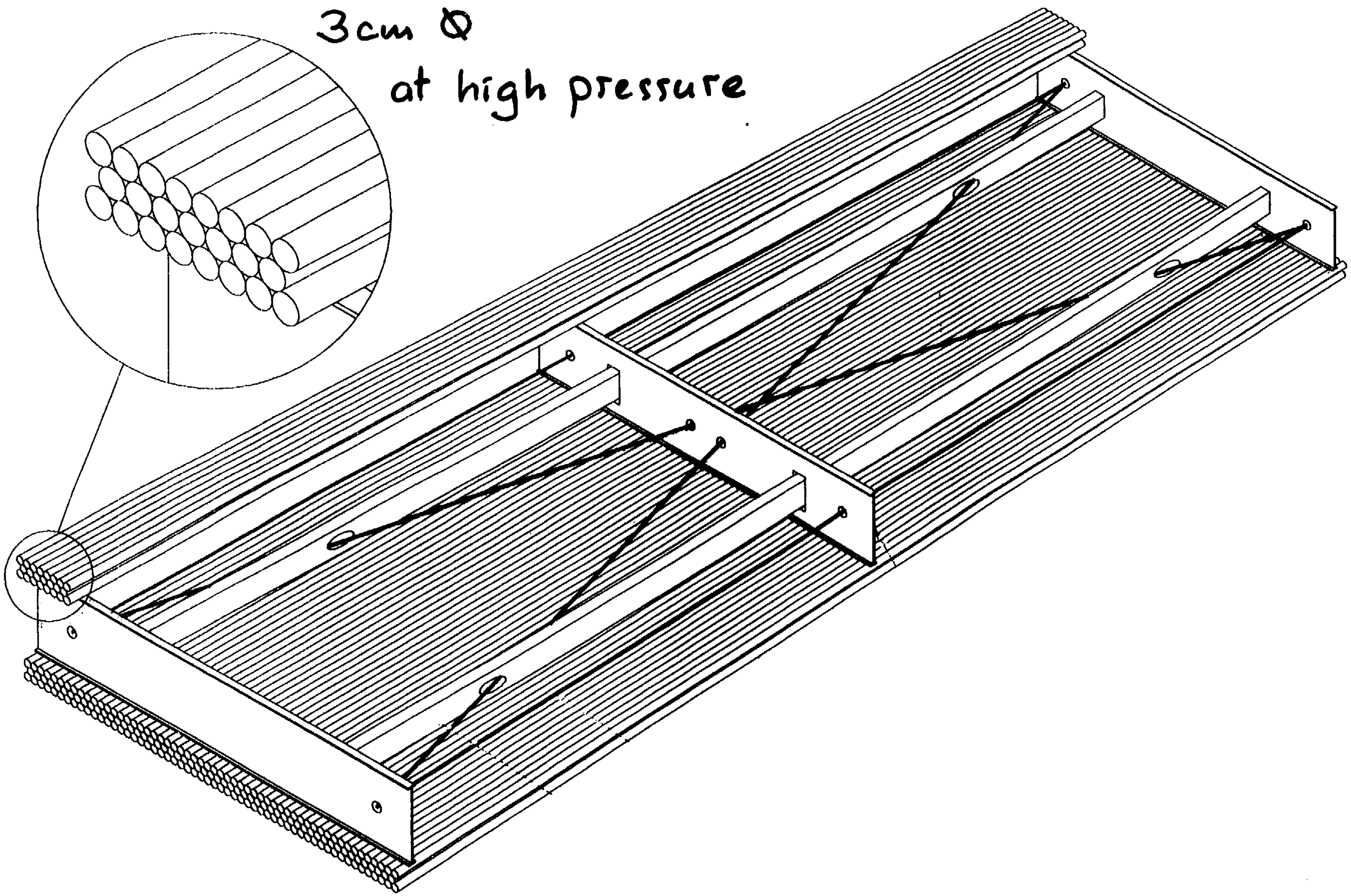

The role of pressure

- ionization $\propto p$

- the Lorentz angle decreases with p

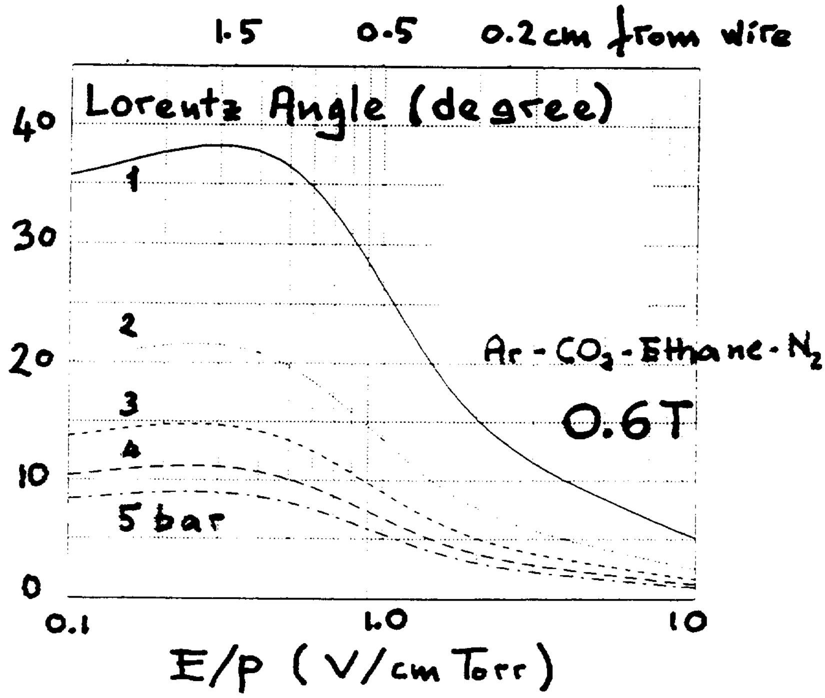

- diffusion decreases with p

  → single tube layer accuracy: $\sigma \sim 60 \mu m$

MDT preliminary performance (no $\vec{B}$)

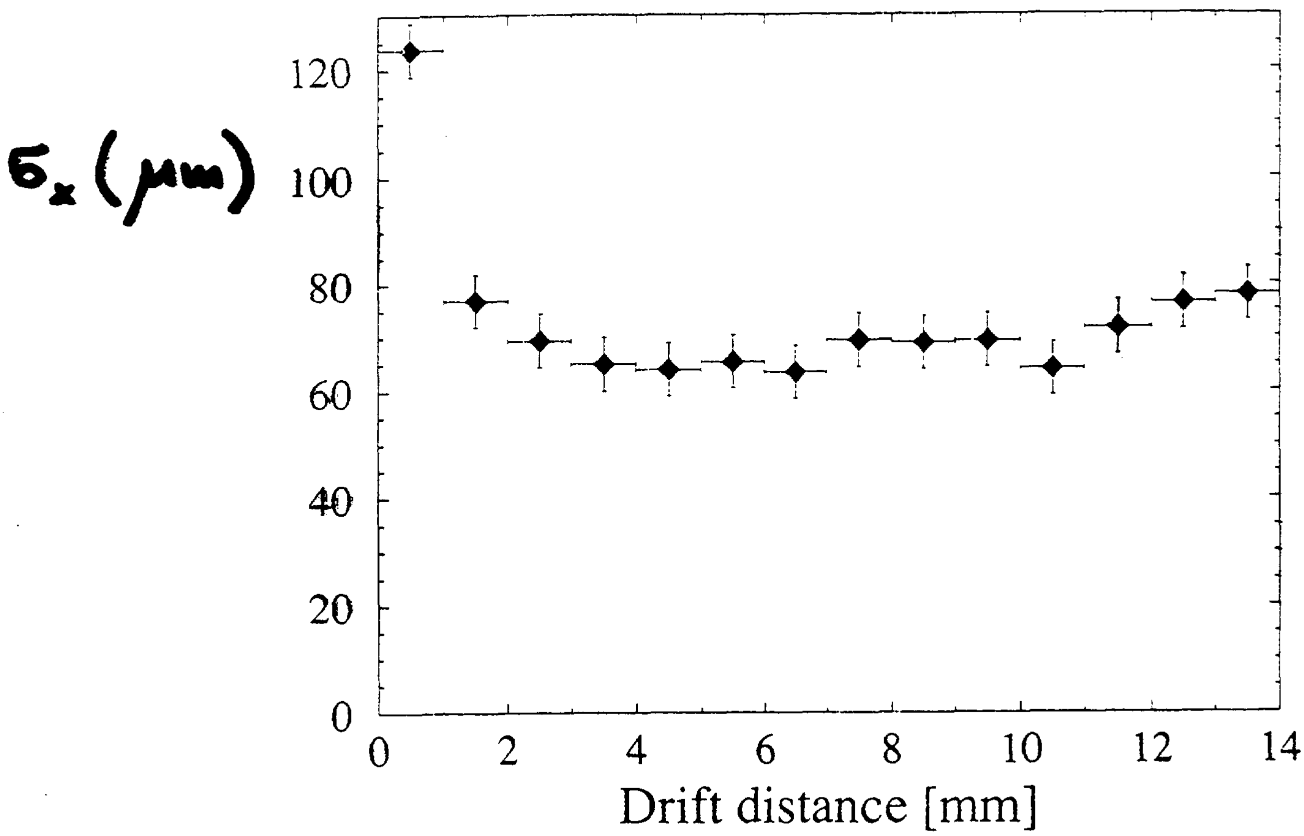

- 3 cm diameter, 50 μm wire
- Ar/N_2/Ethane = 90/5/5 at 3 bar
- HV = 3.1 kV
- Gain $\approx 10^5$
- Threshold $\approx$ 5 electrons

- Complexity : 1/r field, Lorentz, non flammable gas, pressure → many gas mixture needed
- Essential tool : simulation (MAGBOLTZ, GARFIELD) + testing : work just started

Very linear Space - Driftime - Relation

$Ar-CO_2$-Ethane-N_2

88-2-5-5

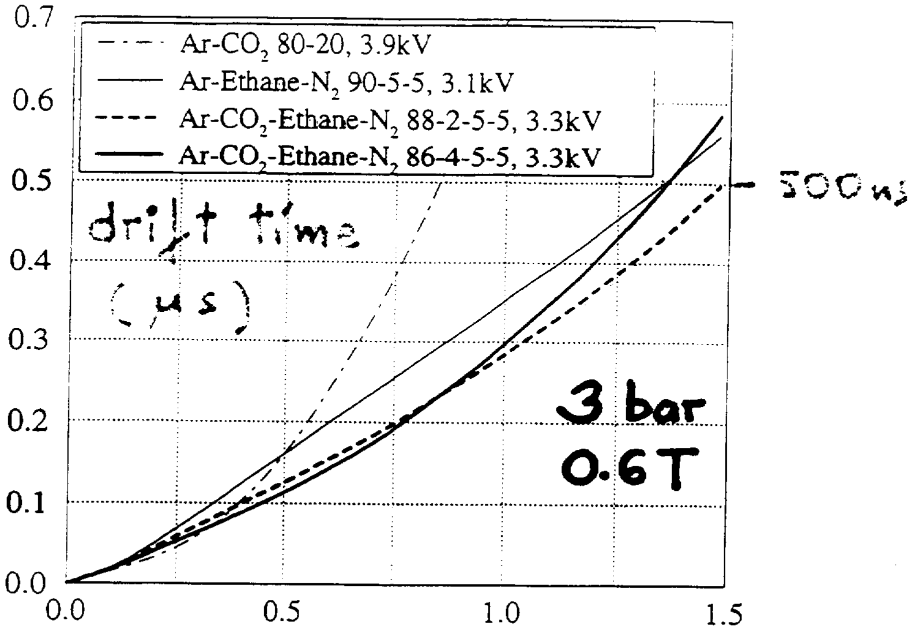

distance from wire (cm)

1.5 0.5 0.2 cm from wire

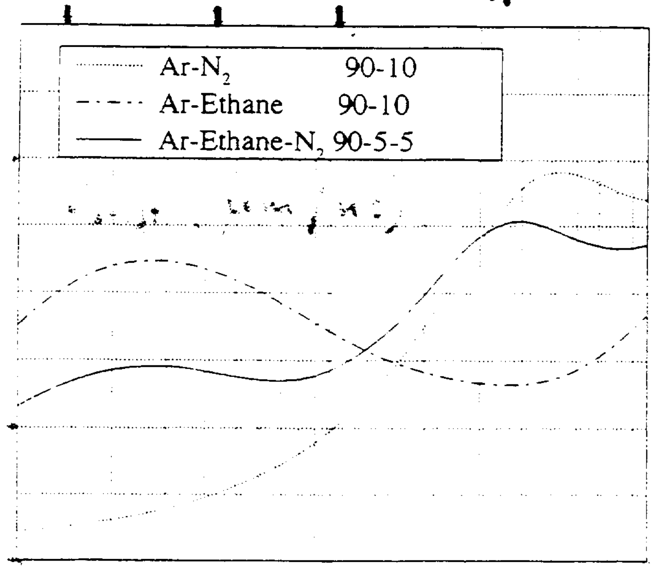

Lorentz Angle (degrees)

The influence of CO_2 at 3bar, 0.6T

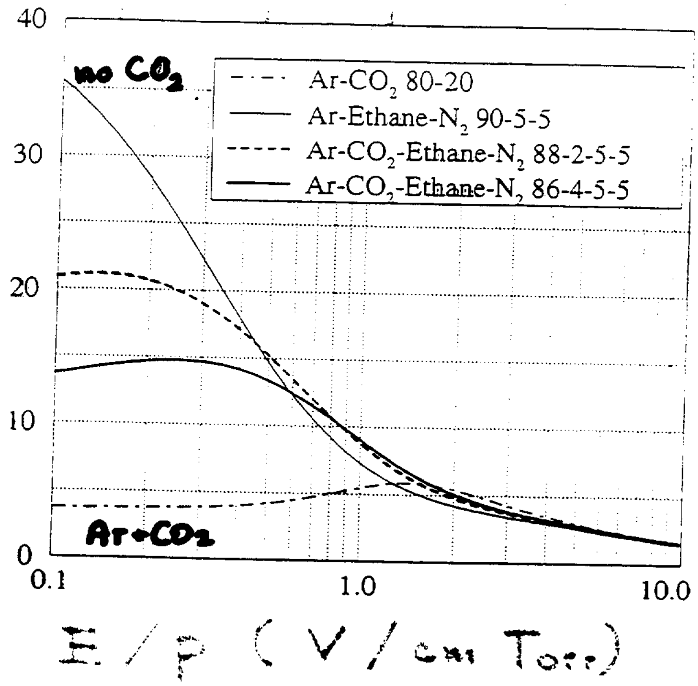

An example of comparison with experiment: Ar + Ethane + N_2 (90 + 5 + 5) at 3bar, 2.1kV, 0T

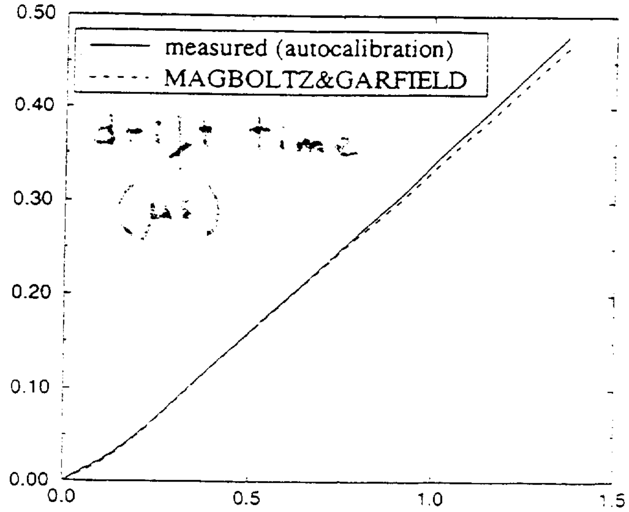

Goal: wire position monitoring ~
~ tube position accuracy

Concept:

- monitor position of rigid support
- wire ends in precise position with respect to the support
- rely on sag of wire and tube (no spacers)

sag (μm)

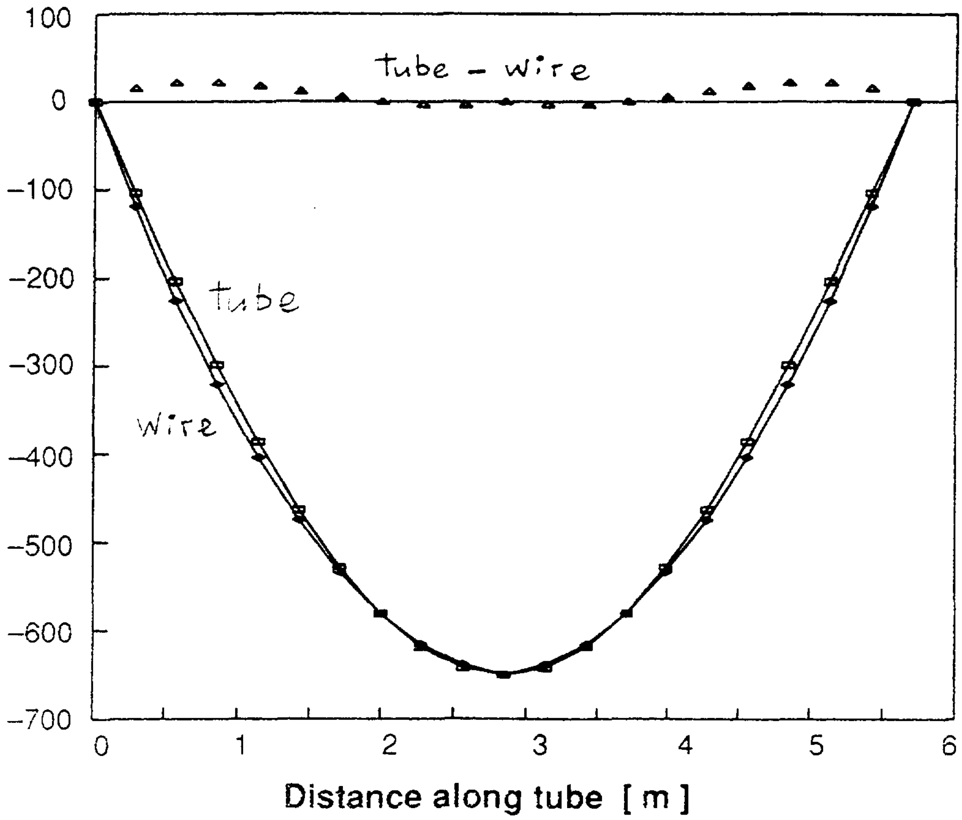

MDT : example of reconstruction of a single track

Inner chamber tube occupancy = 30% ~ 10 × present estimates

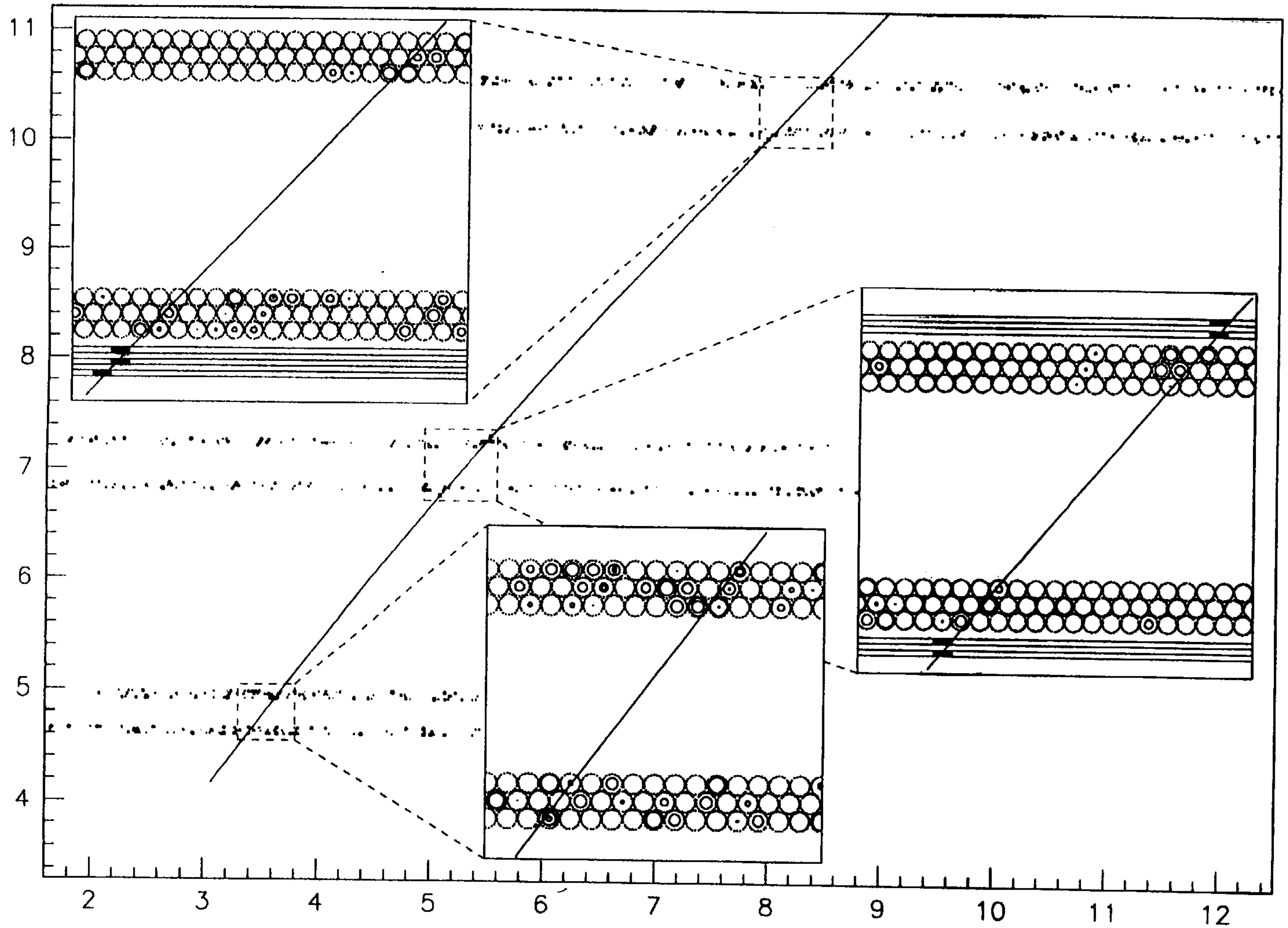

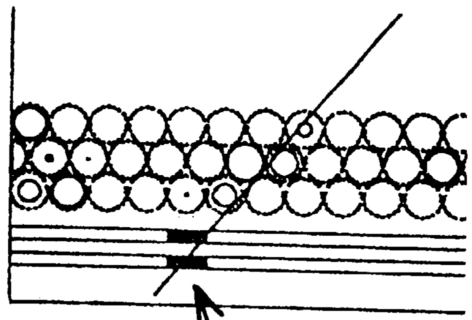

CMS Drift Tubes with meantiming
in the barrel iron return yoke

Precision goal:
200 μm

Drift
Cell

with 3 cathodes

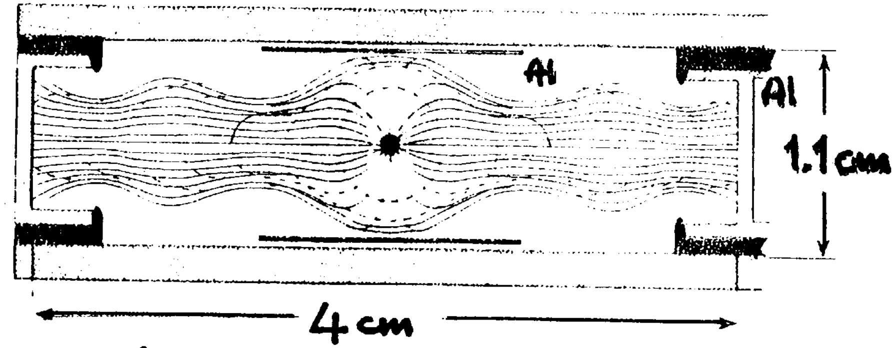

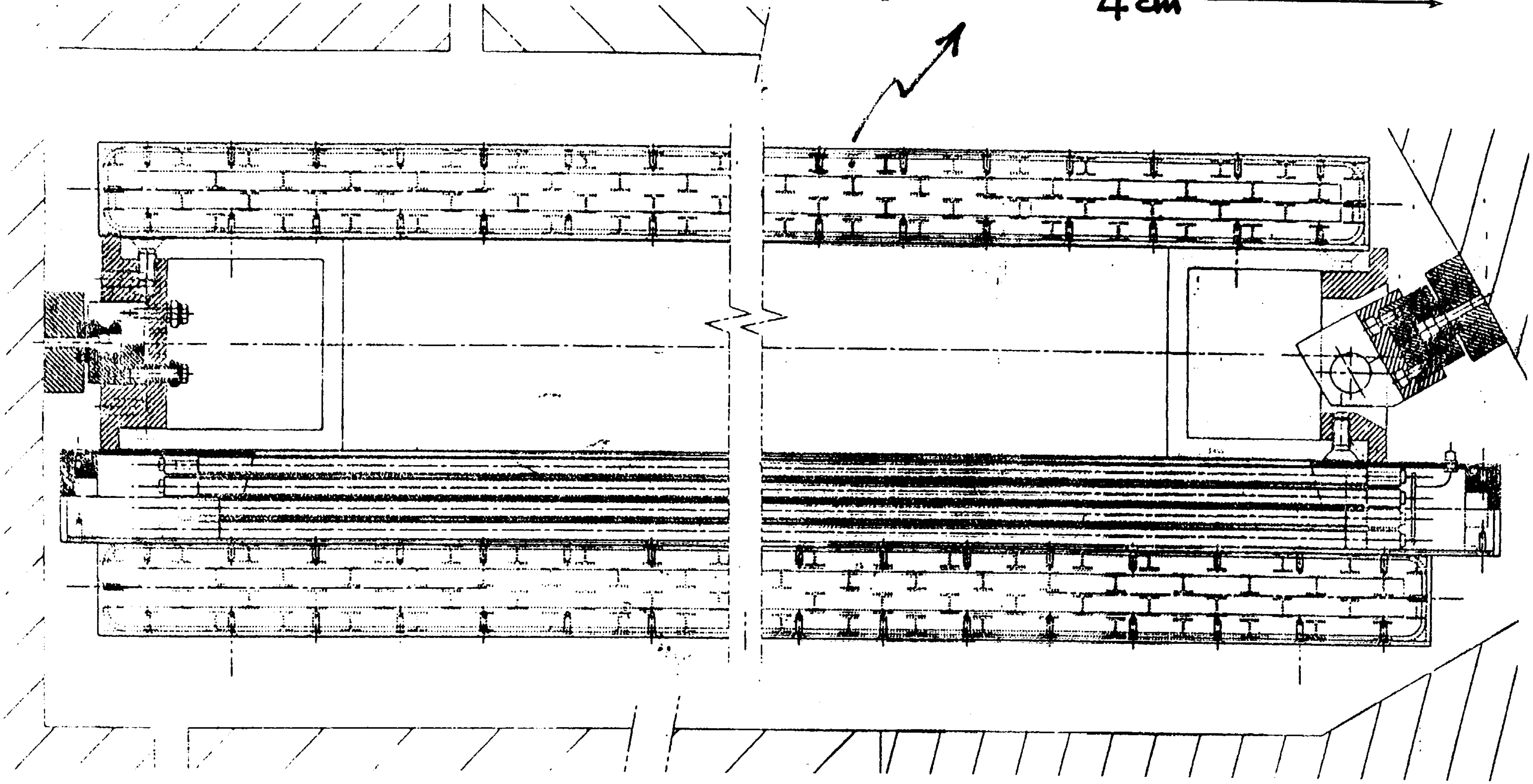

Meantimer concept

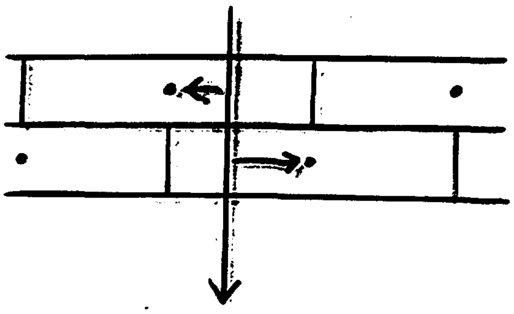

$T_1 + T_2 = \text{const}$

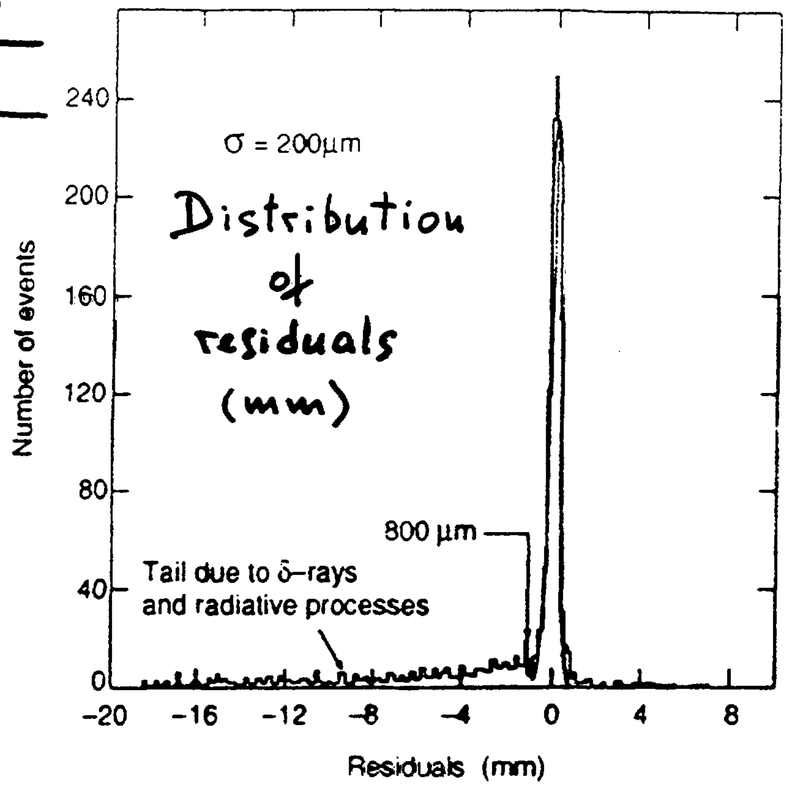

How the tail is generated

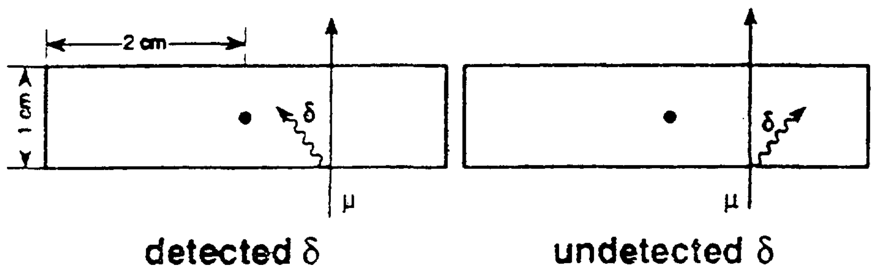

Majority coincidence to suppress the influence of the tail

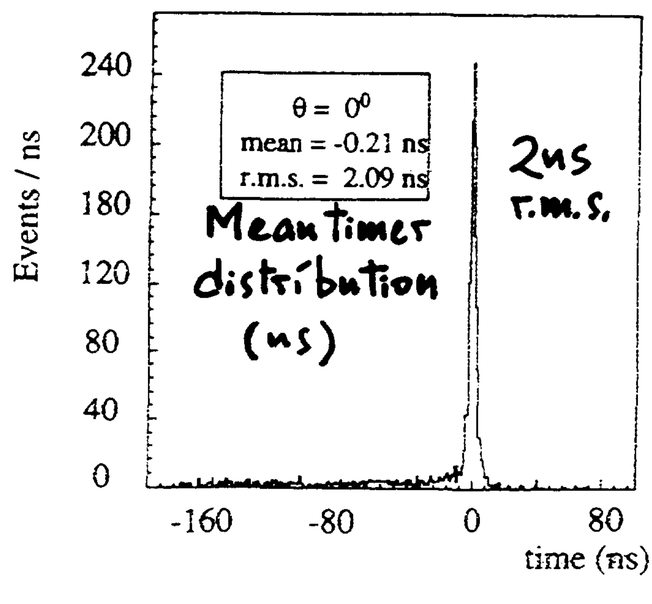

"Meantiming" with Shift Registers

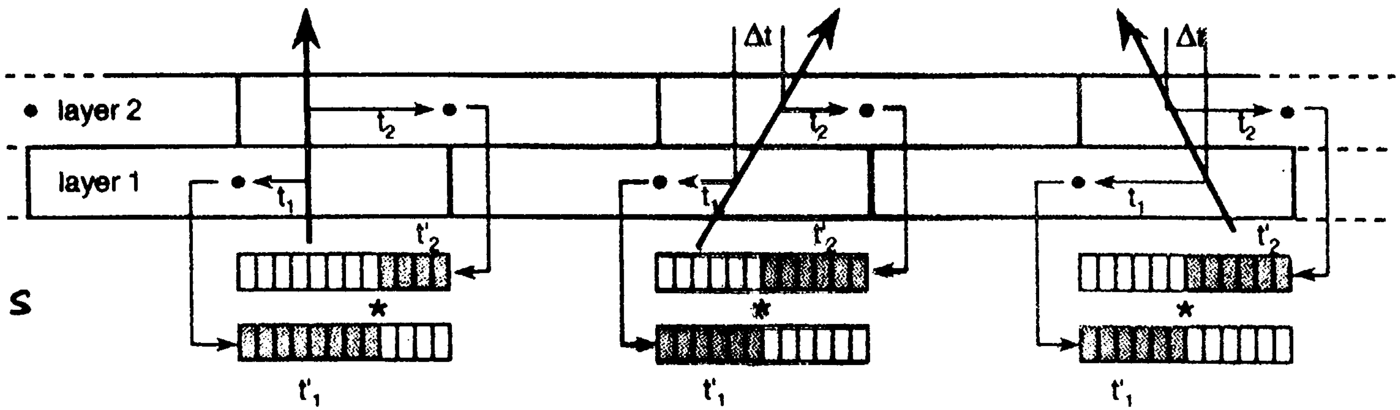

* they meet after $T_{drift\,max}$ * they meet at a different time

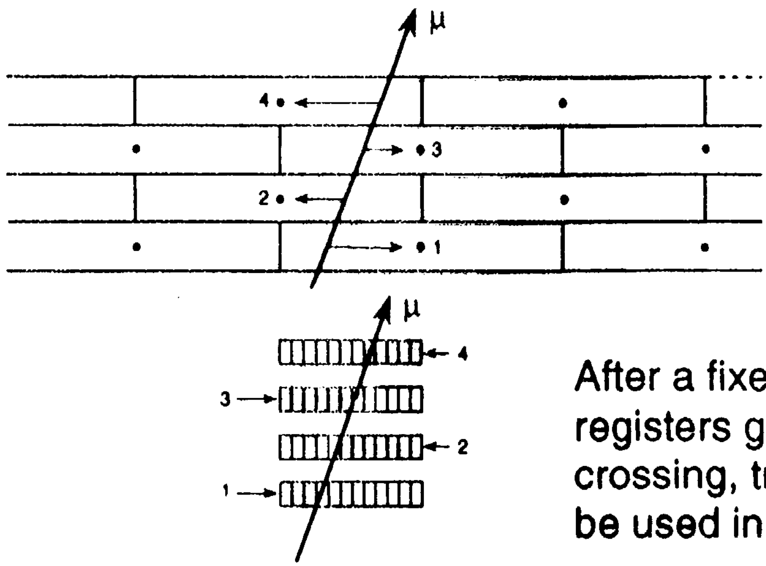

The Meantimer makes a majority coincidence every clock period of 25 ns of all possible slopes and requires 3 matching slopes.

After a fixed delay (= $T_{drift\ max}$) the shift registers give the corresponding bunch crossing, track position and angle to be used in muon trigger.

- **25ns clock → 1.2 mm accuracy**

The meantiming technique requires a linear drift time - position relation

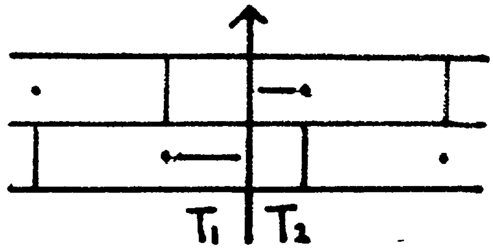

Simple 2-cathode tube

too low

$Ar + CO_2 = .82 + .18$ $Ar + CO_2 = .88 + .12$

T_1 vs T_2 (ns)

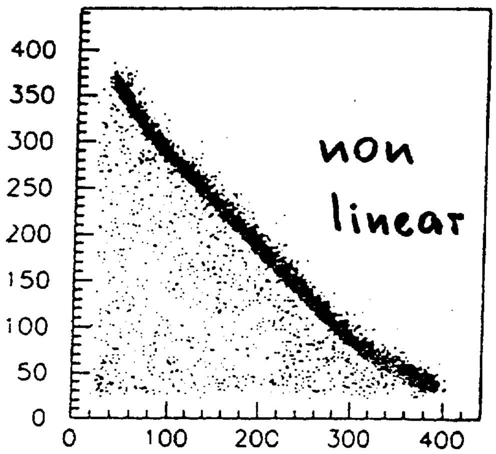

T1 VS T2

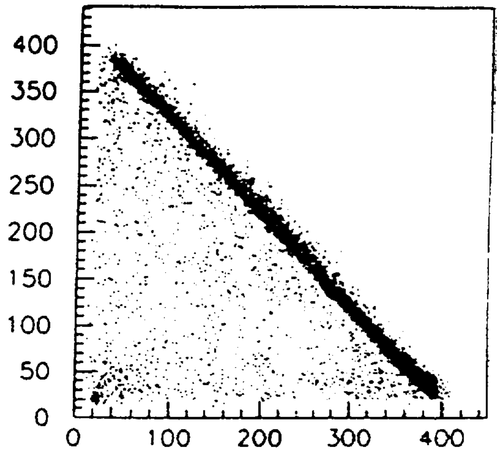

T1 VS T2

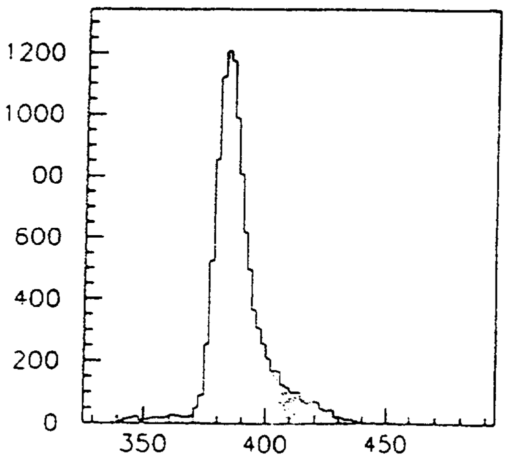

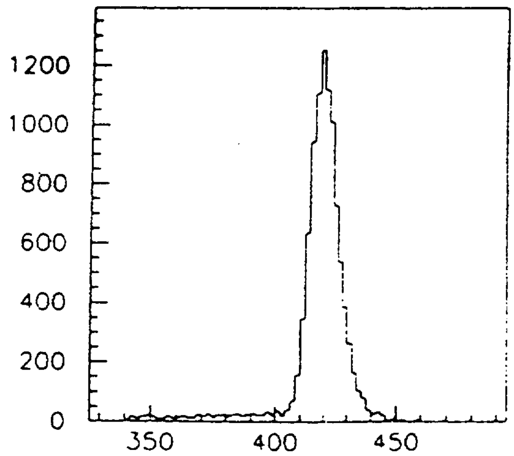

$T_1 + T_2$ (ns) $T_1 + T_2$ (ns)

The 3-cathode structure improves electric field uniformity and gives the desired linearity with the simple mixture: $Ar/CO_2 = 80/20$

Single layer accuracy : $\sigma = 150\,\mu m$

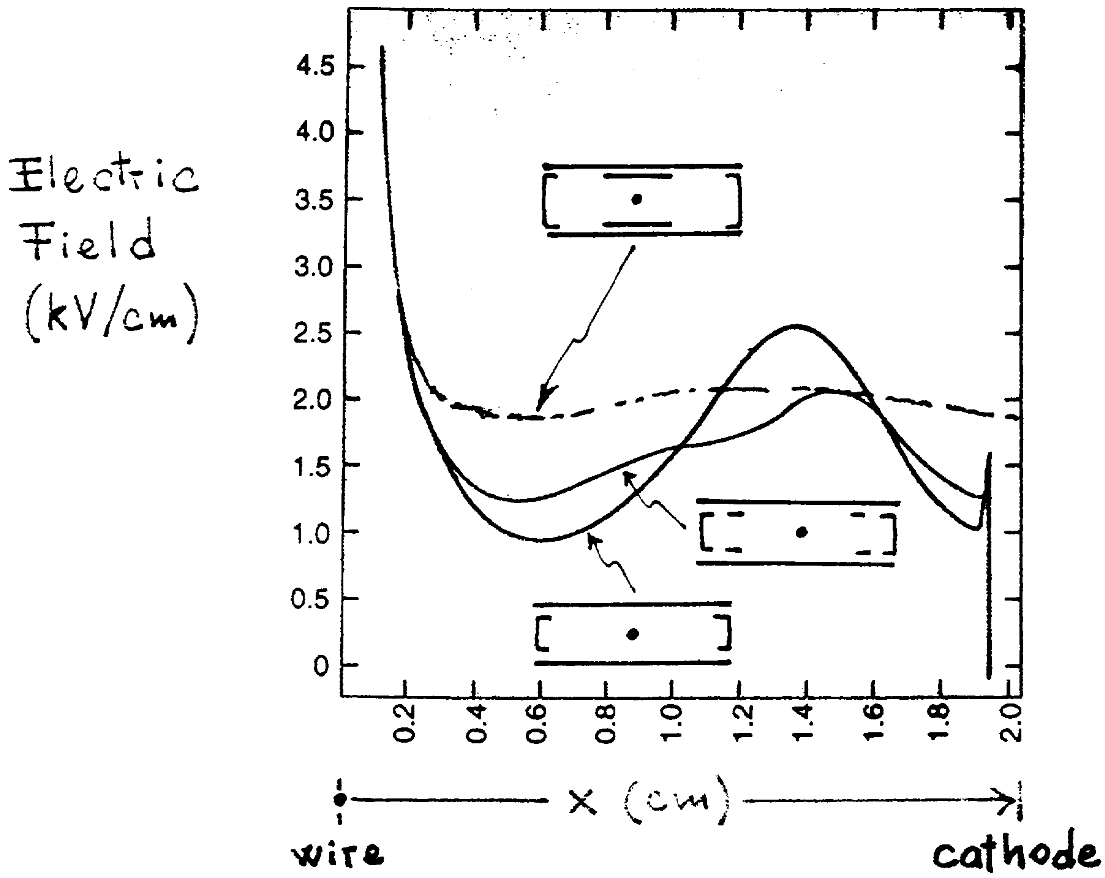

The Meantiming DT's also tolerate the influence of $\vec{B}$ field which is estimated not to exceed 0.6 T

+2.0 kV
central electrode

-1.6 kV
side cathode
(I beam)

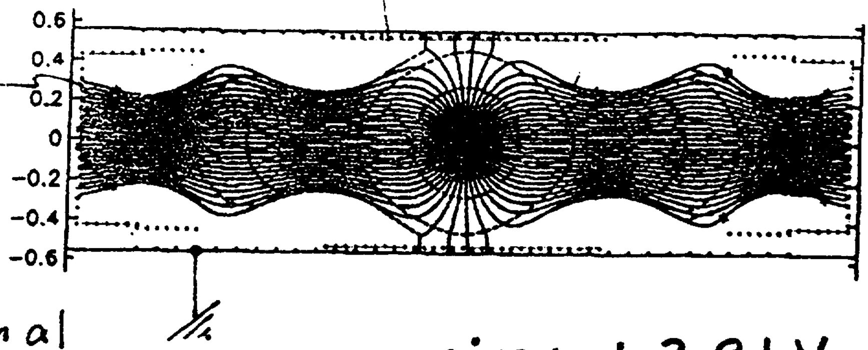

no $\vec{B}$

external
aluminum foils

wire : + 3.9 kV
(50μm stainless steel)

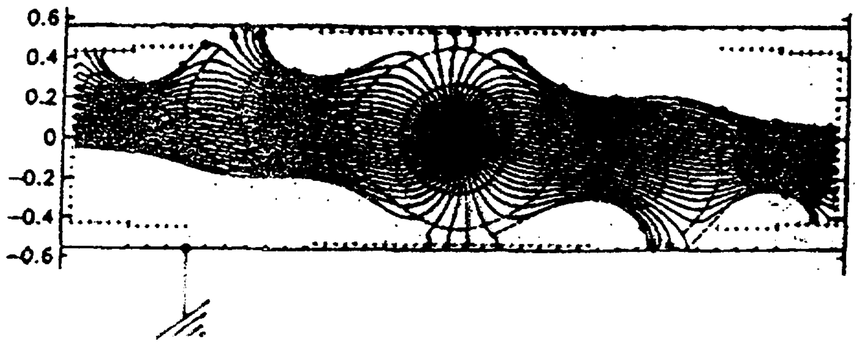

0.6T
⊙

* linearity is maintained

End Cap muon detectors

High rate (10^3 Hz/cm^2) and intense $\vec{B}$ (≤ 3 T)
$\rightarrow$ CSCs for both ATLAS and CMS

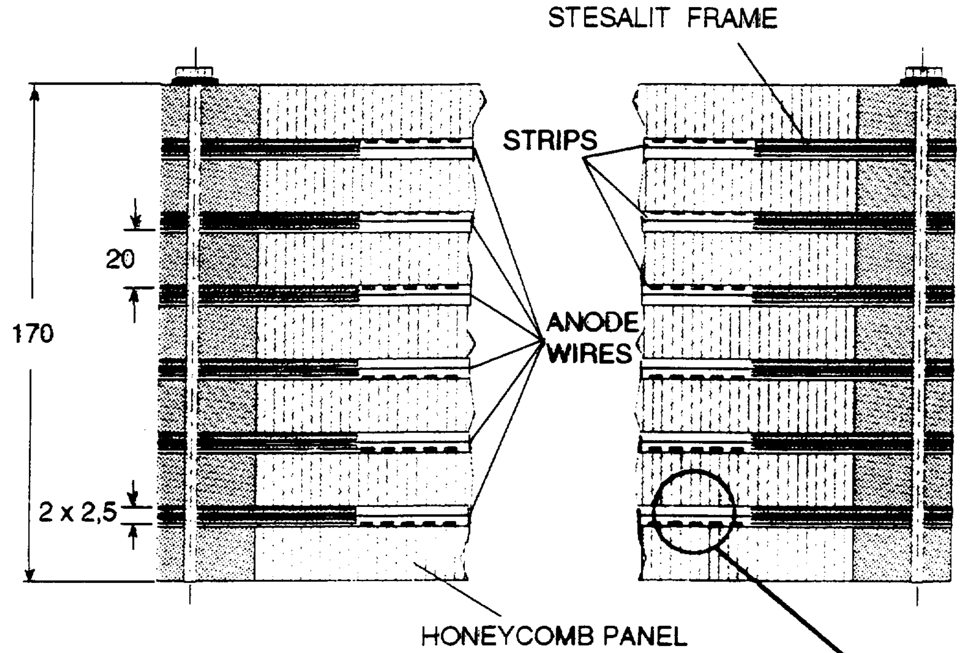

CMS design for one station

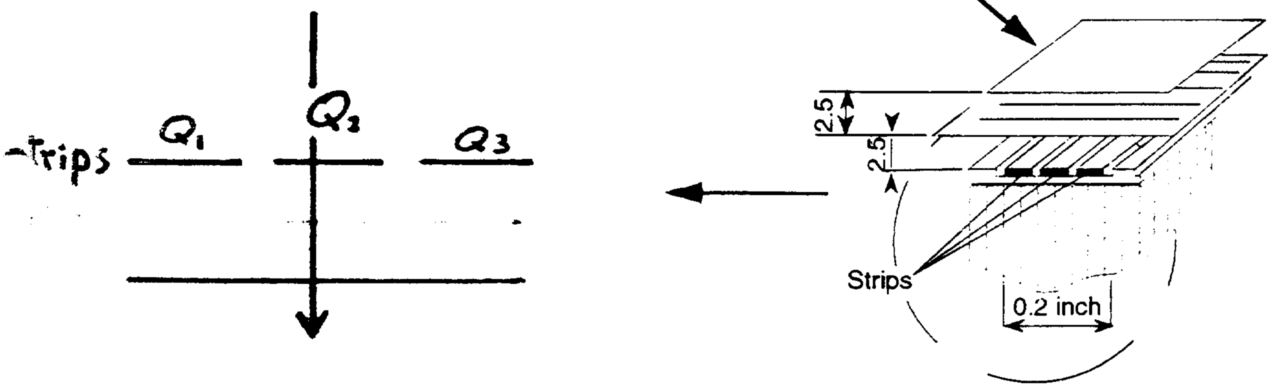

Geometry optimized
for charge centroid method:

- wire pitch 2.5mm
- wire-cathode gap "
- strip pitch 5mm

$$\sigma_x \sim \sqrt{2} \cdot \text{strip width} \cdot \frac{\Delta Q}{Q_{tot}}$$

The Lorentz force due to axial $\vec{B}$ perpendicular to wire plane: the effect and its compensation

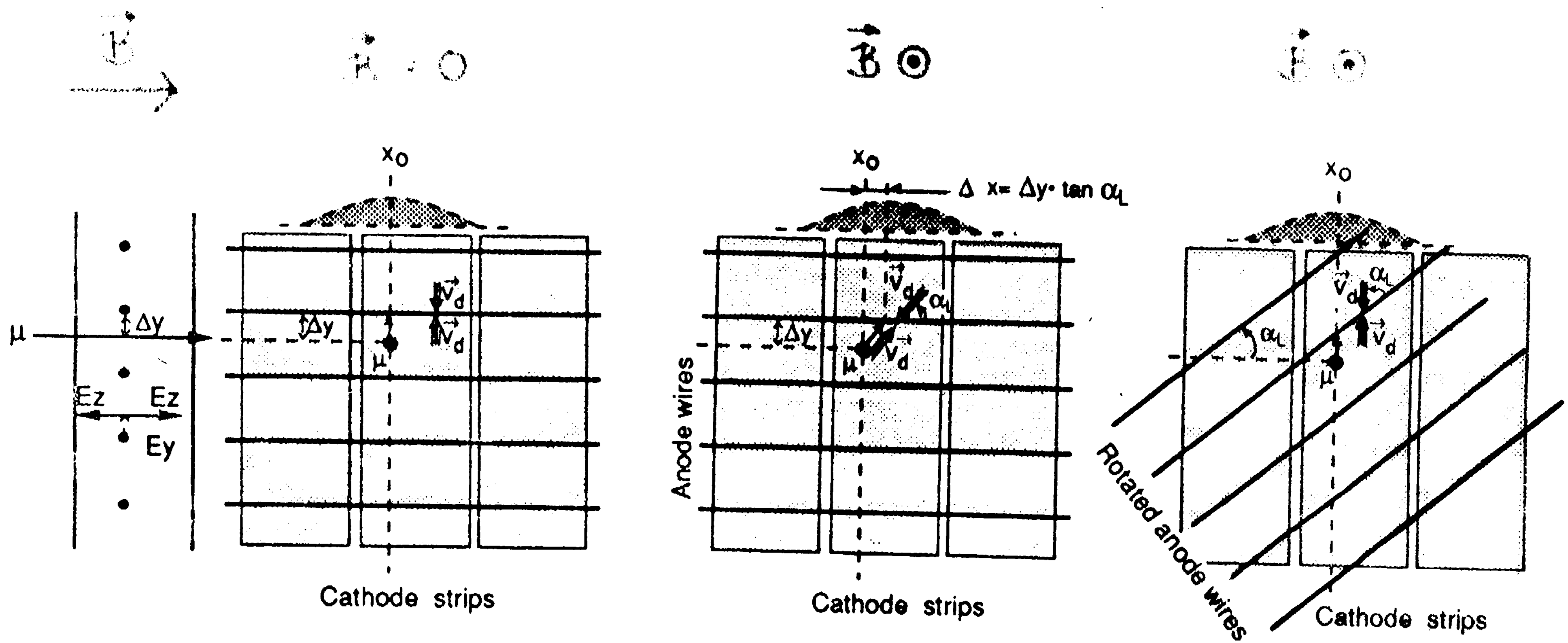

- Problem:
  $\vec{v}_D$ is not parallel to the strips
  $\rightarrow \Delta x = \Delta y \cdot tg\, \alpha_L$
- Compensation:
  $\vec{v}_D$ is parallel to the strips

The effect of Lorentz force due to $\vec{B}$ // strips:
loss of resolution similar to that due to angle of incidence

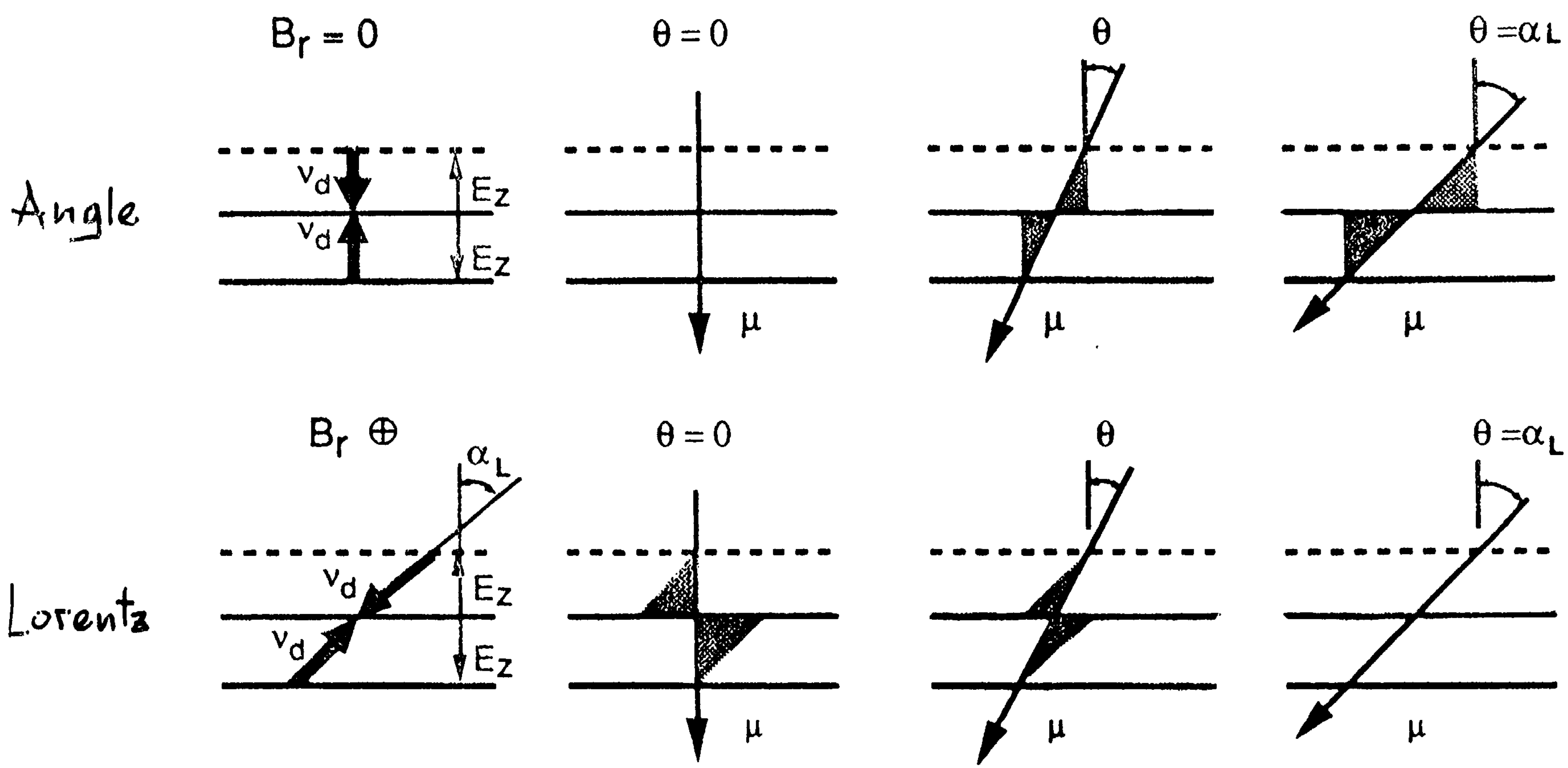

• loss of resolution due to non uniformity of ionization

Compensation (by chamber rotation) not possible.
However this component of $\vec{B}$ is small.

Measurement of Lorentz angle:

with $\vec{B}$ // strips α_L = angle of minimum σ_x

Resolution σ (μm)

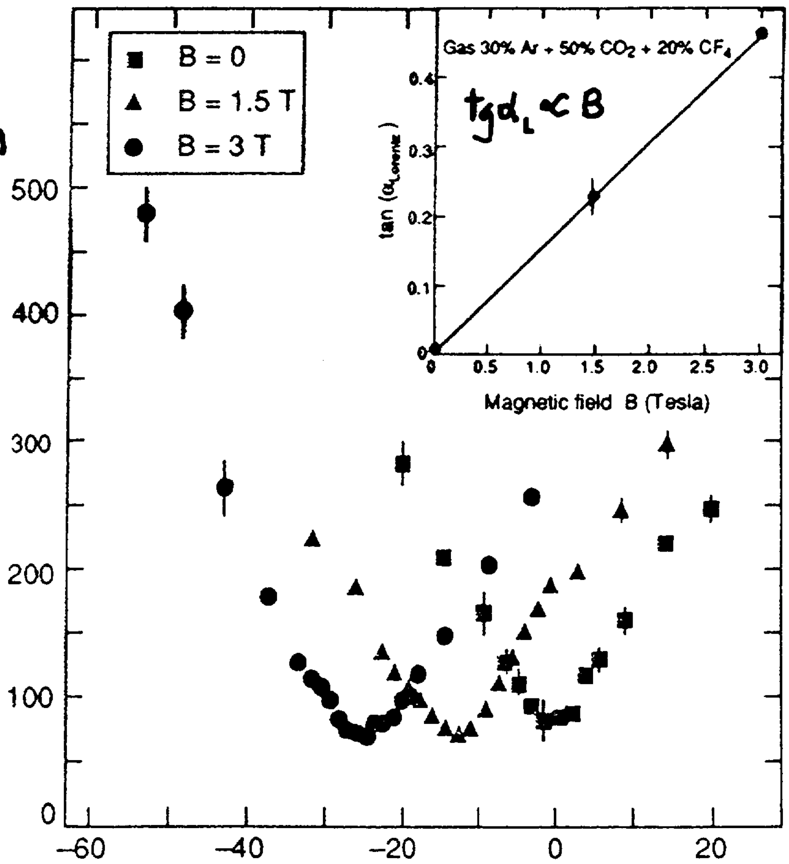

Angle of incidence (degree)

Gas: $Ar + CO_2 + CF_4$ = 30 + 50 + 20

optimized for high drift velocity and small Lorentz angle

σ_t ~ few ms per station

- Strips ↑ ↑ ↑ are radial

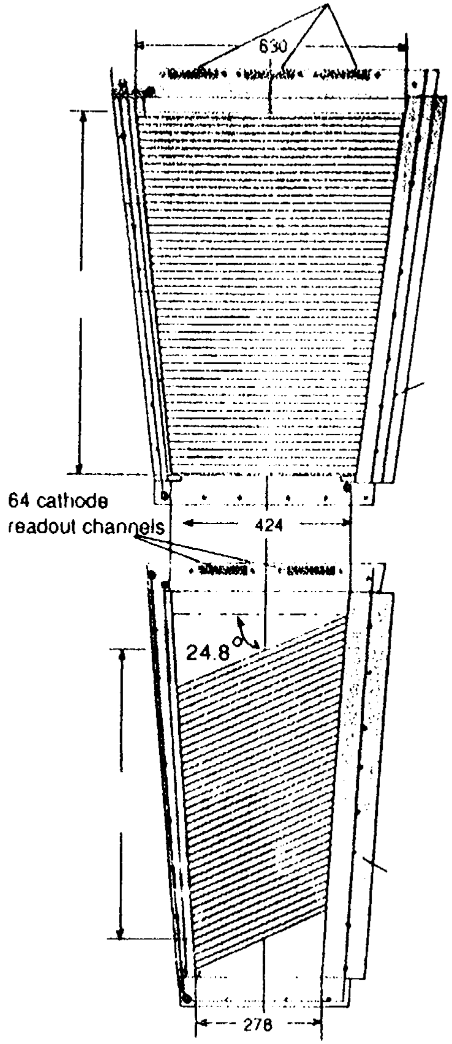

Sketch of a full size prototype of an MF1 sector.
All dimensions are in mm

- $\vec{B} = 0 \rightarrow \sigma = 50\mu m$

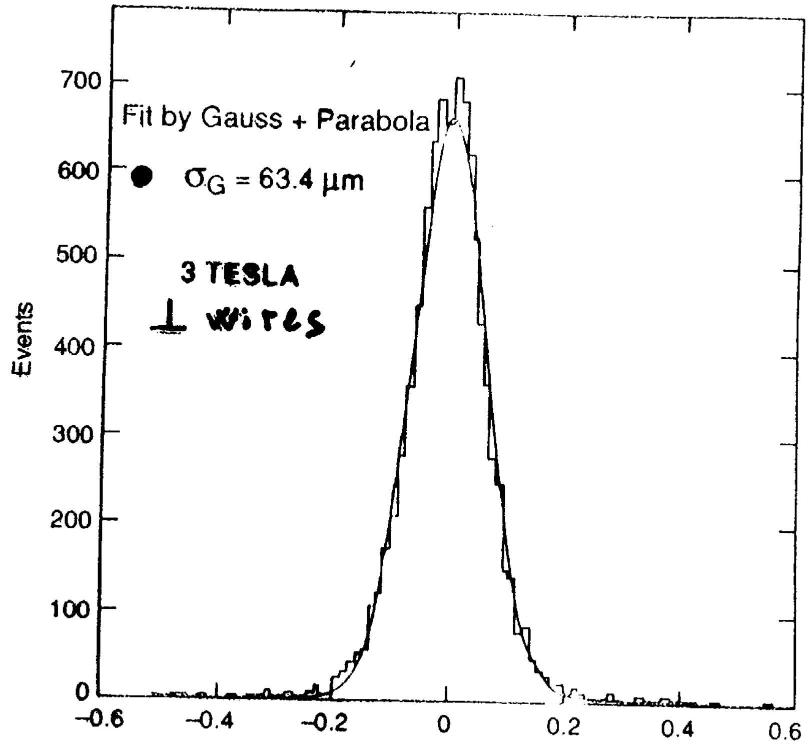

An average spatial resolution over the full sensitive CSC area with cosmic ray and Endcap configuration of 3 Tesla magnetic field

RESISTIVE PLATE CHAMBERS

The muon trigger chambers for CMS everywhere and ATLAS in the barrel

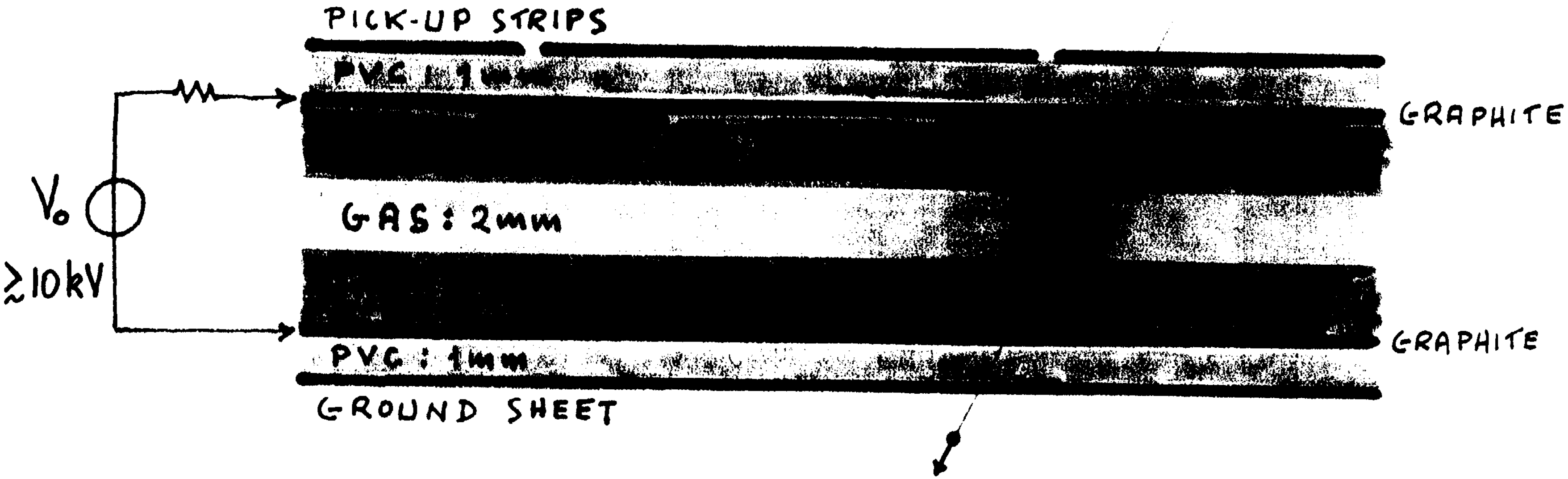

Gas : Ar + quencher + freon

Mode: streamer/avalanche confined by voltage drop and U.V. absorption

Accuracies : $\sigma_t \sim 1$ns → bunch crossing identification
($\sigma_x \sim 0.5$mm by pulse height interpolation on strips)

Double gap RPC with single strip layer in between to read both gaps

→ ~100% efficiency

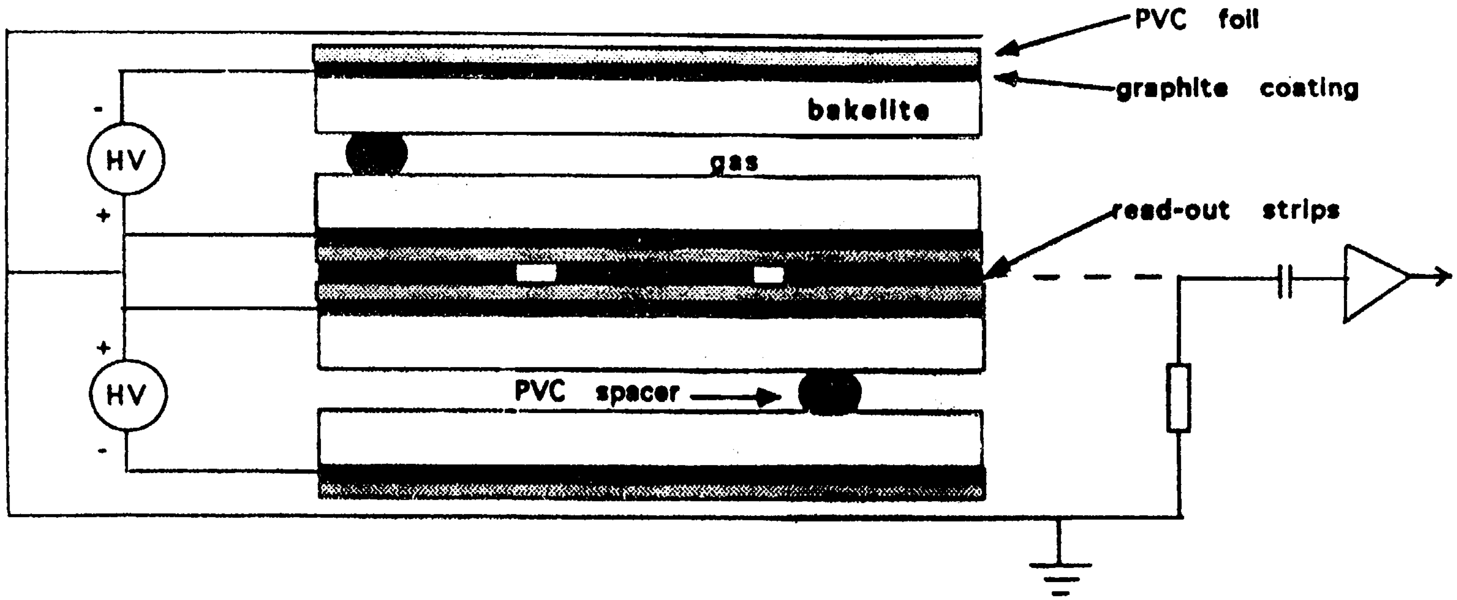

The rate capability of RPCs has been improved by using Ar + freon = 20 + 80 which reduces pulse height and therefore recovery time

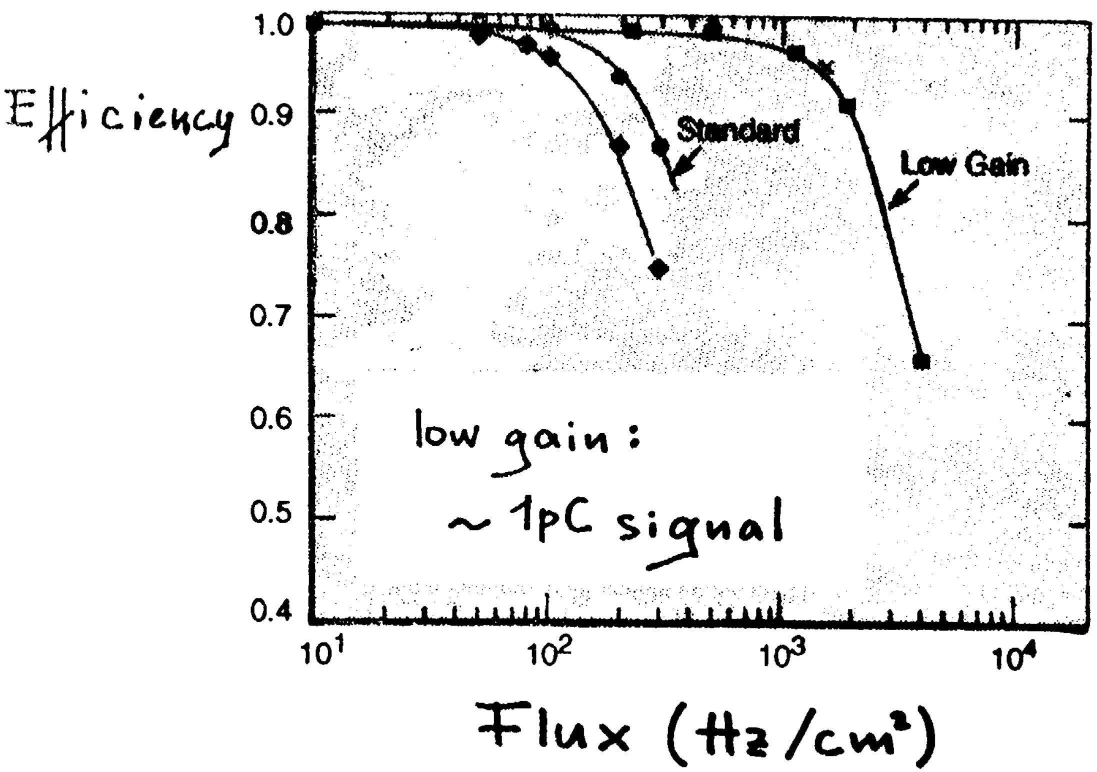

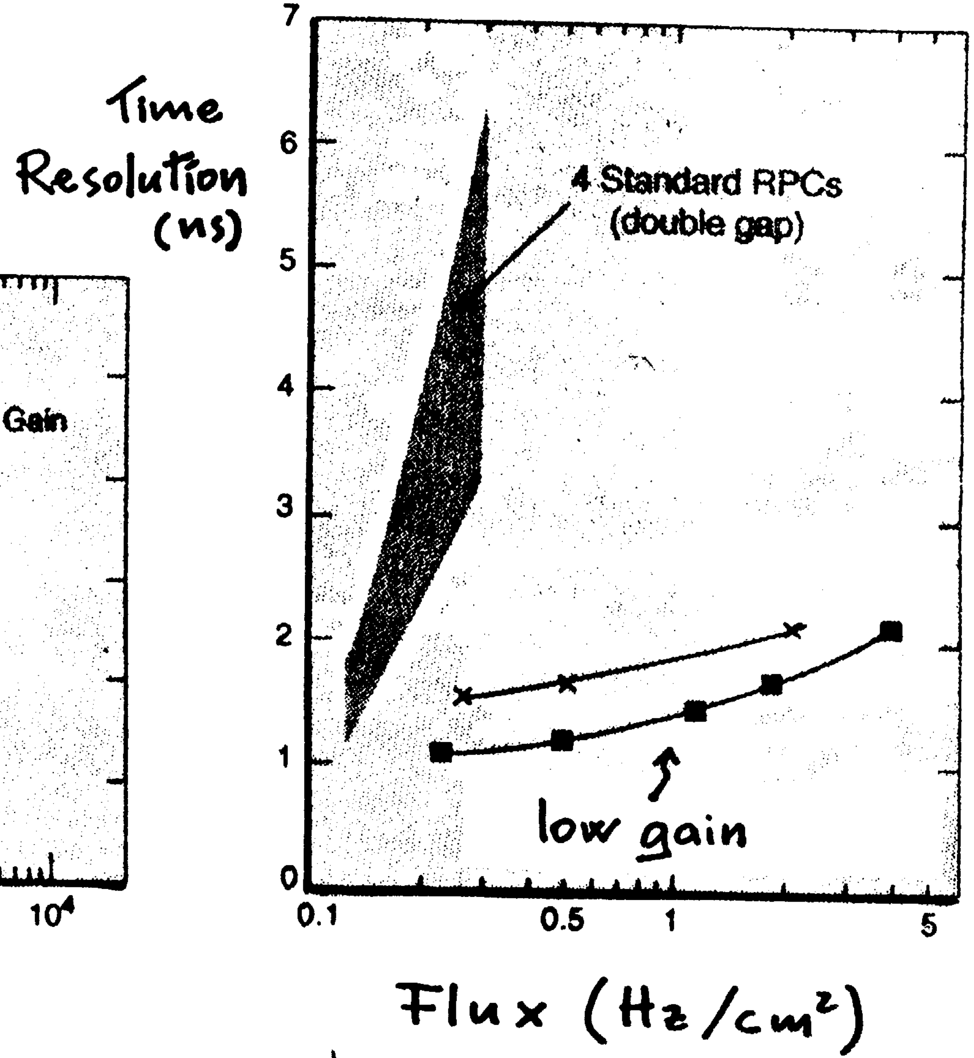

The Thin Gap Wire Chamber

ATLAS μ trigger chamber in End Cap: cathode strip chamber optimized for time accuracy

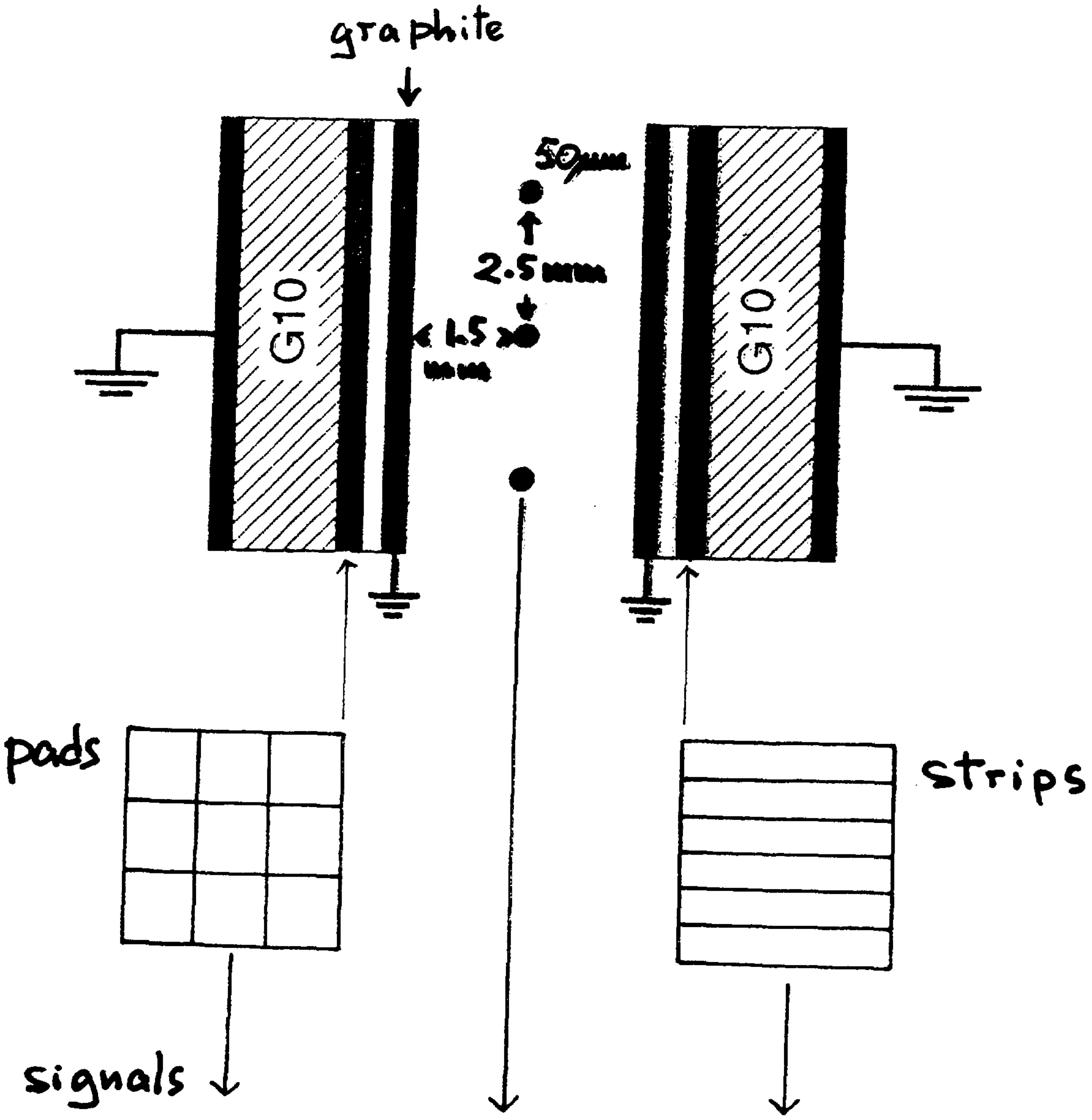

- saturated mode: gain $> 10^5$
- high rate capability: $\sim 0.3\ \mathrm{MHz/cm^2}$
- time accuracy: $\sigma_t \sim 5\ \mathrm{ns}$
- time distribution contained in 20ns

→ bunch crossing identification

Solid State detectors

- Introduction
- LHC detectors
  - Si microstrips RD2, RD20
  - Si pixels RD19
  - GaAs RD8
  - Diamond RD42

Drift and collection of ionization charges: from gases and liquids to solids

non electronegative Gas or Liquid

→ no problem for "contact"

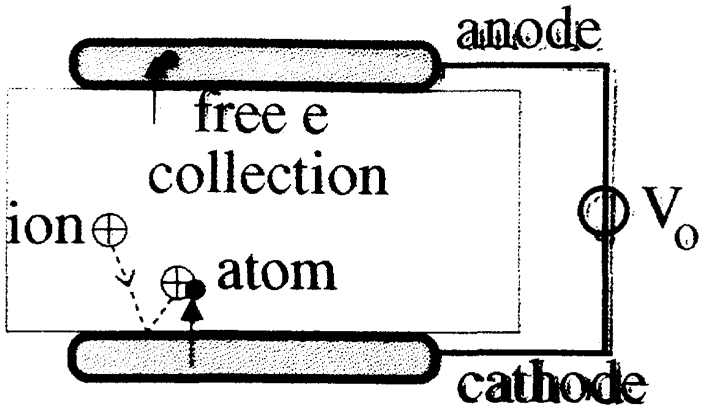

- On the average: a gas or liquid at the microscopic level is a "regular" structure (only imperfections: impurities) → no problem of microscopic structure

- Amorphous solids: beyond impurities there are microscopic structure defects: traps for e and h (few 10 μm Si layers have been studied (Saclay))

→ • Single crystals: insulators or reverse biased semiconductor junctions

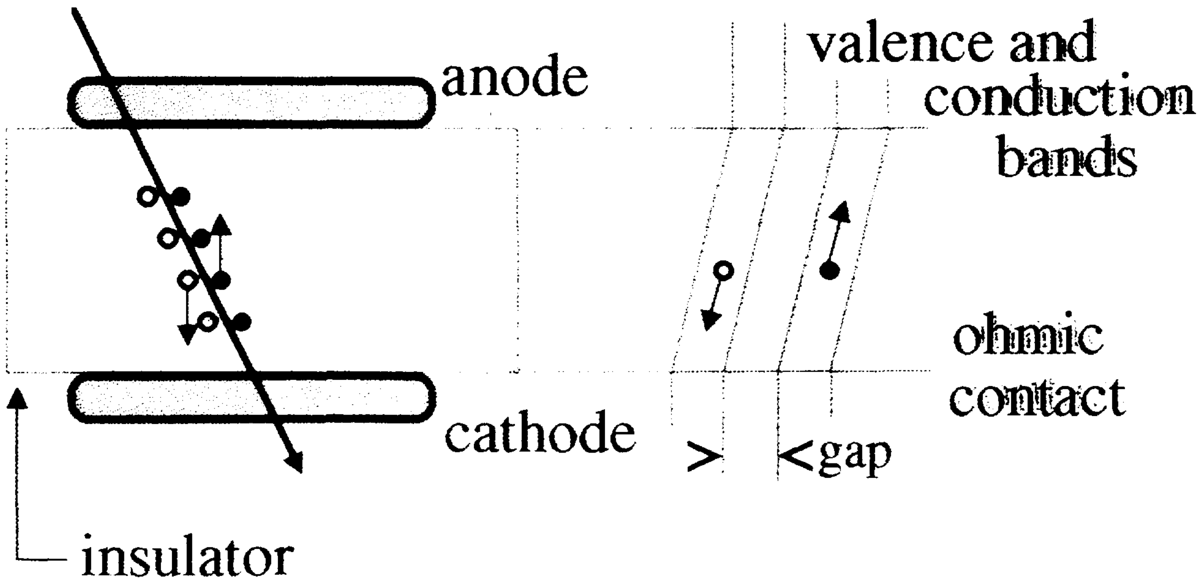

Si detector: reverse biased junction to create a carrier free thickness (except for thermal generation of e-h)

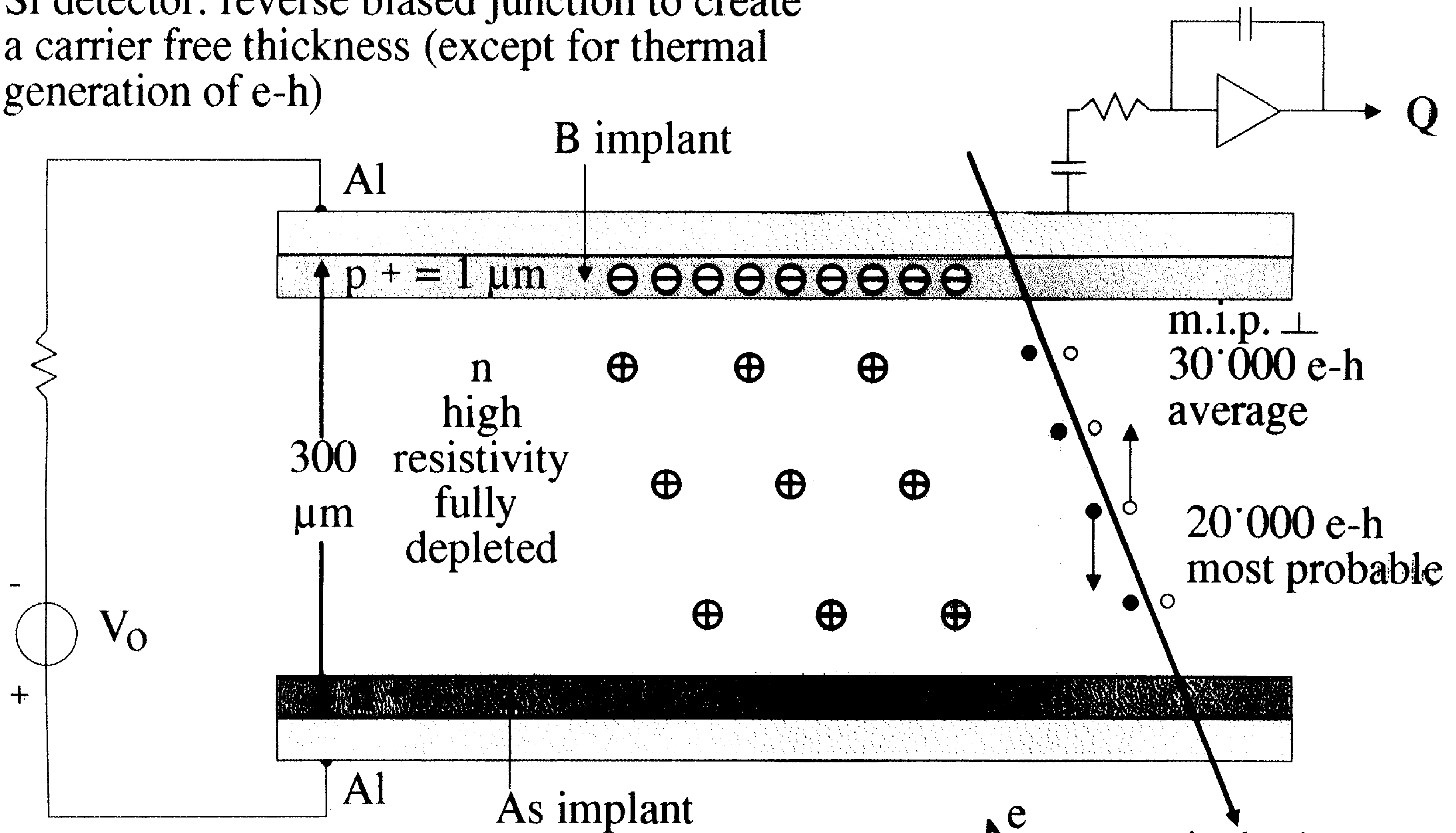

free charge yields

silicon	≡	3.6 eV/e-h
gas & liquids	~	30 eV/e-ion
plastic scint	~	300 eV/p

x ≡ distance from junction

$E(x) \propto x$

$V(x) \propto x^2$

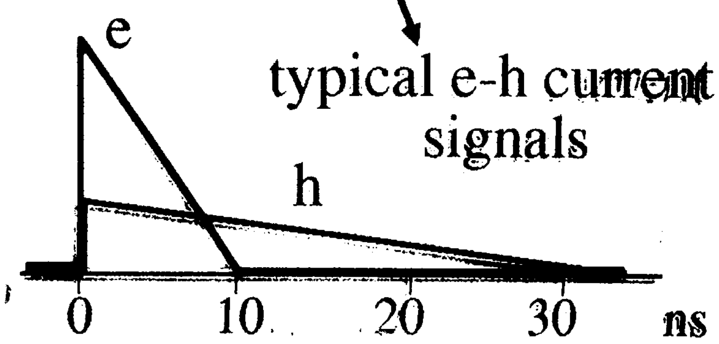

Si μ-STRIP DETECTOR

$20 \div 200 \mu m$ PITCH

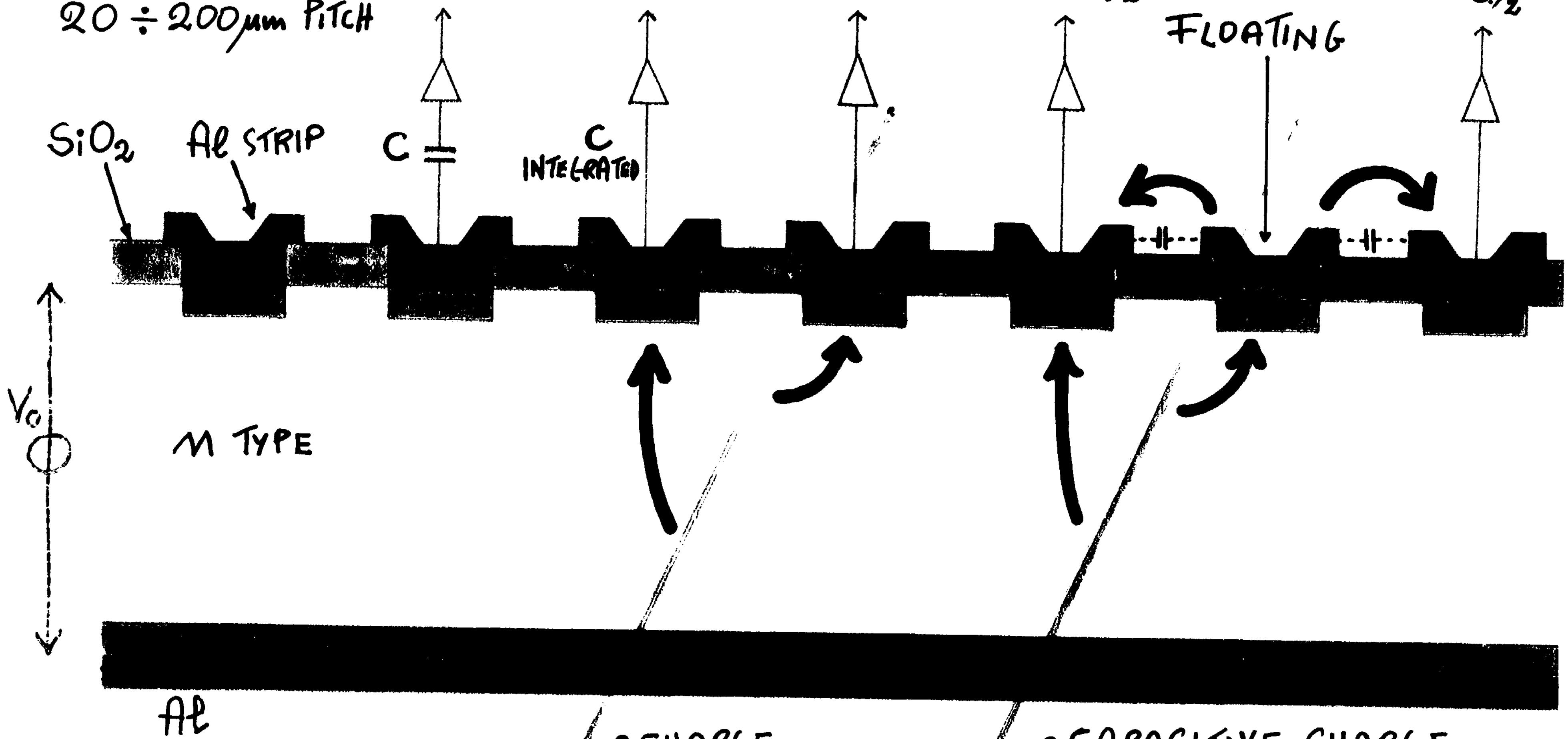

- MINIMUM ACCURACY $\sigma_x = \text{PITCH}/\sqrt{12}$
- CHARGE SHARING BY ANGLE AND LATERAL DIFFUSION (~20μm) IMPROVES ACCURACY
- CAPACITIVE CHARGE DIVISION → ENCODED TRACK POSITION (NOT CENTROID)
- LIMITATION : NOISE
- ENC = a + bC ~ 700e

? PURE INDUCTION SIGNALS ... ~20ns, Q=0 : UNDETECTABLE

2-Dimensional Si μ-strip detectors (LEP,...)

p-side x-strips and n-side y-strips

- undesired effect

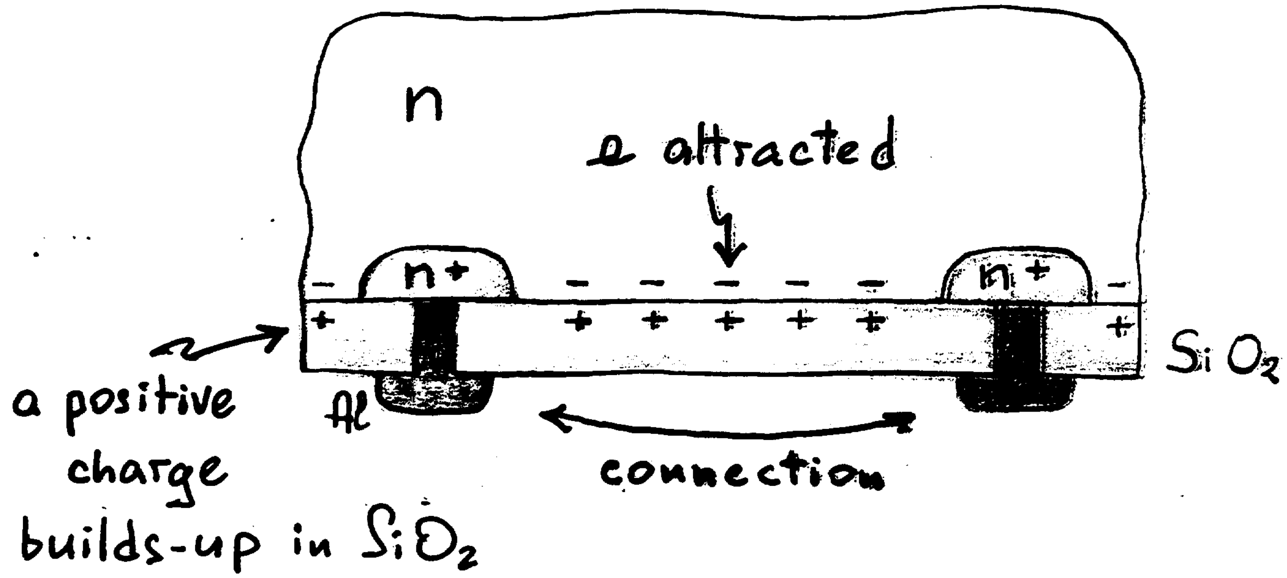

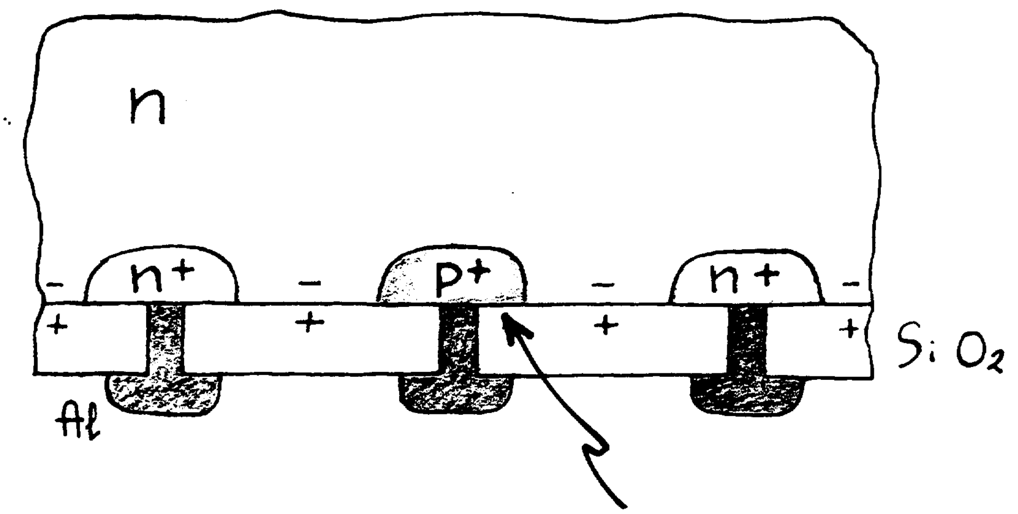

- effect suppressed by p-stops

Double-metal double-sided a.c.-coupled microstrip detector

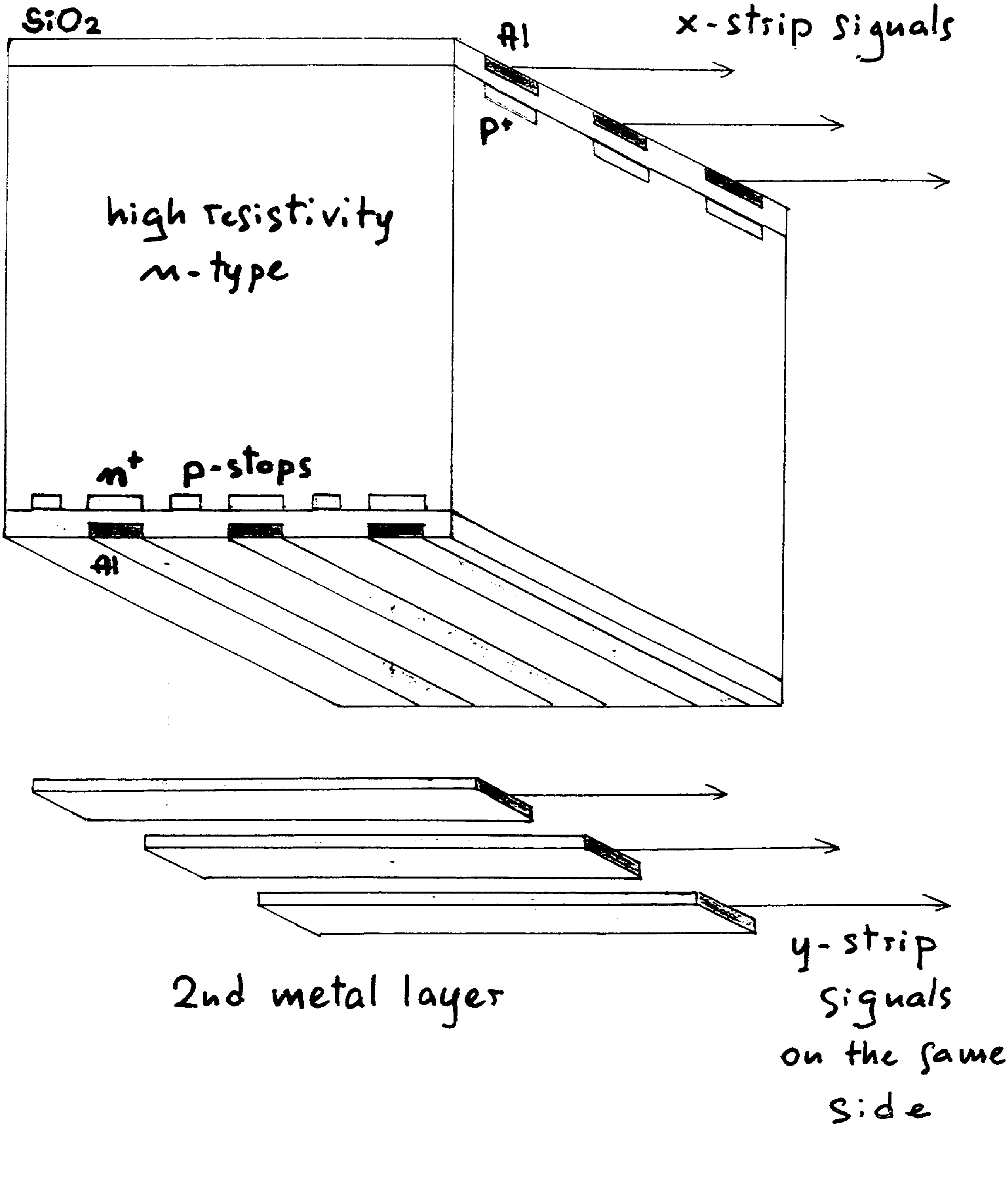

Si microstrip detector development for LHC

- RD2, outer tracker: 100 ÷ 200 μm strip pitch
- RD20, inner tracker: 50 μm strip pitch
  100 μm readout pitch

The most critical issues:

- detector radiation hardness (10 LHC years)
- few 10^6 channels (occupancy ≤ 1%
- complex readout in rad.-hard technology
- power dissipation ~ 10 kW
  (given transistor principle, detector capacitance, and the II Principle of Thermodynamics, a minimum is determined)

Radiation damage:
doping changes

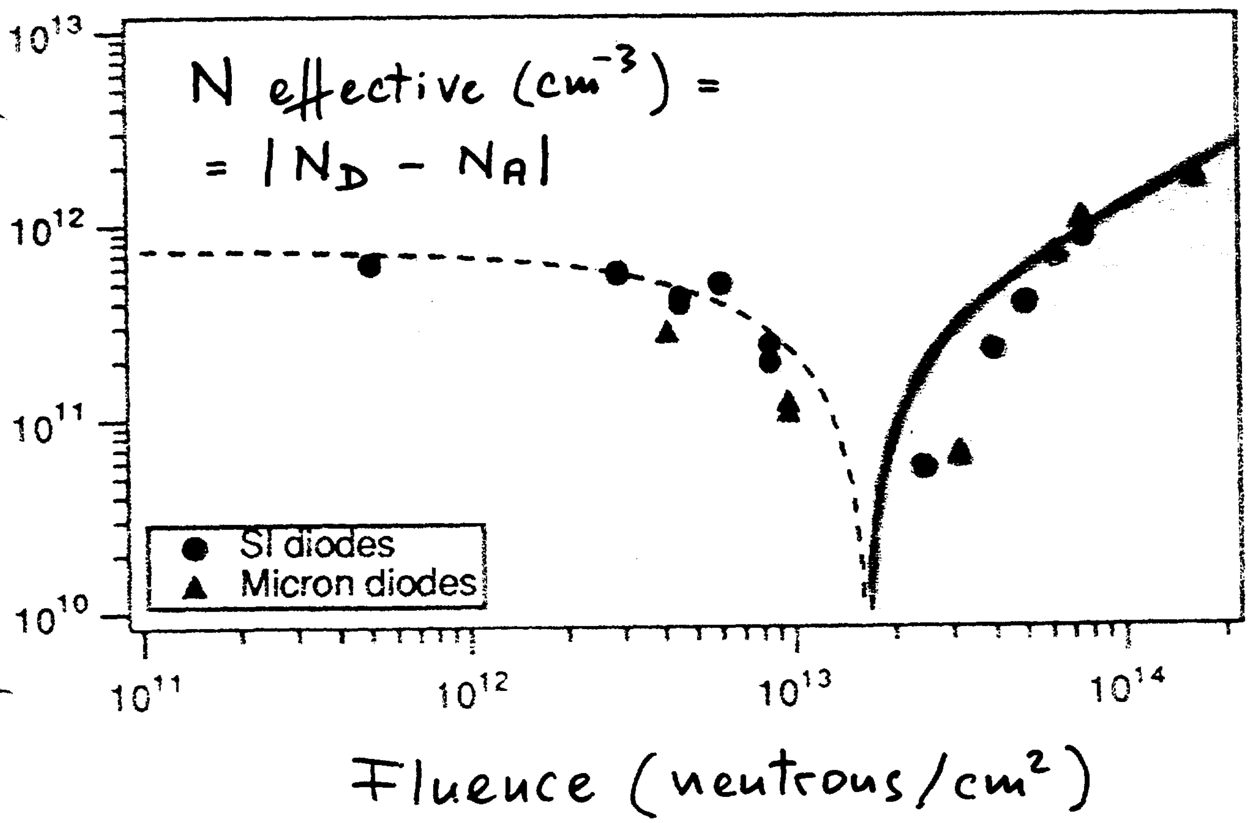

- bulk n-type becomes p-type

- "Anti-annealing" effect
- Can be controlled by 5-10 °C operation

Depletion voltage (Volts)

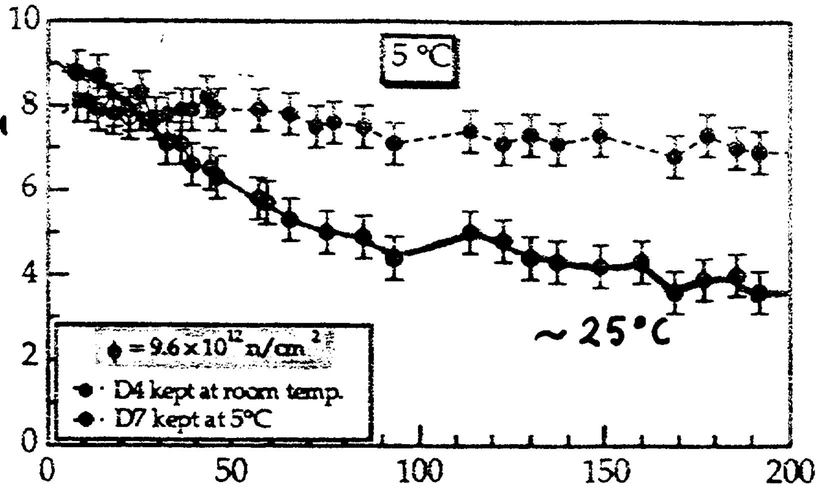

after 10^{13} n/cm^2

(Volts)

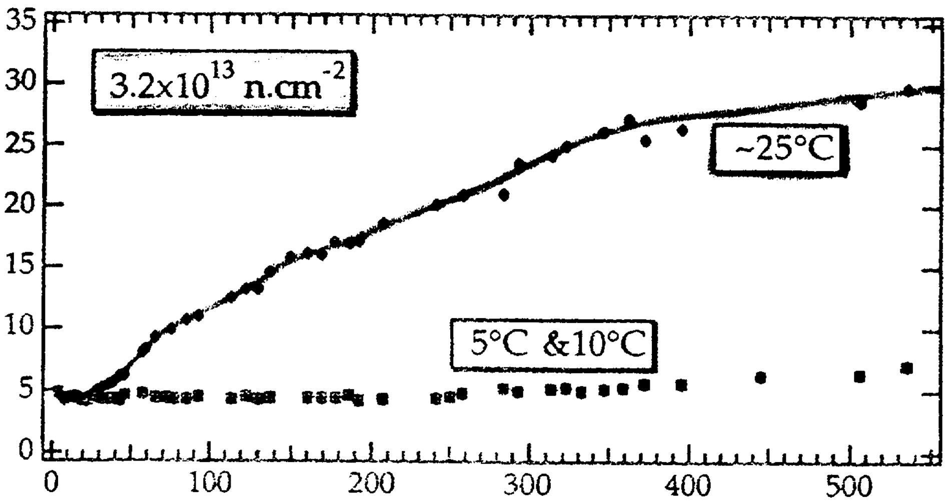

$3 \cdot 10^{13}$ n/cm^2

(Volts)

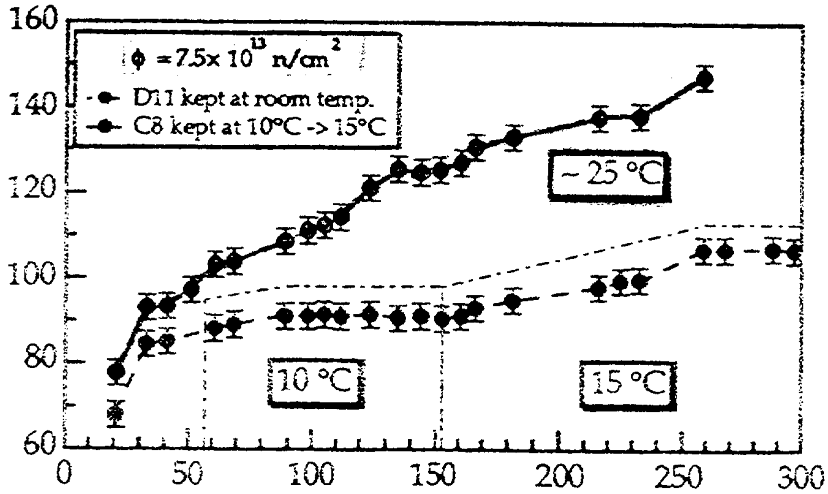

$7.5 \cdot 10^{13}$ n/cm^2

Days

Radiation damage of Si in the bulk

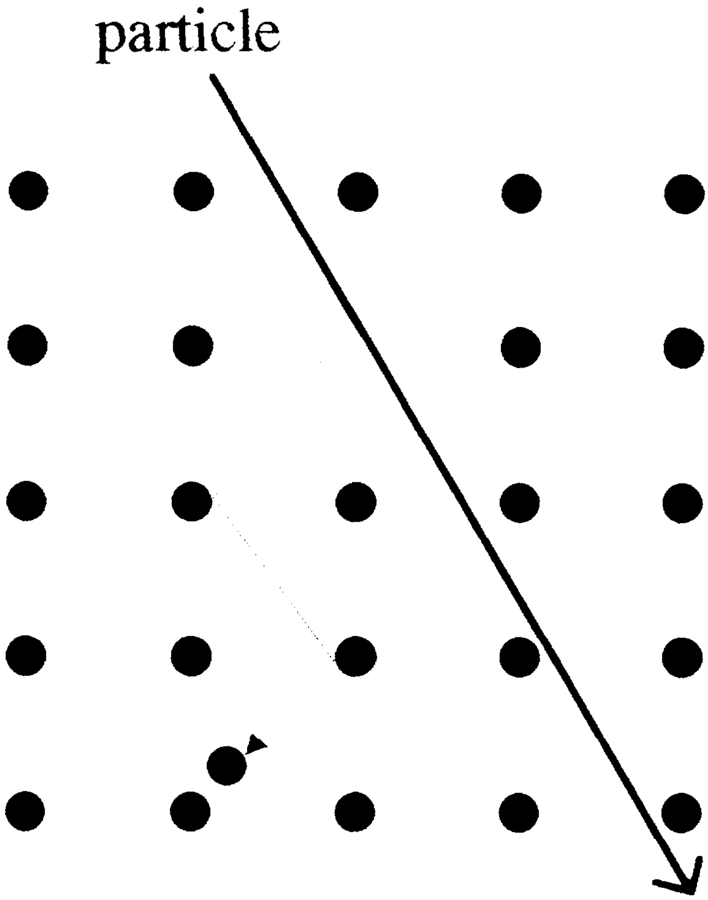

- ~ 15 eV recoil energy is sufficient to create a vacancy and an interstitial atom

- both defects are mobile and chemically active, giving rise to temperature dependent behaviours

- interstitials and vacancies go around and stop at more damaging sites

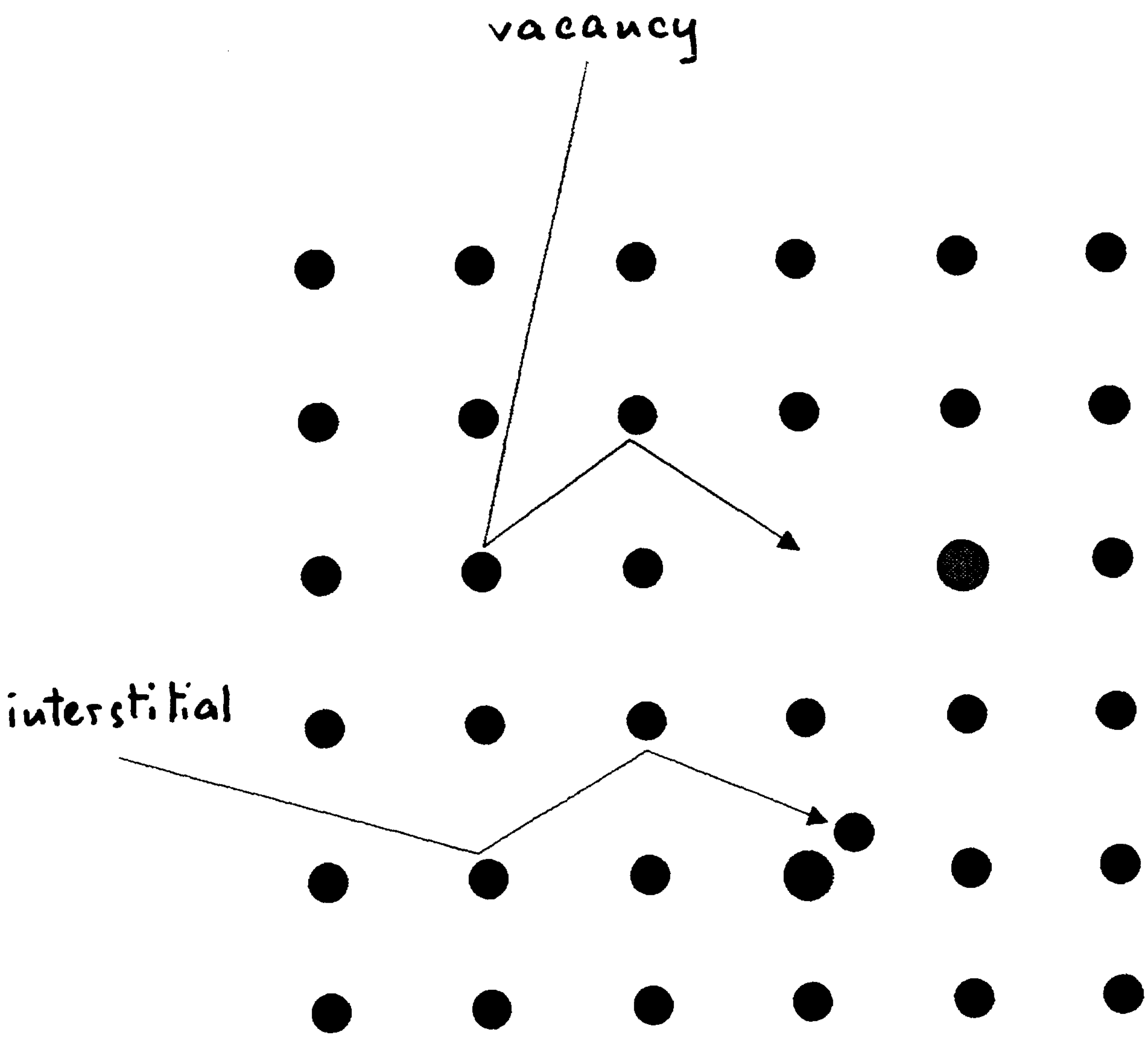

- the control of impurities could improve the situation